UNIVERSIDADE FEDERAL DO RIO GRANDE DO SUL
ESCOLA DE ENGENHARIA
PROGRAMA DE PÓS-GRADUAÇÃO EM ENGENHARIA ELÉTRICA

GUSTAVO LIMA ASCHIDAMINI

A FRAMEWORK FOR RELIABILITY ASSESSMENT IN EXPANSION PLANNING OF POWER DISTRIBUTION SYSTEMS

Porto Alegre
2022

GUSTAVO LIMA ASCHIDAMINI

A FRAMEWORK FOR RELIABILITY ASSESSMENT IN EXPANSION PLANNING OF POWER DISTRIBUTION SYSTEMS

Thesis presented to Programa de Pós-Graduação em Engenharia Elétrica of Universidade Federal do Rio Grande do Sul in partial fulfillment of the requirements for the degree of Master in Electrical Engineering.
Area: Energy

ADVISOR: Prof. Dr. Mariana Resener

Porto Alegre
2022

GUSTAVO LIMA ASCHIDAMINI

A FRAMEWORK FOR RELIABILITY ASSESSMENT IN EXPANSION PLANNING OF POWER DISTRIBUTION SYSTEMS

This thesis was considered adequate for obtaining the degree of Master in Electrical Engineering and approved in its final form by the Advisor and the Examination Committee.

Advisor: _____
Prof. Dr. Mariana Resener, UFRGS
Universidade Federal do Rio Grande do Sul – Porto Alegre, Brazil

Examination Committee:

Prof. Dr. Fernanda Caseño Trindade Arioli, UNICAMP – Campinas, Brazil
PhD from Universidade Estadual de Campinas – Campinas, Brazil

Prof. Dr. Mauricio Sperandio, UFSM – Santa Maria, Brazil
PhD from Universidade Federal de Santa Catarina – Florianópolis, Brazil

Prof. Dr. Daniel Gazzana, UFRGS – Porto Alegre, Brazil
PhD from Universidade Federal do Rio Grande do Sul – Porto Alegre, Brazil

Coordinator of PPGEE: _____
Prof. Dr. Sérgio Haffner

Porto Alegre, October 2022.

DEDICATION

This thesis is dedicated to my family.

ACKNOWLEDGEMENTS

First and foremost, I am grateful for the unwavering support from my supervisor Dr. Mariana Resener.

A special thanks to my research colleagues from the R&D project titled "Planejamento Integrado para Definição de Obras de Expansão na Rede de Distribuição Considerando Critérios Probabilísticos" [Integrated Planning for Definition of Expansion Projects in the Distribution Network Considering Probabilistic Criteria], [in Portuguese]. This project was funded by CEEE Grupo Equatorial Energia and regulated by ANEEL, project number PD-05707-2006/2020. I would also like to express my gratitude to: Gederson Alvaro da Cruz, Roberto Chouhy Leborgne, Luís Alberto Pereira, Lara Colognese de Almeida, Bibiana Petry Ferraz, and José David Doria Garcia.

Thank you to PPGEE (Graduate Program in Electrical Engineering) and the Power Systems Modeling and Analysis Group (GMASP), for the opportunity to research in the field of power systems.

I am thankful for the guidance from my professors, especially, Roberto Chouhy Leborgne, Sérgio Haffner and Daniel Gazzana.

I would also like to thank Fernanda Trindade, Mauricio Sperandio and Daniel Gazzana for all valuable comments and suggestions to the final version of this thesis.

This study was financed in part by the Coordenação de Aperfeiçoamento de Pessoal de Nível Superior – Brasil (CAPES) – Finance Code 001. Last but not least, I thank CAPES for providing me with a full-time scholarship to dedicate exclusively to my research.

ABSTRACT

This work proposes a framework that utilizes a method of analytical assessment of reliability to guide the expansion planning of power distribution systems (PDS) considering reliability criteria. The framework allows the estimation of reliability indices with and without the execution of expansion projects, thus supporting the decision-making process on investments in expansion projects. In the analytical assessment of reliability, failure rates of zones and restoration times are calculated from past data of interruptions in the primary distribution network. Additionally, the estimated reliability indices are adjusted to historical values through failure rates proportionate to the length of each zone. To test and validate the proposed framework, it was applied to a distribution network of the Roy Billinton Test System (RBTS). To validate the framework with real data of interruptions, two case studies were developed, one using a primary distribution feeder and another using a large-scale primary distribution network, both located in Southern Brazil. The results indicated that the proposed framework could help find the most attractive investments leading to improvements in reliability indices and reduction in unsupplied energy. This work formulates the impact of those alternatives of expansion that most affect reliability, namely: (i) the installation of normally closed sectionalizing switches, (ii) the installation of normally open switches with interconnection to adjacent feeders, (iii) the replacement of manual switches by remote controlled switches, and (iv) the replacement of existing bare overhead conductors by covered conductors. Nevertheless, the proposed framework allows the inclusion of other expansion alternatives. The computational performance of the adjustment processes of the estimated indices to the historical indices was evaluated for different reliability parameters, proving convergence and advantages for the chosen parameters. Finally, the proposed framework proved to be practical and useful for real-life applications by power distribution companies.

Keywords: Reliability assessment, power distribution system, expansion planning, reliability indices, energy not supplied.

RESUMO

Este trabalho propõe um *framework* que utiliza a avaliação analítica da confiabilidade para orientar o planejamento da expansão de sistemas de distribuição considerando critérios de confiabilidade. O *framework* proposto permite estimar indicadores de confiabilidade com e sem a execução de projetos de expansão, auxiliando assim a tomada de decisão sobre investimentos em projetos de expansão. Na avaliação analítica da confiabilidade, as taxas de falhas das zonas e os tempos de restabelecimento são calculados a partir de dados históricos de interrupções na rede de distribuição primária. Além disso, os indicadores de confiabilidade estimados são ajustados a valores históricos por meio de taxas de falhas proporcionais ao comprimento de cada zona. Para testar e validar o *framework* proposto, ele foi aplicado à uma rede de distribuição do *Roy Billinton Test System* (RBTS). Para validar o *framework* com dados reais de interrupções, foram desenvolvidos dois estudos de caso reais, um com um alimentador de distribuição primário e outro com um conjunto de oito alimentadores de distribuição primários de uma subestação, ambos localizados na região Sul do Brasil. Os resultados indicaram que o framework proposto pode ajudar a definir os investimentos mais atrativos levando a melhorias nos indicadores de confiabilidade e redução de energia não fornecida. Neste trabalho foi formulado o impacto das alternativas de expansão que mais afetam a confiabilidade: (i) a instalação de chaves de seccionamento normalmente fechadas (ii) a instalação de chaves normalmente abertas com interligação com alimentadores adjacentes, (iii) a substituição de chaves manuais por chaves telecomandadas, e (iv) a substituição de condutores aéreos nus de média tensão por condutores protegidos. No entanto, devido à flexibilidade do *framework* proposto, este permite a inclusão de outras alternativas de expansão que impactam na confiabilidade. O desempenho computacional dos processos de ajuste dos indicadores estimados aos indicadores históricos do framework foi avaliado para diferentes parâmetros de confiabilidade, provando a convergência e vantagens dos parâmetros escolhidos. Finalmente, o *framework* proposto provou ser prático e útil para aplicações reais por empresas de distribuição de energia.

Palavras-chave: Avaliação da confiabilidade; sistemas de distribuição; planejamento da expansão; indicadores de confiabilidade; energia não suprida.

LIST OF FIGURES

LIST OF TABLES

LIST OF ABBREVIATIONS

AENS	Average Energy Not Supplied
AL	Addition of Lines
ANEEL	National Agency of Electric Energy
ASAI	Average Service Availability Index
CB	Circuit Breakers
CDF	Customer Damage Function
CIC	Customer Interruption Cost
CID	Customer Interruption Duration
CIF	Customer Interruption Frequency
CS	Charging Stations
CWIDM	Consumers Weighted Interruptions Duration Matrix
CWIM	Consumption Weighted Interruption Matrix
CWIQM	Consumers Weighted Interruptions Quantity Matrix
DEC	Equivalent Interruption Duration per Consumer Unit
DER	Distributed Energy Resources
DG	Distributed Generation
DIC	Individual Interruption Duration per Consumer Unit or Connection Point

ECOST	Expected Interruption Cost Index
EENS	Expected Energy Not Supplied
ESS	Energy Storage Systems
EV	Electric Vehicles
FEC	Equivalent Interruption Frequency per Consumer Unit
FIC	Individual Interruption Frequency per Consumer Unit or Connection Point
FIM	Fault Incidence Matrix
I	Unrecoverable Zone
IDM	Interruptions Duration Matrix
IEEE	Institute of Electrical and Electronics Engineers
IQM	Interruptions Quantity Matrix
LP	Load Point
MAIFI	Momentary Average Interruption Frequency Index
MAIFIe	Momentary Average Interruption Event Frequency Index
MILP	Mixed Integer Linear Programming
MV	Medium-Voltage
N	Unaffected Zone
NC	Normally Closed
NO	Normally Open
OMS	Outage Management System
PDS	Power Distribution Systems
PL	Parking Lots
PRODIST	Electricity Distribution Procedures in the National Electric System

R	Recoverable Zone
RBTS	Roy Billinton Test System
SAIDI	System Average Interruption Duration Index
SAIFI	System Average Interruption Frequency Index
SS	Substation
SW	Switching or Protection Devices
T	Transferable Zone
TC	Total Number of Consumers
V2G	Vehicle-to-Grid
ZCM	Zone Classification Matrix

LIST OF SYMBOLS

$\mathbf{A}$	Adjacency matrix.
$cEENS_i$	Contribution of faults in zone i to the index $EENS$ (MWh/year).
$cSAIDI_i$	Contribution of faults in zone i to the $ESAIDI$ (h/year).
$cSAIFI_i$	Contribution of faults in zone i to the $ESAIFI$ (interruptions/year).
E	Vector of edges.
$EASAI$	Expected value of average service availability index (%).
$ECID_j$	Expected value of index customer interruption duration in zone j (h/year).
$ECIF_j$	Expected value of index customer interruption frequency in zone j (interruptions/year).
$EENS$	Expected energy not supplied (MWh/year)
$ESAIDI$	Expected value of system average interruption duration index (h/year).
$ESAIFI$	Expected value of system average interruption frequency index (interruptions/year).
G	Definition of a graph.
l_i	Length of zone i (km).
n	Number of zones.
NO_e	End zones of normally open switches.
NO_s	Start zones of normally open switches.

p_l	Percentage of ${t_l}^h$ in relation to ${t_R}^h$ (%).
p_r	Repair time in percentage (%).
$\mathbf{R}$	Reachability matrix.
$SAIDI_h$	Historical average system average interruption duration index (h/year).
$SAIFI_h$	Historical average system average interruption frequency index (interruptions/year).
t_l	Average fault location time (h).
${t_l}^h$	Historical average fault location time (h).
t_r	Average time to repair a failure (h).
t_{res}	Average restoration time (h).
${t_{res}}^i$	Initial restoration time (h).
${t_{res}}^s$	Step for t_{res} (h).
${t_R}^h$	Historical average restoration time (h).
t_{sw}	Average manual switching time (h).
V	Vector of vertices.
Δ^s	Failure rate step per length (failure/km.year).
λ_i	Failure rate of zone i (failure/year).
${\lambda_i}^c$	Calculated failure rate of zone i (failure/year)
${\lambda_i}^h$	Historical failure rate of zone i (failure/year).

CONTENTS

1 INTRODUCTION

Nowadays, great interest resides in the study of the quality of electricity supply, since it is related to technical and economic losses affecting utilities and end-users (MASOUM; FUCHS, 2015). In this respect, the services offered by power distribution companies must meet quality requirements imposed by regulatory agencies. Consequently, power distribution companies in general follow given strategies when they plan the operation and the expansion of their distribution network. In addition, new solutions are constantly needed to modernize the distribution network and simultaneously assure high-quality services (GEORGILAKIS; HATZIARGYRIOU, 2015; ESCALERA; HAYES; PRODANOVIć, 2018; ALOTAIBI *et al.*, 2020; CHAVES *et al.*, 2021).

On the other hand, low investment costs in the network compete with improvement in reliability indices, making thus necessary support tools to define those projects that best improve reliability at the lowest cost (BILLINTON; ALLAN, 1992). Therefore, the essential aspects to be considered to make decisions on the expansion of the system are (i) estimation of the reliability indices, (ii) identification of the points of the network that most need improvements, and (iii) the assessment of the impact of expansion projects on reliability. In this context, it then becomes relevant to develop software tools to support power distribution utilities to better choose expansion projects during the planning stages.

Reliability is defined as the ability to continuously meet the load demand of consumers in terms of both quantity and quality (WILLIS, 2004; CHOWDHURY; KOVAL, 2009). Failures in power distribution systems (PDS) are responsible for more than 80% of the interruptions of the energy supply to consumers, showing that investments in reliability at the

distribution level can improve the reliability of the entire power system (CHOWDHURY; KOVAL, 2009). Thus, to simultaneously meet economic and reliability requirements, when formulating the problem of planning the expansion of PDS, it is necessary to consider reliability indices.

Reliability can be measured using several indices, such as the system average interruption duration index (SAIDI), system average interruption frequency index (SAIFI), average service availability index (ASAI), customer interruption frequency (CIF), customer interruption duration (CID), and expected energy not supplied (EENS) (BILLINTON; ALLAN, 1996; LOTERO; CONTRERAS, 2011; IEEE, 2012). These indices are related to frequency, duration, or energy not supplied due to interruptions. In addition, SAIFI and SAIDI are among the commonest reliability indices used by power distribution companies (ESCALERA *et al.*, 2019).

Reliability indices can be obtained through analytical methods or simulation, such as the sequential Monte Carlo simulation (BILLINTON; ALLAN, 1992; CHOWDHURY; KOVAL, 2009). Analytical methods represent the system through formulated models with fixed values or parameters, from which the reliability indices are estimated. In contrast, methods based on sequential Monte Carlo simulation estimate the reliability indices by simulating the random behavior of the system (BILLINTON; LI, 1994). Furthermore, analytical methods generally provide average values for reliability indices, whereas methods based on simulation provide probability distributions of possible values of the reliability indices (BROWN, 2008).

Analytical methods for reliability assessment require lower computational effort to estimate reliability indices when compared to methods based on simulation (BILLINTON; ALLAN, 1992; LóPEZ-PRADO; VéLEZ; GARCIA-LLINáS, 2020). In addition, analytical methods can be readily applied to real distribution systems, given that distribution utilities usually have feeder models suitable for some commercial software used for network analysis. Moreover, this type of method is more adequate for sensitivity analysis due to the better accuracy of the results that can be obtained (BROWN, 2008).

Utilities are responsible for supplying electricity to consumers while meeting reliability

requirements established by regulatory agencies. Towards this end, utilities must invest in expansions of the network and follow maintenance practices in their concession areas that help reduce their costs (BILLINTON; ALLAN, 1996). To quantify the PDS reliability and assess the performance of utilities, both on the regulator side and on the utility side, reliability indices are used. These indices can be related to momentary interruptions or sustained interruptions; further, they can also be based on loads of PDS. IEEE Standard 1366-2012—Guide for Electric Power Distribution Reliability Indices defines the fundamental terms to be used in studies of the reliability of distribution systems as well as several reliability indices (IEEE, 2012).

The horizon of PDS expansion planning can be divided into short term (1–5 years) or long term (5–20 years) (GONÇALVES; FRANCO; RIDER, 2015). Within the context of reliability, short-term expansion planning usually encompasses the installation of protection and/or switching devices and the reconductoring of existing circuits, while long-term expansion planning may include the construction of substations and new feeders, as well as increasing the capacity of existing substations.

Furthermore, the reliability of active distribution networks can be improved through additional alternatives, such as islanded operation through post-fault reconfiguration and energy supply through distributed generation, energy storage systems, and electric vehicle charging stations (ASCHIDAMINI *et al.*, 2022a). These alternatives can help reduce the duration of interruptions and thus improve reliability indices.

The problem of planning the expansion of PDS considering reliability is usually approached through optimization models, aiming to define a set of expansion projects. However, the problem can be addressed through the use of analytical assessment of reliability, which allows the verification of critical points in the distribution network. In this approach, the method does not define a set of expansion projects. Instead, the analytical assessment of reliability can be used with the sensitivity analysis of network and reliability parameters to assess the impact of executing projects in the network on reliability. This approach provides flexibility in indicating alternatives for expansion projects to be evaluated during the expansion planning stages, presenting potential practical applications

by power distribution companies.

Although reliability assessment has already been used for sensitivity analysis and to quantify the impacts of expansion projects on reliability of PDS, most published works disregard reliability when developing tools to plan the expansion of power distribution systems. To improve this aspect, an analytical framework to consider reliability criteria when planning the expansion of PDS is proposed in this thesis. Toward this goal, data available from power distribution utilities are used, and procedures leading to reliability indices, considering the effective execution of expansion projects, and without the execution of expansion projects, are defined.

To validate the proposed framework, as well as demonstrate its use, the proposed framework was applied to a distribution network of the Roy Billinton Test System (RBTS) (BILLINTON, 1996). To test the framework with real data of interruptions, two case studies using real primary distribution feeders from a power distribution utility were developed, with the results being subsequently discussed.

1.1 Objectives

Within this context, the main objective of this thesis is to propose a framework to incorporate the reliability assessment within the expansion planning of power distribution systems. In this framework, a proposed method of analytical assessment of reliability is used to evaluate reliability indices concerning the primary distribution network level. This method employs historical data of interruptions and the network length of each zone, which are the sections of the primary distribution network between protection and/or sectionalizing devices, to calculate failure rates and adjust the estimated reliability indices to the average historical indices of the primary distribution network.

1.2 Contributions and Innovations

In this thesis, a comprehensive framework to evaluate the reliability of PDS and estimate the impacts that the execution of expansion projects produces on reliability indices is proposed. One of the main contributions of this thesis is the process of adjustment of

reliability indices, which are estimated from historical data of faults in each zone. A further contribution is that unlike (DIAS, 2002; ZHANG *et al.*, 2020), failure rates are determined considering (i) the length of each zone of the distribution network and (ii) the history of faults of each zone, thus allowing the identification of the most critical zones.

Moreover, as yet another contribution, the proposed method allows the evaluation of the expected indices SAIFI, SAIDI, and EENS, as well as the load node indices CIF and CID, both not considered by (ZHANG *et al.*, 2020). Additionally, the proposed framework includes the evaluation of the impact on the reliability of expansion alternatives such as (i) installation of normally closed (NC) sectionalizing switches, (ii) installation of normally open (NO) switches with interconnection to adjacent feeders, (iii) replacement of manual NC sectionalizing switches by remote controlled switches, and (iv) replacement of existing bare overhead conductors by covered conductors.

1.3 Thesis Outline

This thesis is organized in the following chapters:

- Chapter 2 presents the background related to the reliability of PDS and the problem of planning the expansion of PDS considering reliability. Subsequently, the proposed framework is compared with other approaches to the problem cited above;
- In Chapter 3, the proposed framework is presented. Initially, the procedures for assessing the reliability of PDS assuming no expansion of the distribution network and considering expansion projects are described in flowcharts, from obtaining the data of power distribution companies to assessing reliability indices. Subsequently, the model of the distribution network is detailed, and the proposed method of analytical assessment of reliability is formulated based on matrices that allow obtaining reliability indices. Finally, the formulation for assessing the impact of expansion projects on the reliability of the primary network is developed;
- Chapter 4, presents a case study using a distribution network of the RBTS, to validate the proposed framework and show the advantages of the proposed framework over a

correlated method;

- In Chapter 5, to use real data of interruptions from a power distribution utility, the framework is applied to two case studies; one using a real distribution feeder and another using a large-scale real distribution network. Furthermore, the computational performance of parts of the framework is evaluated;

- Finally, Chapter 6 concludes this thesis and offers recommendations for future studies.

2 BACKGROUND

This chapter is excerpted, modified, and reproduced with permission, from the following papers that I co-authored:

- **Aschidamini, G.L.**; da Cruz, G.A.; Resener, M.; Leborgne, R.C.; Pereira, L.A. A Framework for Reliability Assessment in Expansion Planning of Power Distribution Systems. Energies 2022, 15. doi:10.3390/en15145073.

- **Aschidamini, G.L.**; da Cruz, G.A.; Resener, M.; Ramos, M.J.S.; Pereira, L.A.; Ferraz, B.P.; Haffner, S.; Pardalos, P.M. Expansion Planning of Power Distribution Systems Considering Reliability: A Comprehensive Review. Energies 2022, 15. doi:10.3390/en15062275.

Sections of this chapter have been adapted from the above papers to fit the scope and formatting of the thesis.

This chapter introduces essential aspects of the reliability of distribution systems. Subsequently, different approaches to the problem of planning the expansion of PDS considering reliability criteria are discussed. In the specialized literature, works with different approaches are found, and for this reason, the main works related to the problem mentioned above will be analyzed in a brief bibliographic review in Section 2.2. Finally, the proposed method will be compared with the main correlated works.

2.1 Reliability of Power Distribution Systems

The reliability of power distribution systems is usually measured by indices and, for this reason, the main indices at the distribution level are initially examined. Subsequently, alternatives for expanding the distribution network with an impact on reliability are discussed. Finally, the distribution test systems used in distribution systems studies are analyzed.

2.1.1 Reliability Indices

In the IEEE Standard 1366-2012—Guide for Electric Power Distribution Reliability Indices (IEEE, 2012), indices aiming to measure the reliability of the distribution network level are defined. The expected indices SAIFI, SAIDI and ASAI are determined as follows.

The expected value of SAIFI (ESAIFI) indicates how many sustained interruptions an average customer expects to experience, as expressed by:

$$ESAIFI = \frac{\text{Total number of customer interruptions}}{\text{Total number of customers served}}. \tag{2.1}$$

The expected value of SAIDI (ESAIDI) indicates the expected number of hours of interruption of an average customer, as follows:

$$ESAIDI = \frac{\sum \text{Customer interruption duration}}{\text{Total number of customers served}}. \tag{2.2}$$

The expected value of ASAI (EASAI) indicates the percentage of time an average customer is supplied without interruption:

$$EASAI = \frac{\text{Customer hours service availability}}{\text{Customer hours service demand}}. \tag{2.3}$$

Furthermore, the indices expected customer interruption frequency (ECIF) and expected customer interruption duration (ECID) can also be used. They express the frequency and duration of interruptions for each load node, respectively.

In contrast, the indices EENS and average energy not supplied (AENS) are load-oriented, both being equivalent to the energy not consumed due to interruptions. Note that

AENS is normalized by the number of consumers of the electrical set, defined as a group of consumers according to (BILLINTON; ALLAN, 1996).

Reliability can also be measured using the customer interruption cost (CIC) due to interruptions related to the distribution system level. The expected interruption cost index (ECOST) can be used, which, in turn, is based on the EENS index. ECOST uses the customer damage function (CDF), which estimates the cost of outages normalized by the load and the duration of the outage of each customer (WACKER; BILLINTON, 1989). Note that each customer class has a CDF, given that consumers can be divided into classes, such as residential, commercial, industrial, agriculture, government/institutional, large consumers, and offices (BILLINTON, 2001).

The reliability assessment considering the costs of interruption to customers requires the definition of the financial losses for the energy that was not consumed during interruptions, which is an imprecise parameter, mainly due to the uncertainties of the methods for estimating this parameter (KüFEOğLU; LEHTONEN, 2015). This imprecision in the input parameters of the reliability assessment makes the use of the index ECOST unattractive for use in software tools with potential use by power distribution companies, which aim to evaluate the reliability of real distribution networks.

Among the most relevant reliability indices related to momentary interruptions are the momentary average interruption frequency index (MAIFI) and the momentary average interruption event frequency index (MAIFIe) (BROWN, 2008). The indices MAIFI and MAIFIe are essential in studies that aim to assess the impact of temporary failures, due to the increase in the amount of sensitive loads, such as loads found in homes, businesses, and industries, and also due to the relevance of avoiding temporary interruptions to keep consumers satisfied (VIEIRA POMBO; MURTA-PINA; FERNãO PIRES, 2017).

In Brazil, the National Agency of Electric Energy (ANEEL), Brazil's regulatory agency, defines the sets of distribution networks to assess reliability in operation of each power distribution company, and also determines goals for the reliability indices. ANEEL establishes in Module 8 (Quality of Electricity Supply) of the Electricity Distribution Procedures in the National Electric System (PRODIST), reliability indices, which are used

to measure the reliability level of distribution networks.

The reliability of distribution networks is usually defined considering the customers connected to distribution feeders supplied by a substation. The reliability of distribution network is measured by the reliability indices equivalent interruption duration per consumer unit (DEC) and equivalent interruption frequency per consumer unit (FEC) (ANEEL, 2022). The DEC and FEC indices are analogous to the SAIDI and SAIFI, respectively.

Power distribution companies are penalized when they fail to meet the goals for the indices DEC and FEC. In addition, financial compensation is provided for customers for violating the limits of indices assessed by load-node, some of which called individual interruption duration per consumer unit or connection point (DIC) and individual interruption frequency per consumer unit or connection point (FIC). The indices DIC and FIC are analogous to the indices CID and CIF, respectively.

2.1.2 Expansion Alternatives for Power Distribution Systems

Planning the expansion of PDS takes into account the addition, replacement or reinforcement of different types of devices, distribution lines, or substations (RESENER *et al.*, 2018; GEORGILAKIS *et al.*, 2021). To maintain the quality of electricity supplied to customers, power distribution companies propose expansion projects in the primary and secondary distribution networks. Reliability is one of the factors of power quality, which is essential to improve the quality of electricity distribution services.

Figure 1 illustrates expansion alternatives for power distribution systems that can help reduce the frequency or duration of interruptions, thus improving reliability. The expansion alternatives were categorized into seven groups: the addition of lines (AL), reconductoring (RE), switching or protection devices (SW), substation construction or increasing the capacity of existing substations (SS), distributed generation (DG), energy storage systems (ESS), and parking lots (PL) with charging stations (CS) for electric vehicles (EV). Further, among the expansion alternatives related to SW are reclosers, fuses, sectionalizing switches, tie-lines, and circuit breakers (CB).

The installation of protection and switching devices can be considered as an expansion alternative in short-term planning, given that the installation requires less time compared

Figure 1 – Expansion alternatives for power distribution systems.

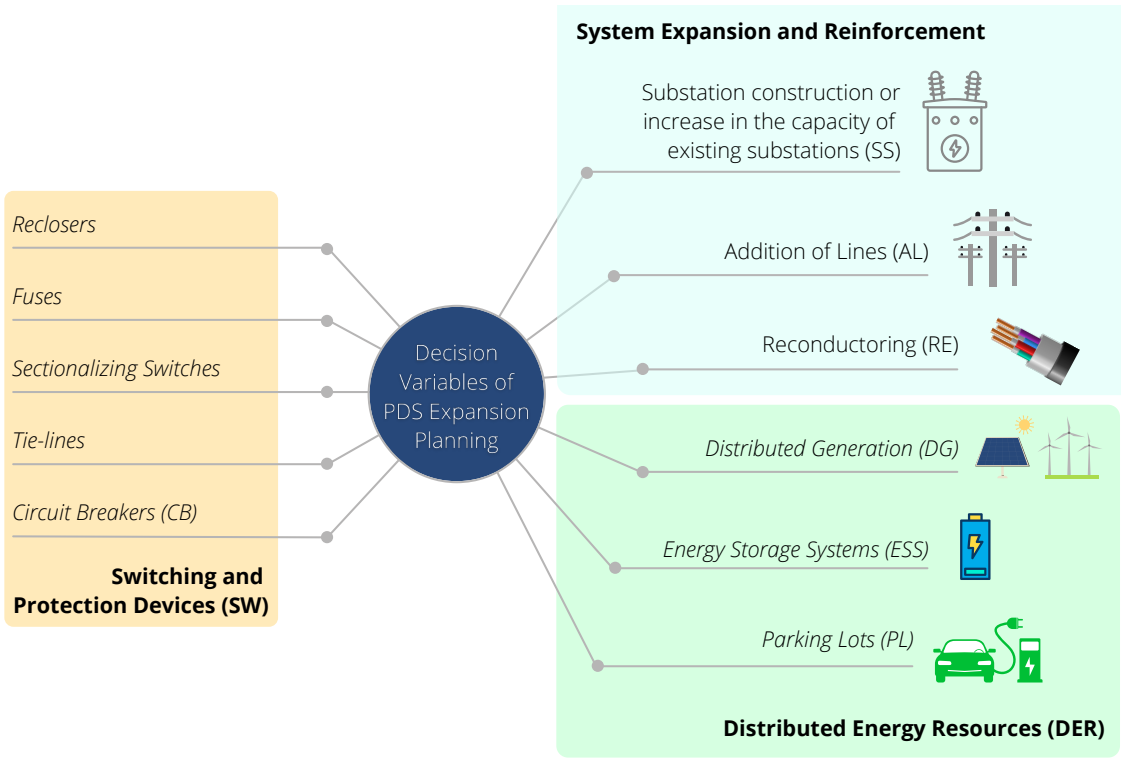

Source: ASCHIDAMINI *et al.* (2022a)

to other alternatives, such as the construction of substations. In addition, as a short-term alternative, the automation of PDS can also be considered, in which manual protection and/or switching devices are replaced with automated devices. These alternatives are commonly used by power distribution utilities to improve reliability indices so that they meet the requirements of regulatory agencies concerning electricity distribution services.

The growth in consumer load demands expansion projects by power distribution utilities, with some of the alternatives being to increase the capacities of existing substations or the construction of new substations. These alternatives fit within expansion plans considering medium- or long-term horizons, due to the longer execution time required and the need for more significant changes to be made to the network. Furthermore, the construction of new substations usually requires new feeders to supply the load, for instance, when the network is expanded to areas not yet covered by electricity supply (Greenfield planning (MIGUEZ *et al.*, 2002)). In addition, given that switching and protection devices need to be installed along the new feeders, they not only change the

network topology but also have an impact on the reliability of the system. Therefore, it becomes essential to include reliability criteria in optimization models applied to solve the problem of long-term expansion planning.

The integration of distributed energy resources (DER) in the electrical grid can collaborate with the expansion of smart electrical grids, bringing benefits through network operation and reconfiguration strategies (POMBO; MURTA-PINA; PIRES, 2016). The use of renewable DG in distribution systems is increasing, with DG being predominantly associated with wind and solar sources, while in some countries, grid-connected ESS technologies are being implemented. Furthermore, the use of EV is already a reality in many countries. Currently, studies on the expansion of distribution systems considering reliability also allow the inclusion of DER as alternatives, among which are (i) DG, (ii) ESS, and (iii) parking lots with CS for EV with vehicle-to-grid (V2G) capability. Although these DER expansion alternatives are indicated in the literature to improve reliability, in the this work only alternatives for the expansion of passive PDS will be incorporated, which do not consider the insertion of DER.

2.1.3 Power Distribution Test Systems

Test systems can be classified into actual or synthetic systems. Actual systems are modeled through real distribution networks; synthetic systems are generated through real distribution networks but modified through different techniques, as detailed in (MARCOS *et al.*, 2017). Optimal expansion planning studies of PDS usually employ test systems found in the literature, or systems modified according to the needs of the study. A representative example of test systems is the IEEE 123-node system, which is a radial distribution feeder used in several areas of studies involving PDS (KERSTING, 1991).

Further examples of test systems used in PDS studies are the IEEE 13-node, 34-node, and 37-node, described in (KERSTING, 1991), IEEE 33-node introduced in (BARAN; WU, 1989a), and the 69-bus system used in (BARAN; WU, 1989b). On the other hand, a test system widely applied in reliability studies is the RBTS (Roy Billinton Test System) (BILLINTON, 1996), which is composed of six medium-voltage buses with different types of consumers. In contrast, the 54-node test system described in (MIRANDA; RANITO;

PROENA, 1994) is suitable for network expansion planning due to the existence of candidate branches and substations to be constructed. Finally, many studies concerning PDS expansion planning make no use of the test systems found in the literature. On the other hand, the case studies reported are based on actual feeders modeled using data of real distribution networks.

2.2 Expansion Planning of Power Distribution Systems Considering Reliability: A Brief Bibliographic Review

Utilities must follow the standards established by regulatory agencies. For this purpose, they use tools that allow them to assess the network history and to support the decision making in PDS expansion planning. In this context, the historical assessment of reliability helps compare the performance of the system concerning the limit values of indices required by regulatory agencies. On the one hand, this type of assessment helps identify those parts of the network that most need improvements. On the other hand, predictive evaluation aims to estimate future performance, as well as the impact of expansion actions on the PDS reliability; further, predictive evaluation can also support the decision-making process on expansion investments in short- and long-term planning horizons (BILLINTON; ALLAN, 1992).

The specialized literature exhibits many studies addressing the reliability of large PDS, of which the most relevant are discussed in what follows. In (TABARES *et al.*, 2019), a reduction in the computational time needed to analytically evaluate the reliability was obtained through an algebraic formulation in which a system of linear equations is solved. The author of (SPERANDIO, 2008) analytically assessed reliability indices using graph theory and historical data of interruptions of a real distribution network. Besides, in this work, the planning of automation of switches of the primary distribution network was defined through an optimization model. A method based on the fault incidence matrix (FIM) was introduced by (WANG *et al.*, 2018) for the analytical estimation of the reliability of PDS. Although the method proposed in (WANG *et al.*, 2018) can be used to analyze the sensitivity of reliability indices aiming to reduce the computational load, it has not been

yet applied to real or large systems.

The reliability of PDS was assessed through an analytical method with formulation of matrices in (DIAS, 2002). This method is based on the parts of the distribution network between protection and/or sectionalizing devices, which can be called *zones*. Subsequently, a method for reliability assessment, based on the Logically-Structured Matrix (MLE), was proposed by ABAIDE (2005). Variations of this method, using the MLE, were used in (NETO, 2006), (SPERANDIO, 2008), and (DAZA, 2010). As a contribution to the MLE, RODIGHERI (2013) included temporary faults, and in (SOUSA, 2018), a non-sequential Monte Carlo simulation method was used with the MLE, to insert uncertainties in the reliability assessment.

A more recent paper presented an extension of the FIM along with mathematical expressions to quantify the impact of some factors that affect reliability (ZHANG *et al.*, 2020). This study was applied to a real system, showing its potential to contribute to reliability improvements. There is a concern with the assessment of the reliability of large systems, which is explained by the difficulties with the modeling and numerical complexity of such assessment. In addition, modeling of additional resources related to network reconfiguration becomes necessary so as not to overestimate the reliability, which can introduce more computational difficulties. Although the methods proposed by (TABARES *et al.*, 2019; WANG *et al.*, 2018) are suitable for reducing the computational load required for reliability assessment, both works disregarded the impact that expansion projects can have on reliability.

The problem of planning the expansion of PDS with a focus on improvements in reliability is usually treated as an optimization problem, in which the reliability is considered through a multi-objective function or a weighted single-objective function (LI *et al.*, 2017). Besides, the optimization problem considers expansion projects, which are defined by decision variables, such as the number and optimal location of protection and/or sectionalizing devices (GEORGILAKIS *et al.*, 2021; RESENER *et al.*, 2018). In this context, optimization models solved both through exact (JOOSHAKI *et al.*, 2022; TABARES *et al.*, 2022) methods and also approximate (HAMIDAN; BOROUSAN, 2022)

methods are found in the literature; these, however, are predominant over exact methods.

The computational complexity of an optimization problem generally depends on the size of PDS being considered and the number of variables. Therefore, finding solutions to the problem with a reasonable computational load depends strongly on the dimension of the system. Large real systems can have no feasible solution, or the computational time to find feasible solutions may be too long, so that the use of optimization methods when planning the expansion of networks can become unpractical.

In some studies, reliability is assessed using solutions found for optimization problems used for planning the expansion of PDS. In (HEIDARI; FOTUHI-FIRUZABAD, 2016), a method was presented which includes the assessment of reliability in studies of planning the expansion of PDS. The proposed method was applied to evaluate the reliability using the solution found for the multistage optimization model proposed in (HEIDARI; FOTUHI-FIRUZABAD; KAZEMI, 2015). In yet another study, the authors developed a mixed integer linear programming (MILP) model to be applied to multistage expansion planning of PDS (LOTERO; CONTRERAS, 2011). Further, multiple solutions were obtained considering the multistage planning horizon and the estimated reliability was used to compare solutions.

Although on the one hand, the solution of optimization models indicating the best expansion plan may be useful to decide, on the other hand, network diagnosis allows the identification of critical points of the network and thus helps prioritize given expansion projects. Furthermore, the models described in (HEIDARI; FOTUHI-FIRUZABAD; KAZEMI, 2015; HEIDARI; FOTUHI-FIRUZABAD, 2016; LOTERO; CONTRERAS, 2011) cannot be applied to analyze the impacts of expansion projects on reliability, such as the installation of successive sectionalizing switches.

In addition to studies that propose (i) the assessment of reliability in optimization models for planning the expansion of PDS, and (ii) the evaluation of the reliability related to the optimal solutions found for network expansion, studies are also found in the literature that analyzes the sensitivity of reliability indices as well as the impact that the expansion projects can have on the reliability. In (DIAS, 2002), a method for evaluating the impact

of expansion projects on reliability was described and subsequently applied to a real distribution network. In (ZHANG *et al.*, 2020), an analytical reliability assessment method was proposed that helps identify those factors that most impact reliability, such as failure rates, switching and repair times, among others. However, (DIAS, 2002; ZHANG *et al.*, 2020) uses a failure rate given per length unity and equally distributed along the entire feeder which can misrepresent critical zones of the network that could otherwise be prioritized regarding expansion and/or maintenance actions.

In order to compare works correlated to the proposed method, it was decided to separate them into groups, as shown in Table 1. In the first column, the references and the proposed method are indicated. Each group has works that apply reliability assessment in expansion planning of PDS. Group 1 focuses on the insertion of reliability assessment in optimization models. Group 2 focuses on contributions to reliability assessment methods, which allow historical assessment of the network. Finally, group 3 focuses on proposing methods to assess the impact of expansion projects on reliability.

Table 1 – Comparison of the proposed method with the main correlated works.

Works	**Groups**		
	1	**2**	**3**
DIAS (2002)			✓
LOTERO; CONTRERAS (2011)	✓		
HEIDARI; FOTUHI-FIRUZABAD (2016)	✓		
WANG *et al.* (2018)		✓	
ZHANG *et al.* (2019)	✓		
TABARES *et al.* (2019)		✓	
ZHANG *et al.* (2020)			✓
Proposed Method			✓

Among the works of group 1 (see Table 1), ZHANG *et al.* (2019) integrates reliability into the optimization process. On the other hand, in LOTERO; CONTRERAS (2011) and HEIDARI; FOTUHI-FIRUZABAD (2016), the reliability is evaluated for the optimization solutions. In group 2, improvements in reliability assessment processes are proposed, as well as in TABARES *et al.* (2019), which aimed to reduce the computational time to analytically assess reliability; and in WANG *et al.* (2018), that the reliability assessment

served to verify critical points of the network through sensitivity analyzes of reliability and network parameters.

In group 3, DIAS (2002) and ZHANG *et al.* (2020) proposed methods that apply reliability assessment to estimate the impact of possible expansion projects to be carried out on reliability. These works also focus on helping to prioritize expansion projects by assessing critical points in the network, as done by WANG *et al.* (2018) (group 2). Finally, this thesis fits into group 3, as it proposes a strategy for including reliability assessment in the expansion planning of PDS, as well as helping to prioritize expansion projects in the investment stage.

3 PROPOSED FRAMEWORK

This chapter is excerpted, modified, and reproduced with permission, from the following papers that I co-authored:

- **Aschidamini, G.L.**; da Cruz, G.A.; Resener, M.; Leborgne, R.C.; Pereira, L.A. A Framework for Reliability Assessment in Expansion Planning of Power Distribution Systems. Energies 2022, 15. doi:10.3390/en15145073.

- **Aschidamini, G.L.**; da Cruz, G.A.; Almeida, L.C.; Garcia, J.D.D.; Resener, M.; Leborgne. R.C.; Pereira, L.A. Ferramenta Computacional para o Planejamento da Expansão de Redes de Distribuição Considerando Confiabilidade [Software for Power Distribution System Expansion Planning Considering Reliability], XXIV Congresso Brasileiro de Automática [XXIV Brazilian Congress of Automatics], Fortaleza, CE, Brazil, Oct. 16–19, 2022. [in Portuguese].

Sections of this chapter have been adapted from the above papers to fit the scope and formatting of the thesis.

This chapter presents in detail the proposed framework for incorporating reliability criteria in the expansion planning of power distribution systems. The developed framework uses a proposed method for analytical assessment of reliability to provide an estimate of reliability indices without and with expansion projects on the grid. The flowchart of the framework is shown in Figure 2.

Figure 2 – Flowchart of the proposed framework.

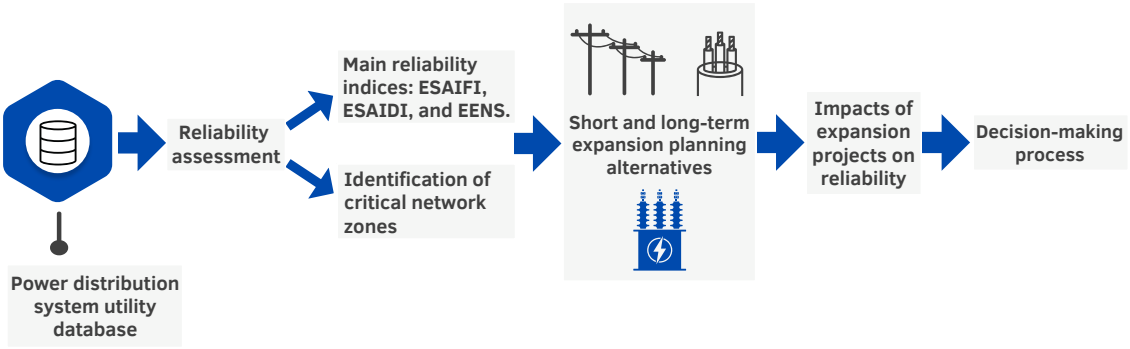

Source: ASCHIDAMINI *et al.* (2022b).

Initially, the information in the power distribution utility database is obtained and used in the process of reliability assessment. As a result, reliability indices concerning the primary level of the distribution network are assessed, such as ESAIFI, ESAIDI, and EENS. Additional data resulting from the assessment of reliability allow the identification of critical network zones of the grid, thus helping the user of the framework to indicate possible alternatives for projects to expand the distribution network. Finally, the framework allows assessing the impact of the expansion projects indicated by the user on reliability, assisting in the decision-making process of the projects to be carried out.

3.1 Input Parameters: Data of the Power Distribution Utility

Due to the reliability requirements imposed by regulatory agencies, power distribution utilities usually keep a database with interruptions data, which is part of outage management systems (OMS) implemented to enhance the quality of services. This database usually contains information about each interruption, such as:

- distribution level affected by each interruption (primary or secondary distribution network);
- date and time at which the interruption was notified;
- date and time of the fault location;
- restoration date and time for each affected transformer;
- number of affected customers;

- interruption type (scheduled or unscheduled).

Power distribution utilities usually have the model of existing distribution feeders in a format compatible with commercial tools used for power flow analysis. Thus, during planning stages involving potential expansion projects, the network can be simulated to assess the impact of each project. In addition, feeders can also be modeled using graphs that indicate the structure of the network and the location of protection and/or sectionalizing devices (SPERANDIO, 2008).

Databases of power distribution utilities can also include the location of transformers, the number of consumers connected to the primary and secondary network, and the energy consumption of each consumer. Further, the model of the distribution network becomes useful in studies concerning power quality, as well as operation and expansion planning. Therefore, the reliability is assessed using the network model, as presented in what follows.

3.2 Reliability Estimation without Expansion Projects

For comparison and decision-making, it is essential to determine reliability indices of the existing network, considering the situation in which some expansion plans are executed as well as the case that no expansion plan is executed. Thus, this and the next sections describe how the reliability indices can be estimated in both situations. Accordingly, the flowchart in Figure 3 details how the reliability indices are estimated under the assumption that no expansion projects are effectively implemented.

Initially, according to Process 1a in Figure 3, interruptions that (i) occurred unscheduled, (ii) lasted longer than 3 minutes (sustained interruptions), and (iii) originated from the primary distribution network are extracted from the database of the power utility.

In Process 2a, the historical average reliability indices of the primary distribution network ($SAIFI_h$ and $SAIDI_h$) are calculated based on the historical interruptions obtained in Process 1a. The historical average restoration time (${t_R}^h$) and the historical average fault location time (${t_l}^h$) are also calculated. In addition, the distribution network is modeled as will be described in Section 3.4. Furthermore, based on (i) the topology of the feeders, (ii) the type of protection and/or sectionalizing devices, (iii) the history of

Figure 3 – Flowchart of reliability assessment assuming no expansion of the distribution network.

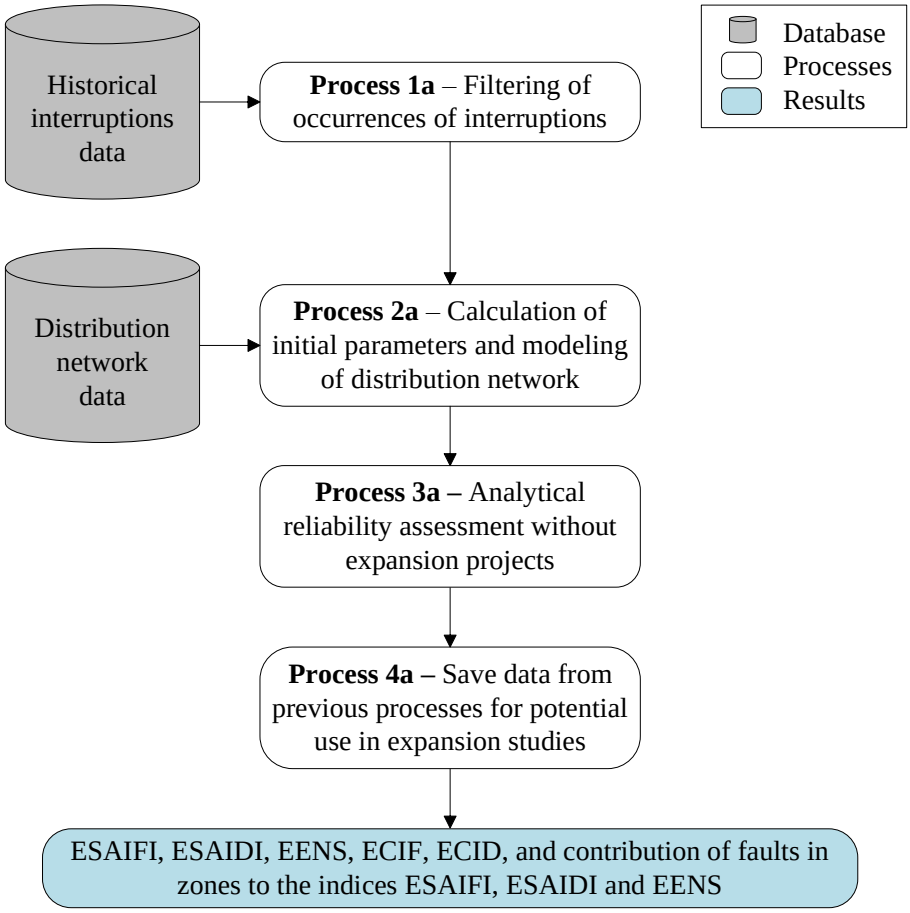

Source: ASCHIDAMINI *et al.* (2022b).

occurrences of interruptions, and (iv) the reported re-connections actions, it is possible to identify those zones of the network where the historical faults occurred, and thus determine the historical failure rate of each zone i ($\lambda_i{}^h$) in failures per year. Finally, the network length of each zone i (l_i) in km is also calculated.

On the other hand, Process 3a assesses the reliability analytically, as will be detailed in Section 3.5. Finally, in Process 4a, data from previous processes are saved for potential use in expansion studies.

3.3 Reliability Estimation Considering Expansion Projects

The procedure described here refers to the reliability indices of the distribution network considering the execution of expansion projects, which are indicated by the user of the

framework as investments during the planning stages. The flowchart in Figure 4 details the procedure proposed to estimate the reliability under the assumption made.

Figure 4 – Flowchart for the estimation of reliability considering expansion projects.

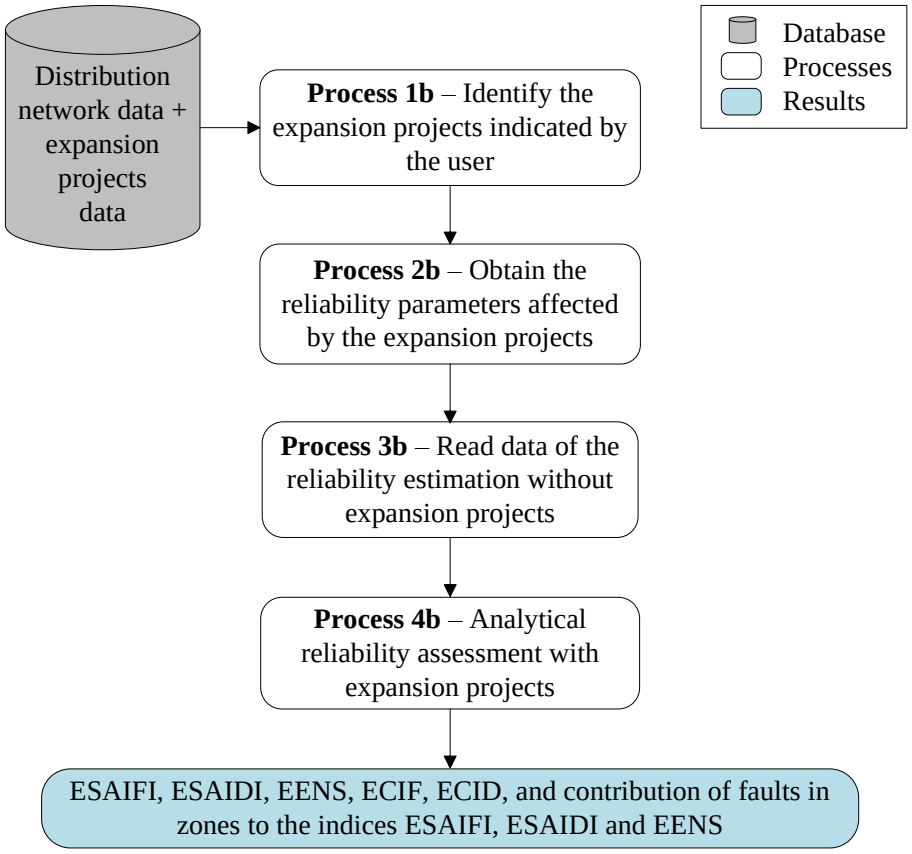

Source: ASCHIDAMINI *et al.* (2022b).

Initially, in Process 1b, the proposed framework identifies the expansion project indicated by the user. In Process 2b, new reliability parameters are estimated according to the expansion project defined. Subsequently, in Process 3b, the indices concerning the reliability without expansion projects are read. Finally, Process 4b assesses the reliability related to the expansion project analytically, as will be described in Section 3.6; this process uses the parameters calculated by Process 2b and the data from Process 3b, as will be detailed in Section 3.5.

3.4 Model of the Distribution Network

Based on the example feeder illustrated in Figure 5, the model of the primary distribution network developed for the proposed framework is detailed here. This elementary

feeder is composed of $n = 4$ zones. In addition, the feeder has two NC switches (NC-1 and NC-2), a NO switch with interconnection to another feeder (NO-3), and a fuse (FUS). Zone 1 in Figure 5 refers to the zone downstream of the circuit breaker at the substation (SS). The other zones refer to those network parts between the protection and/or sectionalizing devices.

Figure 5 – Feeder used as example to derive the model of the network.

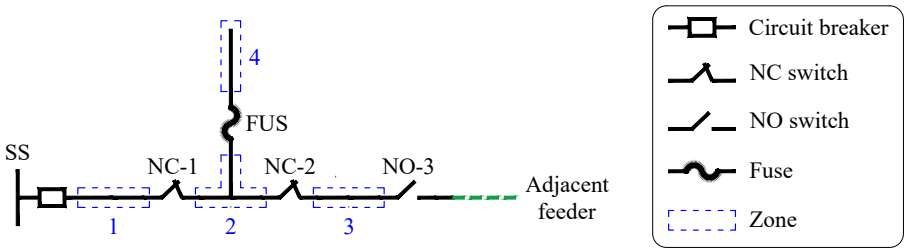

Source: Adapted from ASCHIDAMINI *et al.* (2022b).

A radial distribution feeder can be represented through an oriented graph with the origin vertex belonging to the substation (SPERANDIO, 2008); further, in each edge the direction of the current coincides with the orientation of the edge. A graph G can be defined as a pair of sets $G = (V, E)$, with the elements of V being the vertices (or nodes) and the elements of E being the edges (or arcs), which are also the connections between pairs of vertices (DIESTEL, 2017). Thus, the set of edges E is composed of ordered pairs of V. Furthermore, the first vertex of each pair is the beginning of the edge, and the second the end. In addition, when every edge of a graph starts at the first vertex and ends at the second vertex of the pair, thus defining an orientation, the graph is called oriented, digraph, or directed.

According to the definitions above, the oriented graph that represents the example feeder is shown in Figure 6. The vertices represent the feeder zones, and the edges the protection and/or sectionalizing devices. The oriented graph G is represented through a vector containing all vertices, $V = [1, 2, 3, 4]$, along with an ordered pair of vertices, $E = \{(1, 2), (2, 3), (2, 4)\}$.

The set of NO switches is represented by two vectors (NO_s and NO_e), which, respectively, indicate the start and end zones. In the case of NO switches with connection

Figure 6 – Oriented graph of the example feeder.

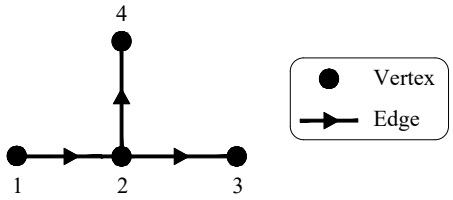

Source: ASCHIDAMINI *et al.* (2022b).

to another feeder, the end vertex is indicated as "0". The example feeder has one NO switch (NO-3), thus resulting in $NO_s = [3]$ and $NO_e = [0]$.

An oriented graph can be represented by the adjacency matrix ($\mathbf{A}$), which in turn can be obtained through V and the ordered pair of vertices E. The matrix $\mathbf{A}$ of a graph with n vertices is binary, has a dimension of $n \times n$, and is denoted as $\mathbf{A} = (a_{ij})_{n \times n}$. Matrix $\mathbf{A}$ contains $a_{ij} = 1$ when an edge exists between the vertices i and j, otherwise $a_{ij} = 0$. For the example feeder (Figure 5), the following adjacency matrix can be determined:

$$\mathbf{A} = \begin{array}{c} \begin{matrix} 1 & 2 & 3 & 4 \end{matrix} \\ \begin{bmatrix} 0 & 1 & 0 & 0 \\ 0 & 0 & 1 & 1 \\ 0 & 0 & 0 & 0 \\ 0 & 0 & 0 & 0 \end{bmatrix} \end{array} \begin{matrix} 1 \\ 2 \\ 3 \\ 4 \end{matrix} \tag{3.1}$$

In contrast, the reachability matrix ($\mathbf{R}$) can be obtained by summing the adjacency matrix ($\mathbf{A}$) with the identity matrix of the same dimension ($\mathbf{I}$) and subsequently raising the result to the exponent $(n-1)$, thus resulting in $\mathbf{R} = (\mathbf{I} + \mathbf{A})^{n-1}$. Further, to obtain a binary matrix, all non-null elements of $\mathbf{R}$ must be made equal to the unity. Consequently, $\mathbf{R}$ indicates all those vertices that a given vertex can reach by traversing the edges of the oriented graph. For the example feeder (Figure 5), the following reachability matrix can be determined:

$$\mathbf{R} = \begin{array}{c} \begin{matrix} 1 & 2 & 3 & 4 \end{matrix} \\ \begin{bmatrix} 1 & 1 & 1 & 1 \\ 0 & 1 & 1 & 1 \\ 0 & 0 & 1 & 0 \\ 0 & 0 & 0 & 1 \end{bmatrix} \end{array} \begin{matrix} 1 \\ 2 \\ 3 \\ 4 \end{matrix} \tag{3.2}$$

To determine the downstream vertices of a given vertex, it is first necessary to evaluate the row of $\mathbf{R}$ where the vertex is located. No-null values (unity) off the main diagonal indicate vertices downstream of the analyzed vertex. For example, the elements in blue

in line 2 indicate that vertices 3 and 4 are downstream of vertex 2. On the other hand, to obtain the vertices upstream from a given vertex to the substation, it is necessary to evaluate the column of the vertex being analyzed. Values equal to unity located off the main diagonal indicate vertices upstream. For example, the elements in green in column 2 indicate that vertex 1 is upstream of vertex 2. Therefore, analyzing $\mathbf{R}$ one can identify the effects on the feeder produced by a fault in each zone, thus allowing algorithms to classify the feeder zones, as will be discussed in Section 3.5.

3.5 Analytical Assessment of Reliability

The proposed method to assess the reliability of primary distribution systems considers that (i) no simultaneous faults occur, (ii) only permanent faults are taken into consideration, and (iii) the current capacity of conductors and switches is not exceeded.

The analytical assessment of reliability is based on the classification of the zones regarding their capacity for restoration after a permanent fault in the distribution feeder. In this way, when a fault occurs in each zone, the zones of the feeder are subsequently classified as follows.

- *Unaffected Zone* (N): when the fault of a given zone does not interrupt the analyzed zone;
- *Recoverable Zone* (R): when the fault of a zone interrupts the analyzed zone, but it is still possible to restore its supply through switching and re-connections within the same feeder;
- *Unrecoverable Zone* (I): when the fault of a zone interrupts the analyzed zone with no possible restoration until the fault is fixed;
- *Transferable Zone* (T): when the fault of a given zone interrupts the supply of the analyzed zone, but it remains possible to restore its supply by transferring the load to another feeder.

Now, using the matrix $\mathbf{R}$ and the classification described above, a matrix of classification can be defined, which will be termed Zone Classification Matrix (ZCM) and whose

lines and columns of ZCM represent the zones of the feeder (Note that the lines represent the zones with fault). The matrix ZCM corresponding to the example feeder is given by (3.3). According to (3.3), the interruption of zone 3 interrupts all remaining zones of the feeders. However, the electricity supply of zones 1, 2 and 4 can be restored after opening a sectionalizing device located upstream of zone 3.

$$ZCM = \begin{array}{c} \begin{matrix} 1 & 2 & 3 & 4 \end{matrix} \\ \begin{bmatrix} \text{I} & \text{T} & \text{T} & \text{T} \\ \text{R} & \text{I} & \text{T} & \text{I} \\ \text{R} & \text{R} & \text{I} & \text{R} \\ \text{N} & \text{N} & \text{N} & \text{I} \end{bmatrix} \end{array} \begin{matrix} 1 \\ 2 \\ 3 \\ 4 \end{matrix} \tag{3.3}$$

From the matrix ZCM, it is also possible to obtain additional matrices with a similar structure which can be used to calculate reliability indices too, as proposed by (DIAS, 2002). These additional matrices are called Interruptions Quantity Matrix (IQM), Consumers Weighted Interruptions Quantity Matrix (CWIQM), Interruptions Duration Matrix (IDM), Consumers Weighted Interruptions Duration Matrix (CWIDM), and Consumption Weighted Interruption Matrix (CWIM).

To obtain the interruption frequency indices, first, the matrix IQM, which indicates the probability of permanent faults, is built according to the classification of the zones of the feeder contained in the matrix ZCM. Those zones classified as N are null in the matrix IQM, as the supply is not interrupted in these zones. In contrast, the failure rate (in failures per year) of the zone under fault (λ_i) is assigned to those zones classified as R, T, or I.

In addition, through the matrix IQM, it is possible to obtain the expected value of index CIF of the consumers in each zone j ($ECIF_j$), expressed in interruptions per year. The $ECIF_j$ is defined as the sum of the elements of each column of the matrix IQM as:

$$ECIF_j = \sum_{i=1}^{n} IQM(i,j) \ , \tag{3.4}$$

$$ECIF_j = \sum_{i=1}^{n} \lambda_i \ . \tag{3.5}$$

Each element of matrix CWIQM contains the number of customers affected by in-

terruptions in a year. The matrix CWIQM is obtained by multiplying IQM, element by element, with the respective number of consumers in the zone j (N_j). The expected value of SAIFI ($ESAIFI$), in interruptions per year, is obtained as the quotient of the sum of all elements of CWIQM and the total number of consumers (TC) according to:

$$ESAIFI = \sum_{i=1}^{n} \sum_{j=1}^{n} \frac{CWIQM(i,j)}{TC} \ , \tag{3.6}$$

$$ESAIFI = \sum_{i=1}^{n} \sum_{j=1}^{n} \frac{\lambda_i N_j}{TC} \ . \tag{3.7}$$

In contrast, the contribution of faults in zone i to the $ESAIFI$ ($cSAIFI_i$), in interruptions per year, is determined by the quotient of the sum of the elements of each line of CWIQM and TC:

$$cSAIFI_i = \sum_{j=1}^{n} \frac{CWIQM(i,j)}{TC} \ , \tag{3.8}$$

$$cSAIFI_i = \sum_{j=1}^{n} \frac{\lambda_i N_j}{TC} \ . \tag{3.9}$$

The interruption duration indices are calculated based on the average restoration time (t_{res}), and on the following parameters: (i) average fault location time (t_l), (ii) average manual switching time (t_{sw}), and (iii) average time to repair (t_r), all expressed in hours. Additionally, the percentage of ${t_l}^h$ in relation to ${t_R}^h$ (p_l) is included in the reliability assessment as follows:

$$p_l = \frac{{t_l}^h}{{t_R}^h} \ . \tag{3.10}$$

Through the parameter p_l, it is possible to insert t_l into the reliability assessment, which is based on historical data of the occurrences of interruptions. In general, an urban feeder has a lower average time to locate a fault than a rural feeder. Therefore, to consider this fact, t_l, in hours, is calculated as a proportion p_l of t_{res} as:

$$t_l = t_{res} p_l \ . \tag{3.11}$$

The time t_{sw} as well as t_r, expressed in hours, are determined using the repair time in

percentage (p_r) of the difference between t_{res} and t_l:

$$t_{sw} = (t_{res} - t_l)(1 - p_r) \ , \tag{3.12}$$

$$t_r = (t_{res} - t_l)p_r \ , \tag{3.13}$$

with p_r being empirically assigned, due to the unavailability of data related to switching and repair time in the historical data of occurrences of interruptions.

To determine the parameter p_r based on data from the history of interruptions, it would be necessary to identify the average time required for manual switching, which may be not a trivial task due to the maneuver of several switches from fault location to restoration of energy supply to all customers. Furthermore, to determine a historical average failure repair time, it would be necessary to identify the beginning and end of the failure repair process.

The average restoration time of each zone depends on their classification in the matrix ZCM and on the protection or switching situation (A, B, C or D), as indicated in Table 2.

Table 2 – Restoration time according to zone classification and protection or switching situation.

Zone	**Restoration Time $t_{res}(i,j)$**			
classification	**A**	**B**	**C**	**D**
N	0	-	-	-
R	-	$t_l + t_{sw}$	-	$t_l + (3 \cdot t_{sw})$
T	-	-	$t_l + (2 \cdot t_{sw})$	$t_l + (3 \cdot t_{sw})$
I	$t_l + t_r$	$t_l + t_{sw} + t_r$	$t_l + (2 \cdot t_{sw}) + t_r$	$t_l + (3 \cdot t_{sw}) + t_r$

Situation A (Table 2) refers only to the blowing of a fuse. Therefore, the restoration times apply only to those zones classified as N and I. In this case, the restoration time of a zone classified as N is null, and the restoration time of zone I is given by the sum of t_l and t_r, as shown in Table 2.

Situation B refers to the opening of the nearest NC switch upstream of the faulted zone. Therefore, the restoration times apply only to zones classified as R and I. In this case, the restoration time of zone R is given by the sum of t_l and t_{sw}. On the other hand, the

restoration time of zone I is given by the sum of t_l, t_{sw} and t_r.

Situation C refers to the opening of the nearest NC switch downstream of the faulted zone and the closing of a NO switch with interconnection to an adjacent feeder. Therefore, the restoration times apply to zones T and I. In this case, the restoration time of zones T is given as the sum of t_l and $2 \cdot t_{sw}$, and the restoration time of zone I is obtained from the sum of t_l, $2 \cdot t_{sw}$, and t_r.

Finally, situation D refers to (i) the opening of the nearest NC switch upstream of the faulted zone, (ii) the opening of an additional NC switch that isolates the fault, and (iii) the closing of a NO switch. Therefore, the restoration times apply to zones R, T, and I. In this case, the restoration time of zones R and T is given as the sum of t_l and $3 \cdot t_{sw}$. On the other hand, the restoration time of zone I is obtained from the sum of t_l, $3 \cdot t_{sw}$, and t_r.

Figure 7 shows zone 4 of the example feeder (Figure 5) under fault. Faults in zone 4 refer to the only occurrence of situation A for this feeder. In this case, the fuse FUS is considered to have blown, isolating the fault. Zone 4 is interrupted; however, the other zones are not affected.

Figure 7 – Situation A for the example feeder – zone 4 under fault.

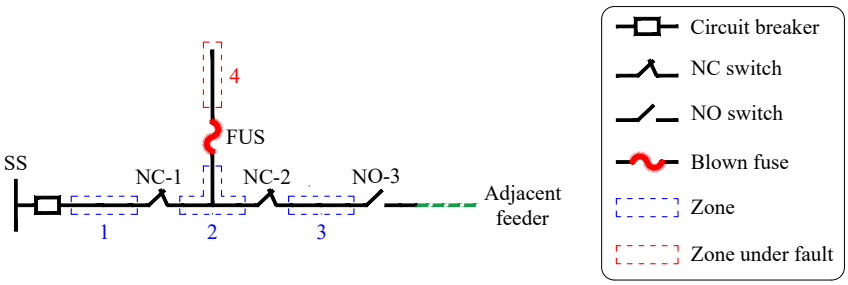

Source: Adapted from ASCHIDAMINI *et al.* (2022b).

Situation B occurs for the example feeder (Figure 5) when zone 3 is under fault, as shown in Figure 8. For a fault in this zone, zones 1, 2, and 4 can be restored after opening the switch NC-2.

Figure 8 – Situation B for the example feeder – zone 3 under fault.

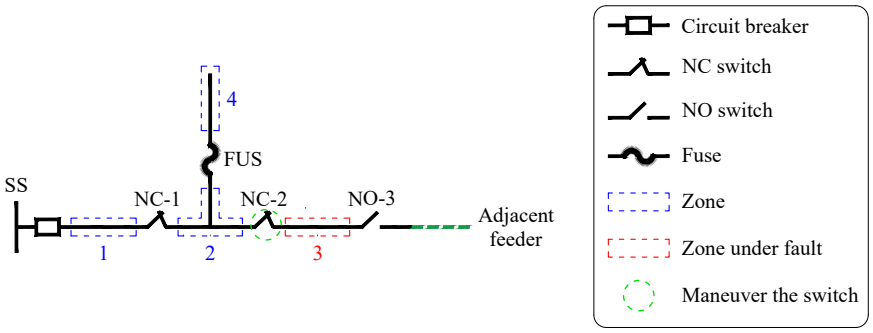

Source: Adapted from ASCHIDAMINI *et al.* (2022b).

Situation C occurs for faults in zone 1 (Figure 9). In this case, the switch NC-1 can be opened and the switch NO-3 can be closed to transfer zones 2–4 to the adjacent feeder.

Figure 9 – Situation C for the example feeder – zone 1 under fault.

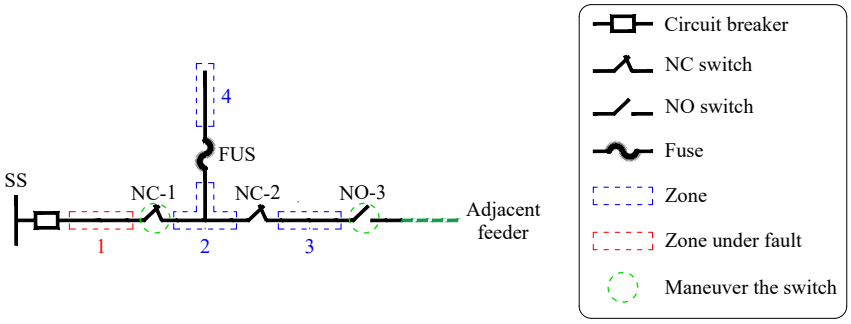

Source: Adapted from ASCHIDAMINI *et al.* (2022b).

Situation D occurs for the example feeder (Figure 5) when zone 2 is under fault. For a fault in zone 2 (Figure 10), the switch NC-1 can be opened to isolate the fault and restore the electricity supply to zone 1. Additionally, the switch NC-2 can be opened, and the switch NO-3 can be closed to transfer zone 3 to the adjacent feeder. The electricity supply can be restored to zones 2 and 4, only after the fault is repaired.

Figure 10 – Situation D for the example feeder – zone 2 under fault.

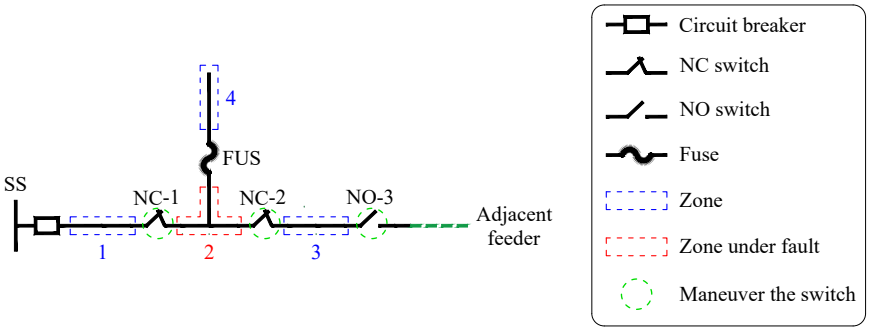

Source: Adapted from ASCHIDAMINI *et al.* (2022b).

The Interruption Duration Matrix (IDM), expressed in hours per year, is determined through the product between the restoration time of each zone and the failure rate of the failed zone (λ_i). The expected value of index CID, in hours per year, of the consumers in each zone j ($ECID_j$) is determined by the sum of each column of the matrix IDM as follows:

$$ECID_j = \sum_{i=1}^{n} IDM(i,j) \ , \tag{3.14}$$

$$ECID_j = \sum_{i=1}^{n} \lambda_i t_{res}(i,j) \ . \tag{3.15}$$

Now, the matrix CWIDM is obtained by multiplying the matrix IDM element by element with the respective number of consumers in the zone j (N_j). On the other hand, the expected value of SAIDI ($ESAIDI$), in hours per year, is obtained by the quotient of the sum of all elements of the matrix CWIDM and the corresponding TC:

$$ESAIDI = \sum_{i=1}^{n}\sum_{j=1}^{n} \frac{CWIDM(i,j)}{TC} \ , \tag{3.16}$$

$$ESAIDI = \sum_{i=1}^{n}\sum_{j=1}^{n} \frac{\lambda_i t_{res}(i,j) N_j}{TC} \ . \tag{3.17}$$

The contribution of faults in zone i to the $ESAIDI$ ($cSAIDI_i$), in hours per year, is determined by the quotient of the sum of the elements of each line of the matrix CWIDM and TC:

$$cSAIDI_i = \sum_{j=1}^{n} \frac{CWIDM(i,j)}{TC} \ , \tag{3.18}$$

or,

$$cSAIDI_i = \sum_{j=1}^{n} \frac{\lambda_i t_{res}(i,j) N_j}{TC} \ . \tag{3.19}$$

From the preceding expressions, the expected value of ASAI ($EASAI$), in pu, can be obtained using the $ESAIDI$:

$$EASAI = 1 - \frac{ESAIDI}{8760} \ . \tag{3.20}$$

The index EENS can be determined using the matrix CWIM. In turn, this matrix is determined by multiplying the matrix IDM element by element with the respective average annual consumption of the zone j, named C_j and expressed in MWh. Subsequently, the index EENS, in MWh per year, is obtained as the sum of all elements of CWIM as:

$$EENS = \sum_{i=1}^{n} \sum_{j=1}^{n} \frac{CWIM(i,j)}{8760} \ , \tag{3.21}$$

$$EENS = \sum_{i=1}^{n} \sum_{j=1}^{n} \frac{\lambda_i t_{res}(i,j) C_j}{8760} \ . \tag{3.22}$$

The contribution of faults in zone i to the index $EENS$ ($cEENS_i$), in MWh per year, is defined as the sum of the elements of each line of CWIM as follows:

$$cEENS_i = \sum_{j=1}^{n} \frac{CWIM(i,j)}{8760} \ , \tag{3.23}$$

or,

$$cEENS_i = \sum_{j=1}^{n} \frac{\lambda_i t_{res}(i,j) C_j}{8760} \ . \tag{3.24}$$

Finally, the expressions introduced and discussed in this section are used to estimate the reliability both with and without considering the execution of expansion projects. When no expansion projects are considered, the reliability indices correspond to the historical indices, as will be detailed in Section 3.5.2. In contrast, when expansion projects are considered, the indices reflect the impact of such projects on the reliability of the primary network, as will be described in Section 3.6.

3.5.1 Analytical Assessment of Reliability for the 3-Zone Example Feeder

In this section, the proposed method for the analytical assessment of reliability, which was formulated in Section 3.5, will be demonstrated in the 3-zone example feeder. The zone diagram of this feeder is shown in Figure 11, and has $n = 3$ zones, and the following devices: a circuit breaker, two NC switches (switches NC-1 and NC-2), and a remote controlled NO switch with interconnection to an adjacent feeder (switch NO-3).

Figure 11 – Zone diagram of the 3-zone example feeder.

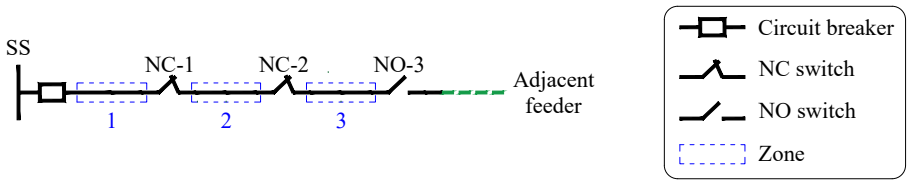

Source: Author.

To assess the reliability indices of the example distribution feeder (Figure 11) using the proposed method for the analytical assessment of reliability, values for the following reliability parameters must be assigned:

- λ_1, λ_2 and λ_3 (failure/year)
- l_1, l_2 and l_3 (km)
- N_1, N_2 and N_3 (customers)
- TC (customers)
- C_1, C_2 and C_3 (MWh/year)
- t_l, t_{sw}, and t_r (h)

The matrix ZCM of the example feeder from Figure 11, has a dimension of $n \times n$, and resulted in:

$$ZCM = \begin{array}{c} \begin{matrix} 1 & 2 & 3 \end{matrix} \\ \begin{bmatrix} \mathrm{I} & \mathrm{T} & \mathrm{T} \\ \mathrm{R} & \mathrm{I} & \mathrm{T} \\ \mathrm{R} & \mathrm{R} & \mathrm{I} \end{bmatrix} \end{array} \begin{matrix} 1 \\ 2 \\ 3 \end{matrix}. \tag{3.25}$$

In fault contingency, the network is reconfigured according to the protection or switching situations considered by the proposed method, therefore, the matrix ZCM was classified as follows:

- When a fault occurs inside zone 1, customers supplied in zones 2 and 3 can be transferred to another feeder by opening switch NC-1 and closing switch NO-3, consequently, these zones are classified as T.
- Given a fault in zone 2, zone 1 can have the electricity supply restored after opening switch NC-1, thus, this zone is classified as R. Additionally, zone 3 can be transferred to the adjacent feeder by opening the switch NC-2 and closing the switch NO-3, therefore, zone 3 is classified as T.
- When a fault occurs in zone 3, customers in zones 1 and 2 can be restored after opening switch NC-2. Consequently, zones 1 and 2 are classified as R.
- The zone under fault is always classified as I, as it is not possible to restore the electricity supply in this zone before the failure is repaired.

The other matrices used by the proposed method for assessing reliability indices have the same dimension as the matrix ZCM ($n \times n$) and are obtained as follows.

The matrix IQM of the example feeder resulted in:

$$IQM = \begin{matrix} \\ 1 \\ 2 \\ 3 \end{matrix} \begin{matrix} \begin{matrix} 1 & 2 & 3 \end{matrix} \\ \begin{bmatrix} \lambda_1 & \lambda_1 & \lambda_1 \\ \lambda_2 & \lambda_2 & \lambda_2 \\ \lambda_3 & \lambda_3 & \lambda_3 \end{bmatrix} \end{matrix} . \tag{3.26}$$

The $ECIF_j$, in interruptions per year, can be obtained by adding all the values of the rows on column j of this matrix. For example, the index $ECIF_1$ is equal to the sum of the values on the first column of the matrix IQM:

$$ECIF_1 = \lambda_1 + \lambda_2 + \lambda_3 \, . \tag{3.27}$$

The matrix CWIQM was obtained using the matrix IQM, resulting in:

$$CWIQM = \begin{matrix} \\ 1 \\ 2 \\ 3 \end{matrix} \begin{matrix} \begin{matrix} 1 & 2 & 3 \end{matrix} \\ \begin{bmatrix} \lambda_1 N_1 & \lambda_1 N_2 & \lambda_1 N_3 \\ \lambda_2 N_1 & \lambda_2 N_2 & \lambda_2 N_3 \\ \lambda_3 N_1 & \lambda_3 N_2 & \lambda_3 N_3 \end{bmatrix} \end{matrix} . \tag{3.28}$$

From the matrix CWIQM, the $ESAIFI$ can be calculated, in interruptions per year, which is equal to the sum of all the elements of this matrix, divided by the TC. Additionally, the values of fault contribution in zones to the $ESAIFI$ are also calculated by the matrix CWIQM. For example, the value of $cSAIFI_1$, in hours per year, is equal to the sum of the values in the first row of this matrix, divided by TC:

$$cSAIFI_1 = \frac{\lambda_1 N_1 + \lambda_1 N_2 + \lambda_1 N_3}{TC} \ . \tag{3.29}$$

The matrix IDM was obtained using the matrix IQM, and resulted in:

$$IDM = \begin{matrix} \\ 1 \\ 2 \\ 3 \end{matrix} \begin{matrix} \begin{matrix} 1 & \quad 2 & \quad 3 \end{matrix} \\ \begin{bmatrix} \lambda_1(t_l + t_{sw} + t_r) & \lambda_1(t_l + t_{sw}) & \lambda_1(t_l + t_{sw}) \\ \lambda_2(t_l + t_{sw} + t_{sw}) & \lambda_2(t_l + t_{sw} + t_{sw} + t_r) & \lambda_2(t_l + t_{sw} + t_{sw}) \\ \lambda_3(t_l + t_{sw}) & \lambda_3(t_l + t_{sw}) & \lambda_3(t_l + t_{sw} + t_r) \end{bmatrix} \end{matrix} \ . \tag{3.30}$$

The $ECID_j$, in hours per year, can be obtained by adding all the row values on column j of this matrix. For example, the index $ECID_1$ is equal to the sum of the values of the first column of the matrix IDM:

$$ECID_1 = \lambda_1(t_l + t_{sw} + t_r) + \lambda_2(t_l + t_{sw} + t_{sw}) + \lambda_3(t_l + t_{sw}) \ . \tag{3.31}$$

Subsequently, the matrix CWIDM can be obtained using the matrix IDM, as:

$$CWIDM = \begin{matrix} \\ 1 \\ 2 \\ 3 \end{matrix} \begin{matrix} \begin{matrix} 1 & \quad 2 & \quad 3 \end{matrix} \\ \begin{bmatrix} \lambda_1(t_l + t_{sw} + t_r)N_1 & \lambda_1(t_l + t_{sw})N_2 & \lambda_1(t_l + t_{sw})N_3 \\ \lambda_2(t_l + t_{sw} + t_{sw})N_1 & \lambda_2(t_l + t_{sw} + t_{sw} + t_r)N_2 & \lambda_2(t_l + t_{sw} + t_{sw})N_3 \\ \lambda_3(t_l + t_{sw})N_1 & \lambda_3(t_l + t_{sw})N_2 & \lambda_3(t_l + t_{sw} + t_r)N_3 \end{bmatrix} \end{matrix} \ . \tag{3.32}$$

From the matrix CWIDM, the $ESAIDI$, in hours per year, can be calculated by the sum of all the elements of this matrix, divided by TC. In addition, the values of fault contribution in zones to the $ESAIDI$ can also be calculated by the matrix CWIDM. For instance, the value of $cSAIDI_1$, in hours per year, is equal to the sum of the values in the

first row of this matrix, divided by TC:

$$cSAIDI_1 = \frac{\lambda_1(t_l + t_{sw} + t_r)N_1 + \lambda_1(t_l + t_{sw})N_2 + \lambda_1(t_l + t_{sw})N_3}{TC} \,. \tag{3.33}$$

The matrix CWIM resulted in:

$$CWIM = \begin{array}{c} \begin{matrix} \quad 1 \quad & \quad 2 \quad & \quad 3 \quad \end{matrix} \\ \left[\begin{array}{ccc} \lambda_1(t_l + t_{sw} + t_r)C_1 & \lambda_1(t_l + t_{sw})C_2 & \lambda_1(t_l + t_{sw})C_3 \\ \lambda_2(t_l + t_{sw} + t_{sw})C_1 & \lambda_2(t_l + t_{sw} + t_{sw} + t_r)C_2 & \lambda_2(t_l + t_{sw} + t_{sw})C_3 \\ \lambda_3(t_l + t_{sw})C_1 & \lambda_3(t_l + t_{sw})C_2 & \lambda_3(t_l + t_{sw} + t_r)C_3 \end{array}\right] \begin{matrix} 1 \\ 2 \\ 3 \end{matrix} \end{array} \tag{3.34}$$

From the matrix CWIM, the index $EENS$, in MWh per year, can be obtained by the sum of all the elements of this matrix, divided by 8760. The values of fault contribution in zones to the index $EENS$ can also be calculated by the matrix CWIM. For example, the value of $cEENS_1$, in MWh per year, is equal to the sum of the values in the first row of this matrix, divided by 8760:

$$cEENS_1 = \frac{\lambda_1(t_l + t_{sw} + t_r)C_1 + \lambda_1(t_l + t_{sw})C_2 + \lambda_1(t_l + t_{sw})C_3}{8760} \,. \tag{3.35}$$

The numerical results obtained by the analytical assessment of reliability for the 3-zone example feeder (Figure 11), considering the assignment of values for the reliability parameters, are available in Appendix A.

3.5.2 Adjustment of Estimated Reliability Indices to Historical Indices

To estimate the reliability without expansion projects, the initial failure rate per zone is calculated based on the historical interruptions. However, the database of the power distribution utility has data concerning the location of only part of the faults. Therefore, this information is assumed as unavailable. Consequently, the failure rate per zone is adjusted to the historical SAIFI ($SAIFI_h$) after determining its initial value. Note also that inserting a failure rate per zone based on actual data of interruptions will incorporate a geographic link to the origin of the fault (SPERANDIO, 2008). In addition, the failure rates per zone have different origins, such as winds, lightning, trees or vegetation, animals, material, or

equipment failure, etc. Thus, for example, the failure rates of zones containing vegetation must consider the presence of this vegetation as a possible cause of failure. Therefore, even with the uncertainties of the input data, the characteristics of the land/environment are weighted with the segmentation of failure rates per zone.

In this work, a procedure like that used to estimate the failure rate to estimate the restoration time is applied, which is also adjusted to the historical SAIDI ($SAIDI_h$) (DIAS, 2002). However, the initial restoration time is assigned before the algorithm begins and is not based on the history of interruptions.

The flowchart in Figure 12 illustrates all the procedures developed to adjust the estimated indices of reliability to their historical values.

Figure 12 – Flowchart for the analytical assessment of reliability.

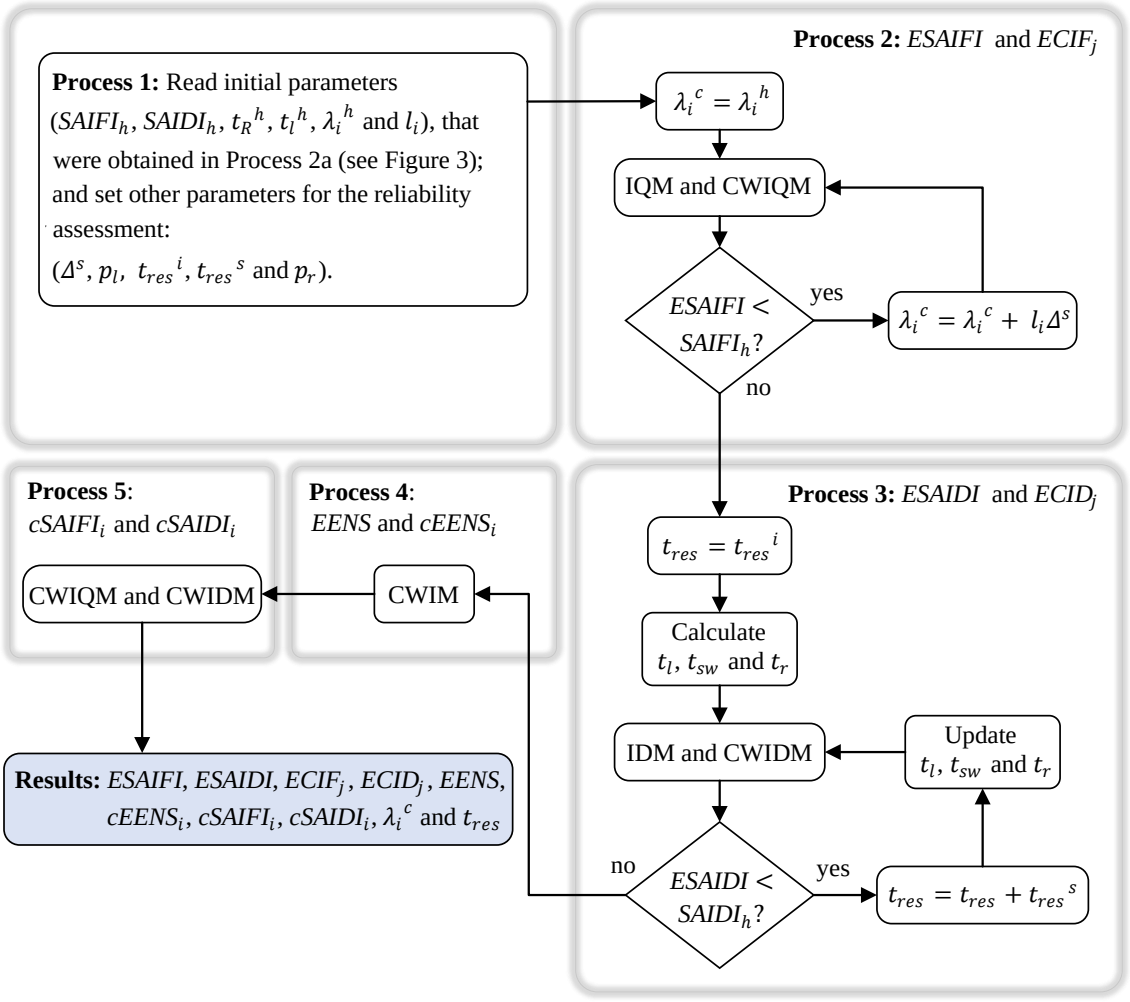

Source: ASCHIDAMINI *et al.* (2022b).

In Process 1 (Figure 12), the initial data obtained in Process 2a (Figure 3) are

read ($SAIFI_h$, $SAIDI_h$, ${t_R}^h$, ${t_l}^h$, ${\lambda_i}^h$ and l_i). In addition, values are assigned to the following parameters: (i) failure rate step per length (Δ^s), in failure/km · year; (ii) parameter p_l; (iii) initial restoration time (${t_{res}}^i$), in hours; (iv) step for t_{res} (${t_{res}}^s$), in hours; and (v) parameter p_r.

In Process 2, the algorithm first calculates the indices concerning the interruption frequency. This is an iterative process, in which the calculated failure rates per zone i (${\lambda_i}^c$) (failures per year) start with the values of ${\lambda_i}^h$; subsequently, after each iteration, a failure rate of $l_i\Delta^s$ in failures per year is added to ${\lambda_i}^c$, until $ESAIFI$ is adjusted to $SAIFI_h$. Finally, the indices $ECIF_j$ are generated through the matrix IQM.

Process 3 is dedicated to the estimation of indices related to the interruption duration. In this iterative process, t_{res} starts with the value of ${t_{res}}^i$, and subsequently t_l, t_{sw} and t_r are calculated. At each iteration, ${t_{res}}^s$ is added to t_{res}; subsequently, t_l, t_{sw} and t_r are updated. The process stops when $ESAIDI$ equals $SAIDI_h$, after which the indices $ECID_j$ are obtained from the matrix IDM.

The indices $EENS$ and $cEENS_i$ are calculated in Process 4 using the matrix CWIM. Finally, in Process 5, the indices $cSAIFI_i$ and $cSAIDI_i$ are calculated through the matrices CWIQM and CWIDM, respectively.

3.6 Assessment of the Impact of Expansion Projects on the Reliability of the Primary Network

After identifying the expansion projects indicated by the framework user and obtaining the reliability parameters affected by expansion projects, the process of analytical assessment of reliability with expansion projects (Process 4b in Figure 4) is performed. This process aims to assess the impact of projects indicated by the framework user on reliability, as will be detailed in this section.

In this process, the proposed method for analytical assessment of reliability in Section 3.5 is used to assess reliability indices considering the modified network. This process uses i) the reliability parameters affected by expansion projects; and ii) data obtained by the estimation of reliability without expansion projects. Furthermore, this section presents the

procedures to evaluate the impact on reliability parameters for each expansion alternative considered in this work.

Although the proposed framework allows the incorporation of different types of expansion projects, this thesis will formulate the impact of those alternatives of expansion that most affect reliability, namely (i) installation of NC sectionalizing switch; (ii) installation of NO switch with interconnection to an adjacent feeder; (iii) replacement of manual NC sectionalizing switches by remote controlled switches; and (iv) replacement of existing bare overhead conductors by covered conductors.

3.6.1 Installation of a NC Sectionalizing Switch

A distribution network can be segmented using sectionalizing devices, which allow fault isolation during contingency situations (XIE; ZHOU; BILLINTON, 2008). Installing a NC switch in a given zone x generates the new zones x_1 and x_2, and hence the number of customers in x_1 and x_2 must be calculated. Further, the failure rate of zone x (λ_x), the length of x (l_x), the length of x_1 (l_{x_1}) and the length of x_2 (l_{x_2}) are subsequently required to determine the failure rates of the new zones, λ_{x_1} and λ_{x_2}, as follows:

$$\lambda_{x_1} = \frac{\lambda_x}{l_x} l_{x_1} \ , \tag{3.36}$$

$$\lambda_{x_2} = \frac{\lambda_x}{l_x} l_{x_2} \ . \tag{3.37}$$

The number of customers in zones x_1 and x_2 (N_{x_1} and N_{x_2}) must also be obtained to calculate the $ESAIFI$ and $ESAIDI$. This process requires the installation of the NC sectionalizing switch in nodes of the distribution network, to calculate the number of customers per zone, considering the number of customers connected to each transformer. Furthermore, it is necessary to update the oriented graph that represents the distribution network, adding the edges that represent the zones generated by the segmentation of the original zone. Moreover, to calculate the index $EENS$, the average annual consumption of zones x_1 and x_2 (C_{x_1} and C_{x_2}) must be determined.

The values of contribution of faults in zones x_1 and x_2 to the $ESAIFI$, in interruptions

per year, can be calculated by (3.9), using the updated values of failure rates and number of customers for these zones. Subsequently, the $ESAIFI$, in interruptions per year, can be calculated by (3.7), using the values of contribution of faults in zones x_1 and x_2 to $ESAIFI$. The $ECIF_j$ can be obtained by (3.5), using the failure rate of these zones.

Values of contribution of faults in zones x_1 and x_2 to the $ESAIDI$, in hours per year, can be recalculated by (3.19), using the updated values of failure rates and number of customers. $ESAIDI$ in hours per year, can be calculated by (3.17) with the updated values of contribution of faults in zones to the $ESAIDI$. Additionally, the $ECID_j$ can be obtained by (3.15).

The values of fault contribution in zones x_1 and x_2 to the index $EENS$, in MWh per year, can be determined by (3.24), using the updated values of failure rates and average energy consumption per year. Finally, using the contribution values of faults in zones x_1 and x_2 to the index $EENS$, the index $EENS$ can be calculated by (3.22).

3.6.2 Installation of a NO Switch with Interconnection to an Adjacent Feeder

Normally open switches between adjacent feeders enable load transfer between feeders, while NO switches with vertices belonging to the same feeder enable restoration within the feeder (ZIDAN *et al.*, 2017). Thus, using this reconfiguration makes it possible to reduce the duration of interruptions for part of the feeder's consumers. According to the proposed framework, installing a NO switch requires updating the vectors that represent NO switches (NO_s and NO_e) by including the respective vertices at which they are installed.

Installing a NO switch may change the classification of zones in the matrix ZCM due to the possibility of restoring the electricity supply to further zones before failure repair occurs. Therefore, the matrix ZCM must be updated to evaluate possible improvements in switching conditions, as possibly more zones could be classified as R or T. For the evaluation of this expansion alternative, the matrices IDM, CWIDM and CWIM must also be updated.

The reliability indices $ECID_j$, $ESAIDI$ and $EENS$ must be calculated considering the modified network using (3.15), (3.17), and (3.22), respectively. Additionally, the contribution of faults in zones to the indices $ESAIDI$ and $EENS$ can be obtained by

(3.19) and (3.24), respectively.

3.6.3 Replacement of Manual Switches by Remote Controlled Switches

The replacement of manual sectionalizing switches by remote controlled ones allows faster switching when faults occur, thus enabling reduced duration of interruptions to part of consumers. Therefore, t_{sw} can be reduced due to the remote-controlled operation. In addition, t_l can be reduced if the fault location can be made easier when switches with protection functionality are used (CONTI *et al.*, 2014). To illustrate the reliability improvement provided by the replacement of existing manual switches by remote controlled switches, t_{sw} can be reduced to zero and t_l decreased in 70% for faults that occur in the first zone downstream of the automated switch (DIAS, 2002).

The impact of replacing an existing sectionalizing switch by a remote controlled one is modeled by changes in the values of average fault location time (t_l) and average manual switching time (t_{sw}) for faults in the first zone downstream of the automated switch. Consequently, the values of time to restore the electricity supply ($t_{res}(i,j)$) for these zones must be updated.

Initially, it is assumed that a NC sectionalizing switch upstream of a zone called x has been replaced by a remote controlled switch. As a result, the parameter $t_{res}(i,j)$ must be updated only for the zone x under fault. The value of $t_{res}(i,j)$ depends on the classification of the zone and the protection or switching situation, as detailed in Table 2. Therefore, this value must be updated with the following steps: i) identify in the matrix ZCM the protection or switching situation for the zone x under fault; ii) read the classification of each zone in the matrix ZCM (for the zone x under fault); and iii) update the value of $t_{res}(i,j)$ according to Table 2, considering the reduction in the values of t_l and t_{sw} from the remote controlled switch. Finally, from the updated parameter $t_{res}(i,j)$, the indices can be calculated using the expressions (3.15), (3.17), and (3.22).

3.6.4 Replacement of Existing Bare Overhead Conductors by Covered Conductors

The replacement of bare overhead conductors of MV feeders by covered conductors is an alternative to expansion plans aiming to improve reliability, since conductors with lower

failure rates can be installed. The adoption of covered conductors in overhead distribution lines may lead to reduced failure rates compared with bare conductors (LI; SU; SHEN, 2010). On the one hand, covered conductors have the advantage of reduced short-circuit currents when distribution lines come into contact, for example, with vegetation. On the other hand, when covered conductors are installed in places close to coast or regions with high air pollution, a phenomenon known as tracking may occur, deteriorating the reliability in mid- to long-term (ESPINO-CORTéS; RAMíREZ-VáZQUEZ; GóMEZ, 2014).

The installation of covered conductors can be carried out in different ways, which may require changing the design standard of the network, with the replacement of poles and other parts (PIHLER; TIčAR, 2005). The replacement of poles may be associated with increase of reliability since poles are critical to the structure of overhead distribution networks (FILHO, 2014). Furthermore, besides insulation type, cables have different characteristics, such as size, material, and impedance (BROWN, 2008).

To estimate and illustrate the impact of replacement of bare conductors by covered conductors, a reduction in the ${\lambda_i}^c$ for the zone i whose conductors have been replaced can be adopted, similar to what was assumed in (DIAS, 2002). Finally, given the replacement of the conductors of a zone called x, and therefore, a change in the failure rate of this zone, the indices can be calculated considering the change in the network using (3.5), (3.7), (3.15), (3.17), and (3.22).

3.6.5 Incorporation of Further Expansion Alternatives

The proposed method for analytical assessment of reliability described in Section 3.5 can be used to assess reliability indices, aiming to verify the impact of expansion alternatives other than the alternatives incorporated in this work. Each expansion alternative must be modeled through the respective modification that it imposes on the reliability parameters of the reliability estimate without expansion projects.

4 NUMERICAL RESULTS FOR A TEST SYSTEM

This chapter is excerpted, modified, and reproduced with permission, from the following paper that I co-authored:

- **Aschidamini, G.L.**; da Cruz, G.A.; Resener, M.; Leborgne, R.C.; Pereira, L.A. A Framework for Reliability Assessment in Expansion Planning of Power Distribution Systems. Energies 2022, 15. doi:10.3390/en15145073.

Sections of this chapter have been adapted from the above paper to fit the scope and formatting of the thesis.

In this chapter, the validation of the proposed framework using the Roy Billinton Test System (RBTS) will be presented (BILLINTON, 1996). Further, the algorithm shown in the flowchart of Figure 3 (Chapter 3) is implemented without considering a failure rate per zone based on the historical faults in each zone. This implementation was called correlated method and will serve the purpose of comparison with the proposed method. Both methods were implemented through algorithms in MatLab® (MATLAB, 2021).

4.1 Roy Billinton Test System

The RBTS consists of five load buses (bus2 – bus6) with different characteristics (BILLINTON, 1996). The distribution network at bus 5 of the RBTS has typical urban loads, such as residences, offices, and commercial buildings, among others. This network also consists of four 11 kV feeders (F1–F4), 43 sections, and 26 load-points (LP), as illustrated in Figure 13. In addition, this network has 8 circuit breakers, 13 NC sectionalizing

switches, and 2 NO switches. The number and the type of consumers, the average and peak loads at each LP, along with the length of each section of the network are available in (BILLINTON, 1996). Thus, due to the characteristics described, the distribution network at bus 5 of the RBTS was chosen to test and validate the proposed method. Additional data for this case study are available in Appendix B.

Figure 13 – Distribution network at bus 5 of the RBTS.

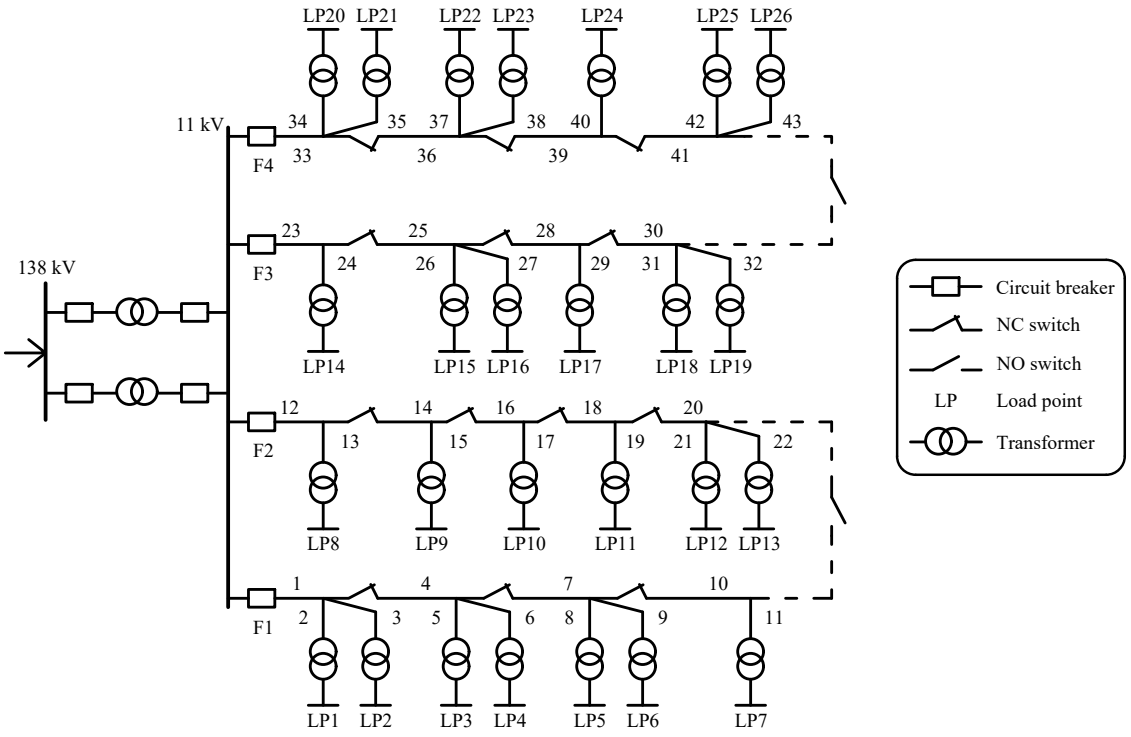

Source: (BILLINTON, 1996).

The zone diagram of the distribution network at bus 5 of the RBTS was obtained from the distribution network in Figure 13, as illustrated in Figure 14. The feeders F1, F3, and F4 have 4 zones and 3 NC sectionalizing switches, while the feeder F2 has 5 zones and 4 NC sectionalizing switches.

Figure 14 – Zone diagram of the distribution network at bus 5 of the RBTS.

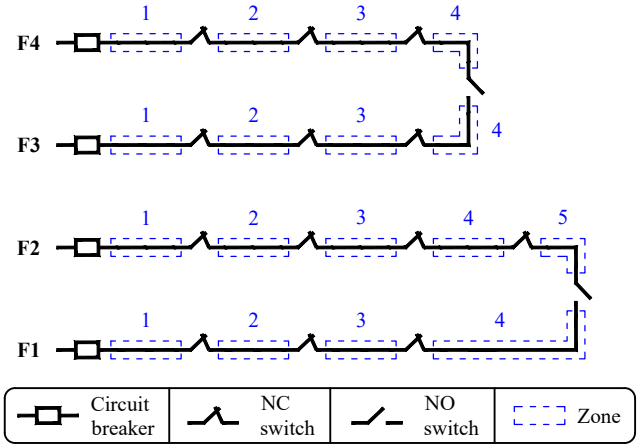

Source: ASCHIDAMINI *et al.* (2022b).

The oriented graphs representing the zone diagram of the power distribution feeders at bus 5 of the RBTS (Figure 14) are illustrated in Figure 15. The zones and sectionalizing switches of the zone diagram are respectively represented by the vertices and edges of the graphs. Therefore, the feeders F1, F3 and F4 have 4 vertices and 3 edges, while feeder F2 has 5 vertices and 4 edges.

Figure 15 – Oriented graphs of the power distribution feeders at bus 5 of the RBTS.

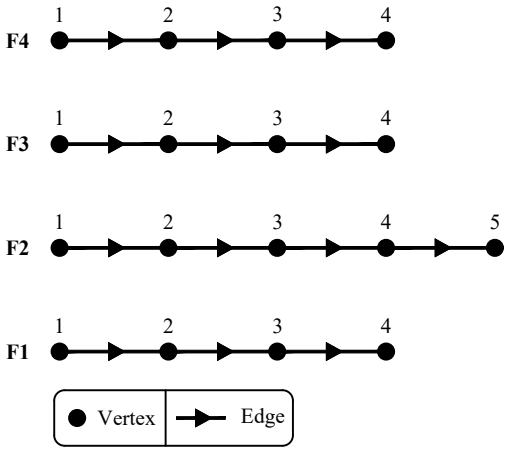

Source: ASCHIDAMINI *et al.* (2022b).

The matrix ZCM for feeders F1, F3, and F4 at bus 5 of the RBTS has a dimension of

4×4, and is presented in:

$$ZCM = \begin{array}{c} \begin{matrix} 1 & 2 & 3 & 4 \end{matrix} \\ \left[\begin{array}{cccc} \mathrm{I} & \mathrm{T} & \mathrm{T} & \mathrm{T} \\ \mathrm{R} & \mathrm{I} & \mathrm{T} & \mathrm{T} \\ \mathrm{R} & \mathrm{R} & \mathrm{I} & \mathrm{T} \\ \mathrm{R} & \mathrm{R} & \mathrm{R} & \mathrm{I} \end{array}\right] \begin{matrix} 1 \\ 2 \\ 3 \\ 4 \end{matrix} \end{array}; \tag{4.1}$$

on the other hand, the matrix ZCM for the feeder F2 at bus 5 of the RBTS has a dimension of 5×5, and is shown in:

$$ZCM = \begin{array}{c} \begin{matrix} 1 & 2 & 3 & 4 & 5 \end{matrix} \\ \left[\begin{array}{ccccc} \mathrm{I} & \mathrm{T} & \mathrm{T} & \mathrm{T} & \mathrm{T} \\ \mathrm{R} & \mathrm{I} & \mathrm{T} & \mathrm{T} & \mathrm{T} \\ \mathrm{R} & \mathrm{R} & \mathrm{I} & \mathrm{T} & \mathrm{T} \\ \mathrm{R} & \mathrm{R} & \mathrm{R} & \mathrm{I} & \mathrm{T} \\ \mathrm{R} & \mathrm{R} & \mathrm{R} & \mathrm{R} & \mathrm{I} \end{array}\right] \begin{matrix} 1 \\ 2 \\ 3 \\ 4 \\ 4 \end{matrix} \end{array}. \tag{4.2}$$

The reconfiguration of the network in situations of contingency of faults for the feeders at bus 5 of the RBTS is used for the classification of the zones in the matrix ZCM, being this detailed in what follows: i) after the occurrence of an interruption and location of the fault, the closest NC switch upstream of the fault is opened to isolate the fault; ii) the electricity supply to the zones upstream of the fault is restored by re-energizing the feeder through closing of the CB; iii) additionally, the NC switch closest downstream of the fault is opened and the NO switch at the end of the feeder is closed to transfer the zones downstream of this NC switch to the adjacent feeder.

Given the post-fault reconfiguration considered, it is possible to observe that given a fault in a zone in the primary network at bus 5 of the RBTS, only the customers of this zone need to wait until the fault repair time with the subsequent re-energizing the feeder to restore electricity supply.

The matrices IQM, CWIQM, IDM, CWIDM, and CWIM, obtained for the analytical assessment of reliability for the feeders at bus 5 of the RBTS, are available in Appendix B.

Given that no historical data are available for RBTS, for this case study, the implemented algorithm assigns historical values for reliability indices, fault location and repair times, and failure rates for each zone. Thus, the indices given in (BILLINTON, 1996)

were considered the historical values of the RBTS. Hence, 0.2325 interruptions/year and 3.5512 h/year were assigned to $SAIFI_h$ and $SAIDI_h$, respectively. Additionally, due to the lack of historical data on fault location and restoration times for the RBTS, the parameters ${t_l}^h$ and ${t_R}^h$ could not be estimated. Therefore, approximately $60\ \%$ to p_l was assigned. Besides, the historical failure rates shown in Table 3 were used. In addition, the following parameters were adopted in the implemented algorithm: $\Delta^s = 10^{-6}$ failure/km·year, ${t_{res}}^i = 17$ h, ${t_{res}}^s = 10^{-4}$ h, and $p_r = 70\,\%$.

Table 3 – Historical failure rates per zone.

	Zone	**1**	**2**	**3**	**4**	**5**
	F1	0.01	0.01	0.01	0.01	–
${\lambda_i}^h$	F2	0.01	0.01	**0.04**	**0.04**	**0.04**
(failure/year)	F3	0.01	0.01	0.01	0.01	–
	F4	0.01	0.01	0.01	0.01	–

4.2 Estimation of Reliability without Expansion Projects

The reliability indices estimated without expansion projects resulted in 0.2325 interruptions/year for $ESAIFI$ and 3.5512 h/year for $ESAIDI$. For comparison, together with those indices obtained through the correlated and proposed methods, Table 4 also contains the reliability indices obtained in (BILLINTON, 1996). Thus, according to Table 4, the $ESAIFI$ and $ESAIDI$ obtained with both methods proposed here correspond to those presented in (BILLINTON, 1996), as expected. This similarity is because the algorithm adjusts $ESAIFI$ and $ESAIDI$ to the values assigned to $SAIFI_h$ and $SAIDI_h$, which proves that both methods (correlated and proposed) converge to the same values. As a further consequence, the $EASAI$ values obtained by the correlated and the proposed methods are the same as those reported by (BILLINTON, 1996).

Table 4 – Reliability indices for the distribution network at bus 5 of the RBTS.

	Ref. (BILLINTON, 1996)	**Correlated Method**	**Proposed Method**
$ESAIFI$ (int./year)	0.2325	0.2325	0.2325
$ESAIDI$ (h/year)	3.5512	3.5512	3.5512
$EASAI$ (%)	99.9595	99.9595	99.9595
$EENS$ (MWh/year)	40.1194	39.6696	38.4903

As can be observed in Table 4, the values of $EENS$ obtained with the correlated and proposed methods are slightly different from that given in (BILLINTON, 1996). This difference arises because, when reliability indices are estimated, both algorithms adjust the failure rate of each zone and repair times based on $SAIFI_h$ and $SAIDI_h$. In contrast, in (BILLINTON, 1996), failure rates and repair times per load node are calculated based on failure rates and repair times for individual components such as transformers, circuit breakers, buses, and lines (ALLAN *et al.*, 1991). The way that each method determines failure rates and repair times changes those indices that are assessed for each load node ($ECIF$ and $ECID$). Consequently, the estimated values for the index $EENS$ are also different for each method.

Concerning the interruption times, $t_{res} = 17.93\,\text{h}$, $t_l = 10.76\,\text{h}$, $t_{sw} = 2.15\,\text{h}$, and $t_r = 5.02\,\text{h}$ were approximately obtained by the correlated and proposed methods. The failure rates per zone, in failures per year, obtained through the proposed method can be seen in Table 5, according to which zones 3, 4, and 5 of feeder F2 (in bold) have the highest failure rates compared to the rates of the remaining zones[1].

Table 5 – Failure rate per zone obtained through the proposed method.

	Zone	**1**	**2**	**3**	**4**	**5**
	F1	0.0587	0.0553	0.0518	0.0471	–
$\lambda_i{}^c$	F2	0.0367	0.0367	**0.0736**	**0.0667**	**0.0853**
(failure/year)	F3	0.0471	0.0483	0.0436	0.0553	–
	F4	0.0553	0.0553	0.0367	0.0587	–

The failure rates per zone in failures per year obtained through the correlated method are given in Table 6. Compared with the failures of other zones, the failure rates of zone 1 of feeder F1 and those of zone 4 of feeder F4 are the highest, which can be in part explained by the fact that these zones are 2.1 km long and, therefore, are the longest, as also indicated in (BILLINTON, 1996).

[1]Note also that these zones coincide with the zones that have the highest historical failure rates (highlighted in Table 3).

Table 6 – Failure rate per zone obtained through the correlated method.

	Zone	**1**	**2**	**3**	**4**	**5**
	F1	**0.0686**	0.0637	0.0588	0.0523	–
$\lambda_i{}^c$	F2	0.0376	0.0376	0.0474	0.0376	0.0637
(failure/year)	F3	0.0523	0.0539	0.0474	0.0637	–
	F4	0.0637	0.0637	0.0376	**0.0686**	–

The results in Tables 5 and 6 also highlight that each method indicates a different zone with highest failure rates. This is because the proposed method considers the historical faults of each zone and, subsequently, distributes the failure rates according to the length of each zone. On the other hand, the correlated method only distributes the failure rates according to the length of each zone.

The expected value of index CIF in each zone j, in interruptions per year, obtained through the proposed method is presented in Table 7. The highest expected values for index CIF were found in zones of the feeder F2, as can be observed by the values highlighted.

Table 7 – Expected value of index CIF per zone obtained through the proposed method.

	Zone	**1**	**2**	**3**	**4**	**5**
	F1	0.2129	0.2129	0.2129	0.2129	–
$ECIF_j$	F2	**0.2990**	**0.2990**	**0.2990**	**0.2990**	**0.2990**
(int./year)	F3	0.1943	0.1943	0.1943	0.1943	–
	F4	0.2059	0.2059	0.2059	0.2059	–

On the other hand, the expected value of index CIF in each zone j, in interruptions per year, obtained through the correlated method, is given in Table 8, according to which the zones of the feeder F1 (in bold) have the highest values for this index.

Table 8 – Expected value of index CIF in each zone obtained through the correlated method.

	Zone	**1**	**2**	**3**	**4**	**5**
	F1	**0.2434**	**0.2434**	**0.2434**	**0.2434**	–
$ECIF_j$	F2	0.2238	0.2238	0.2238	0.2238	0.2238
(int./year)	F3	0.2173	0.2173	0.2173	0.2173	–
	F4	0.2336	0.2336	0.2336	0.2336	–

In a comparison between the Tables 7 and 8, it is shown that the proposed and correlated methods obtained different values for the $ECIF_j$. This is a consequence of the different values of failure rates per zone obtained by both methods. Furthermore, the highest expected values for the index CIF obtained by both methods is different; in the proposed method, 0.2990 interruptions/year were obtained for consumers connected to feeder F2, while in the correlated method, 0.2434 interruptions/year was obtained for consumers of feeder F1. It is worth noting that the proposed method uses historical failure rates, and that higher failure rates were assigned in zones of feeder F2, as can be seen by the values in bold in Table 3.

The expected value of index CID in each zone, in hours per year, obtained through the proposed method is shown in Table 9. Zone 5 of the feeder F2 (in bold) presents the highest expected value for the index CID.

Table 9 – Expected value of index CID in each zone obtained through the proposed method.

	Zone	**1**	**2**	**3**	**4**	**5**
	F1	3.2733	3.2559	3.2384	3.2151	–
$ECID_j$	F2	4.4245	4.4245	4.6100	4.5751	**4.6683**
(h/year)	F3	2.9430	2.9488	2.9255	2.9837	–
	F4	3.1335	3.1335	3.0403	3.1510	–

On the other hand, the expected value of index CID in each zone, in hours per year, obtained through the correlated method can be seen in Table 10. Zone 1 of the feeder F1 (in bold) shows the highest value for this index.

Table 10 – Expected value of index CID in each zone obtained through the correlated method.

	Zone	**1**	**2**	**3**	**4**	**5**
	F1	**3.7593**	3.7346	3.7099	3.6771	–
$ECID_j$	F2	3.3494	3.3494	3.3987	3.3494	3.4809
(h/year)	F3	3.2930	3.3013	3.2684	3.3506	–
	F4	3.5620	3.5620	3.4304	3.5866	–

The proposed and correlated method obtained different expected values for the index CID, as can be observed by comparing the values presented in Table 9 and Table 10. This

difference was expected, due to the differences in the determination of failure rates cited above. Furthermore, Table 9 reveals that higher values were obtained for the expected value of index CID in zones of the feeder F2 when the reliability was assessed using the proposed method.

Table 11 reproduces the contribution of faults in each zone to the indices $ESAIFI$, $ESAIDI$, and $EENS$ obtained through the proposed method. The values in bold indicate the zones in which the faults most contribute to $ESAIFI$ and $ESAIDI$ (zone 5 of feeder F2), as well as the zone in which the faults most contribute to $EENS$ (zone 2 of feeder F1).

Table 11 – Contribution of faults in zones to the reliability indices obtained using the proposed method.

	Zone	**1**	**2**	**3**	**4**	**5**
	F1	0.0188	0.0177	0.0166	0.0151	–
$cSAIFI_i$	F2	0.0100	0.0100	0.0202	0.0182	**0.0233**
(int./year)	F3	0.0045	0.0046	0.0042	0.0053	–
	F4	0.0171	0.0171	0.0114	0.0182	–
	F1	0.2866	0.2904	0.2721	0.1965	–
$cSAIDI_i$	F2	0.1297	0.1638	0.3287	0.2977	**0.3305**
(h/year)	F3	0.0594	0.0899	0.0629	0.0697	–
	F4	0.2619	0.2595	0.1723	0.2799	–
	F1	2.7889	**3.0736**	2.8799	2.1327	–
$cEENS_i$	F2	1.1989	1.3237	2.6572	2.4061	2.8182
(MWh/year)	F3	1.6888	2.0961	1.8572	2.0849	–
	F4	2.4014	2.8120	1.7521	2.5186	–

The contribution of faults in each zone to the indices $ESAIFI$, $ESAIDI$, and $EENS$ obtained through the correlated method are presented in Table 12. The values in bold refer to zones that most contributes to $ESAIFI$ (zone 1 of feeder F1), $ESAIDI$ (zone 1 and 2 of feeder F1), and $EENS$ (zone 2 of feeder F1).

A comparison between the values in bold in Tables 11 and 12 reveals that concerning the highest contributions to $ESAIFI$ and $ESAIDI$, each method indicates a different zone, as the proposed method indicates zone 5 of feeder F2 whereas the correlated method, zones 1 and 2 of feeder F1.

Table 12 – Contribution of faults in zones to the reliability indices obtained using the correlated method.

	Zone	**1**	**2**	**3**	**4**	**5**
	F1	**0.0220**	0.0204	0.0189	0.0168	–
$cSAIFI_i$	F2	0.0103	0.0103	0.0130	0.0103	0.0174
(int./year)	F3	0.0050	0.0051	0.0045	0.0061	–
	F4	0.0198	0.0198	0.0116	0.0213	–
	F1	**0.3356**	**0.3356**	0.3098	0.2184	–
$cSAIDI_i$	F2	0.1331	0.1681	0.2120	0.1681	0.2476
(h/year)	F3	0.0660	0.1006	0.0684	0.0805	–
	F4	0.3027	0.3000	0.1768	0.3278	–
	F1	3.2658	**3.5526**	3.2793	2.3712	–
$cEENS_i$	F2	1.2308	1.3589	1.7134	1.3589	2.1111
(MWh/year)	F3	1.8777	2.3456	2.0205	2.4099	–
	F4	2.7756	3.2503	1.7987	2.9493	–

From the results discussed above, the contribution of faults in zones to reliability indices can help planners to find out and decide which expansion project is more advantageous in terms of reliability improvement. The comparison above also stresses the relevance of the fault history to the estimation of reliability, as it can directly affect the choice of the zone to execute a given expansion project, thus highlighting an advantage of the proposed method over the correlated method.

The reliability indices calculated assuming that no expansion projects are executed help estimate the impact of expansion alternatives on reliability, as these indices are used for sensitivity analysis of parameters related to the zones affected by expansion projects. Thus, the data required to estimate reliability indices without projects are stored and used later to assess the impact of expansion projects on reliability.

4.3 Estimation of Reliability Considering Expansion Projects

The prioritization of the execution of expansion alternatives considers the reliability indices estimated without projects. Note that expansion projects are indicated by the user of the framework; furthermore, the results of the estimation without projects help the designer to select the best expansion alternatives among those possible. Besides, the

fault contributions in zones to $ESAIDI$ will be used to guide the manual sectionalizing switches to be replaced by remote controlled switches. On the other hand, the contribution of faults within zones to $ESAIFI$ will be used afterward to guide the replacement of bare overhead conductors by covered conductors.

4.3.1 Replacement of Manual Switches by Remote Controlled Switches

In what follows, the replacement of manual NC sectionalizing switches by remote controlled switches is shown by replacing the switch upstream of zone 5 of feeder F2, as this zone has the highest fault contribution to $ESAIDI$ without expansion projects. The replacement of this switch reduced the contribution of faults in zone 5 of feeder F2 to $ESAIDI$ from 0.3305 to 0.1046 h/year and the contribution to $EENS$ from 2.8182 to 0.9292 MWh/year. As a result, the interruption duration indices and $EENS$ were also impacted, as shown in Table 13. The $ESAIDI$ decreased $6.36\,\%$ and $EENS$ $4.91\,\%$, whereas $EASAI$ increased. In contrast, the $ESAIFI$ remained unchanged, as the replacement of manual switches by remote controlled switches does not change the frequency of interruptions.

Table 13 – Impact of replacement of manual switches by remote controlled switches on reliability indices.

	Case without Expansion Projects	**Case with Switch Replaced**	**Reduction (%)**
$ESAIFI$ (int./year)	0.2325	0.2325	0
$ESAIDI$ (h/year)	3.5512	3.3254	6.36
$EASAI$ (%)	99.9595	99.9620	–
$EENS$ (MWh/year)	38.4903	36.6013	4.91

Concerning the indices evaluated by load node, the expected value of index CIF of the zones was not affected by the remote controlled switch installed, as expected. However, considering the proposed expansion project, the expected value of index CID for the zones of feeder F2 decreased. The expected value of index CID of zone 5 of feeder F2, which has the highest value without expansion projects, decreased from 4.6683 to 3.8429 h/year.

To evaluate the impact of the replacement of further switches by remote controlled

ones, simulations were carried out considering that each of the NC sectionalizing switches of distribution network at bus-5 of the RBTS (Figure 14) is replaced. The simulations aim to validate the prioritization of replacement of manual switches by remote controlled switches for the upstream switches of the zones with the highest values of contribution of faults to the $ESAIDI$.

The results of the impact of replacement of manual switches by remote controlled switches on the indices $ESAIDI$ and $EENS$ are shown in Table 14. Replaced switches are identified by their downstream zone and the feeder to which it belongs.

Table 14 – Impact of replacement of manual NC sectionalizing switches by remote controlled switches on the reliability of the distribution network at bus 5 of the RBTS.

Feeder	**Zone Downstream of the Replaced Switch**	$ESAIDI$ (h/year)	$EENS$ (MWh/year)
F1	2	3.3796	36.7001
	3	3.3904	36.8129
	4	3.4048	36.9633
F2	2	3.4540	37.6774
	3	3.3561	36.8584
	4	3.3746	37.0126
	5	**3.3254**	**36.6013**
F3	2	3.5066	37.2668
	3	3.5109	37.3844
	4	3.5001	37.0904
F4	2	3.3854	36.8668
	3	3.4411	37.4123
	4	3.3749	36.7646

The replacement of the upstream switch of zone 5 of the feeder F2 by a remote controlled switch resulted in a more significant reduction for the values of the indices $ESAIDI$ and $EENS$, which resulted in respectively 3.3254 h/year and 36.6013 MWh/year (values highlighted in Table 14). The replacement of the other manual NC sectionalizing switches by remote controlled switches resulted in higher values for the indices $ESAIDI$ and $EENS$, compared to the switch that had its replacement by remote controlled one prioritized. Therefore, it can be verified that prioritizing the replacement of manual switches based on the zones with the highest values of contribution of faults to the $ESAIDI$, can

help in the definition of alternatives for replacement of switches to be evaluated during the planning stage.

4.3.2 Replacement of Existing Bare Overhead Conductors by Covered Conductors

Initially, the replacement of bare conductors of zone 5 of feeder F2 by covered conductors is shown, given that the fault contribution to $ESAIFI$ of this zone is the highest of the distribution network (Table 11). The execution of this expansion project reduces the failure rate for this zone from 0.0853 to 0.0427 failure/year, which is due to the assumed reduction of 50 % in the failure rate of the zone with conductors replaced. As a result, the contribution of faults in zone 5 of feeder F2 to $ESAIFI$ reduced from 0.0233 to 0.0117 interruptions/year, the contribution to $ESAIDI$ reduced from 0.3305 to 0.1652 h/year, while the contribution to $EENS$ reduced from 2.8182 to 1.4091 MWh/year. Furthermore, other reliability indices also changed, as shown in Table 15. The $ESAIFI$ reduced by 5.03 %, while $ESAIDI$ by 4.65 %, and $EENS$ by 3.66 %; in contrast, the $EASAI$ increased.

Table 15 – Impact of replacement of bare overhead conductors of zone 5 of the feeder F2 by covered conductors on reliability indices.

	Case without Expansion Projects	**Case with Replacement of Conductors**	**Reduction (%)**
$ESAIFI$ (int./year)	0.2325	0.2208	5.03
$ESAIDI$ (h/year)	3.5512	3.3860	4.65
$EASAI$ (%)	99.9595	99.9614	–
$EENS$ (MWh/year)	38.4903	37.0812	3.66

Given that the feeder has a circuit breaker at the beginning, the proposed replacement of bare overhead conductors impacted only those reliability indices evaluated by load nodes of feeder F2 ($ECIF$ and $ECID$). Thus, the expected value of index CIF decreased from 0.2990 to 0.2563 interruptions/year and the index CID of all zones of feeder F2 also decreased. The expected value of index CID of zone 5 of feeder F2, which was the highest for the distribution network for the case without expansion projects, decreased from 4.6683 to 3.9040 h/year. Note also that this expansion project will not affect the expected values

of CIF or CID of the other zones if a fuse upstream of a zone that has its bare conductors replaced by covered conductors is assumed, due to the characteristic of this device. In the event of a fault in this zone, the other zones will then be classified as N in the matrix ZCM.

The process of replacement of bare overhead conductors by covered conductors was performed for each zone of the distribution network at bus 5 of the RBTS to validate the prioritization of replacement of bare conductors in zones with the highest values of contribution of faults to the $ESAIFI$. The results of the impact of replacement of bare conductors by covered conductors for each of the zones in the indices $ESAIFI$, $ESAIDI$ and $EENS$ are shown in Table 16.

Table 16 – Impact of replacement of bare conductors by covered conductors of zones on the reliability of the distribution network at bus 5 of the RBTS.

Feeder	**Zone with Conductors Replaced**	$ESAIFI$ (int./year)	$ESAIDI$ (h/year)	$EENS$ (MWh/year)
F1	1	0.2231	3.4079	37.0958
	2	0.2236	3.4060	**36.9535**
	3	0.2242	3.4152	37.0503
	4	0.2249	3.4530	37.4239
F2	1	0.2275	3.4864	37.8908
	2	0.2275	3.4693	37.8284
	3	0.2224	3.3869	37.1616
	4	0.2234	3.4024	37.2872
	5	**0.2208**	**3.3860**	37.0812
F3	1	0.2303	3.5215	37.6458
	2	0.2302	3.5063	37.4422
	3	0.2304	3.5198	37.5617
	4	0.2299	3.5164	37.4478
F4	1	0.2239	3.4203	37.2896
	2	0.2239	3.4215	37.0842
	3	0.2268	3.4651	37.6142
	4	0.2234	3.4113	37.2309

The most significant reduction to the value of $ESAIFI$ comes from the replacement of conductors of zone 5 of feeder F2 by covered conductors, which resulted in 0.2208 interruptions/year (highlighted in Table 16). Additionally, the lowest value for $ESAIDI$ was found when the replacement of conductors was carried out in this same

zone, as it resulted in 3.3860 h/year. On the other hand, the lowest value for the index $EENS$ was obtained when the conductors of zone 2 of feeder F1 are replaced, which is the zone that has the highest value of contribution of faults to index $EENS$ for the estimation of reliability without expansion projects (Table 11). Therefore, it can be verified that the values of contribution of faults in zones to the indices can serve to guide the user of the framework in the definition of potential zones to be indicated for evaluation of the impact of replacement of bare conductors of MV feeders by covered conductors on reliability.

5 APPLICATION EXAMPLES

This chapter is excerpted, modified, and reproduced with permission, from the following papers that I co-authored:

- **Aschidamini, G.L.**; da Cruz, G.A.; Resener, M.; Leborgne, R.C.; Pereira, L.A. A Framework for Reliability Assessment in Expansion Planning of Power Distribution Systems. Energies 2022, 15. doi:10.3390/en15145073.

- **Aschidamini, G.L.**; da Cruz, G.A.; Almeida, L.C.; Garcia, J.D.D.; Resener, M.; Leborgne. R.C.; Pereira, L.A. Ferramenta Computacional para o Planejamento da Expansão de Redes de Distribuição Considerando Confiabilidade [Software for Power Distribution System Expansion Planning Considering Reliability], XXIV Congresso Brasileiro de Automática [XXIV Brazilian Congress of Automatics], Fortaleza, CE, Brazil, Oct. 16–19, 2022. [in Portuguese].

Sections of this chapter have been adapted from the above papers to fit the scope and formatting of the thesis.

In this chapter, the proposed framework is applied in case studies using data from real distribution networks and the history of interruptions. Two real case studies will be presented, one using a primary distribution feeder in Section 5.1; and another using a large-scale primary distribution network in Section 5.2. Finally, the framework was implemented through algorithms in MatLab® (MATLAB, 2021).

5.1 60-Zone Real Primary Distribution Feeder

A primary distribution feeder located in Southern Brazil was used to test the proposed method using initial failure rates by zone and the available historical data of interruptions. The topology of the 60-zone distribution feeder is shown in Figure 16. This feeder consists of a primary network operating at 23.1 kV and having bare overhead conductors with a total length of 49.86 km. Besides, the feeder has 10,947 customers connected at low voltage. Figure 17 shows the zone diagram of the feeder, which is composed of 60 zones and the following devices: 36 fuses, 23 manual NC sectionalizing switches, 6 manual NO switches connected to the same feeder, and a point to install a NO switch with interconnection to an adjacent feeder. Additional data and results for this case study are available in Appendix C.

Figure 16 – Topology of the 60-zone real primary distribution feeder.

Source: Author

Figure 17 – Zone diagram of the 60-zone real primary distribution feeder.

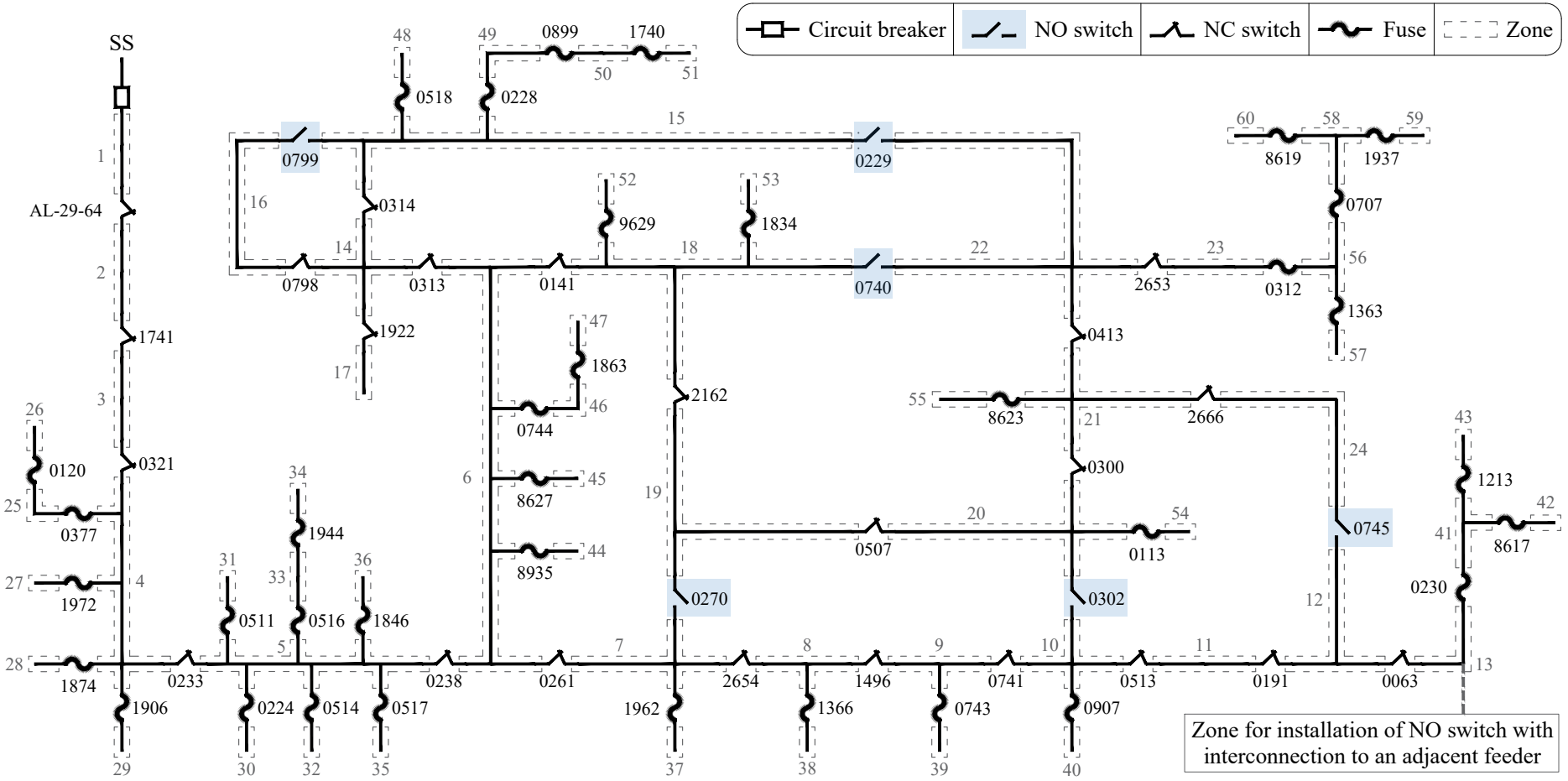

Source: ASCHIDAMINI *et al.* (2022b).

5.1.1 Estimation of Reliability without Expansion Projects

Initially, as described in Section 3.2, the data received from the power distribution utility and referring to the feeder were processed in order to generate a database. Based on the data of interruptions for a three-year period, the historical reliability indices were calculated, resulting in 19.66 interruptions/year for $SAIFI_h$ and 10.86 h/year for $SAIDI_h$. Similarly, ${t_R}^h = 2.86$ h and ${t_l}^h = 1.97$ h were obtained, thus leading to $p_l = 70\,\%$. In addition, the algorithm assumed $\Delta^s = 10^{-7}$ failure/km·year, ${t_{res}}^i = 0.3$ h, ${t_{res}}^s = 10^{-4}$ h, and $p_r = 70\,\%$. The computational performance of the numerical results obtained in this section will be presented in Section 5.3.

Table 17 shows reliability indices obtained through the correlated and proposed methods. According to this table, due to the adjustment of these indices to the values of $SAIFI_h$ and $SAIDI_h$, respectively, the $ESAIFI$ and $ESAIDI$ obtained by both methods converged to the same value. As a further consequence, the $EASAI$ for both methods is the same too. The difference between $ESAIFI$ and $SAIFI_h$ is related to the parameter Δ^s adopted, while the difference between $ESAIDI$ and $SAIDI_h$ to the parameter ${t_{res}}^s$ adopted. Increasing the values of parameters Δ^s and ${t_{res}}^s$ can reduce the computational load required for the simulation, but simultaneously reduce the accuracy of the estimations. From Table 17, a good agreement between the values obtained for the $EENS$ can be recognized.

Table 17 – Reliability indices obtained for a real distribution feeder.

	Correlated Method	**Proposed Method**
$ESAIFI$ (interruptions/year)	19.66	19.66
$ESAIDI$ (h/year)	10.86	10.86
$EASAI$ (%)	99.8760	99.8760
$EENS$ (MWh/year)	32.38	32.31

Using the proposed and the correlated method, $t_{res} = 0.63$ h, $t_l = 0.44$ h, $t_r = 0.13$ h and $t_{sw} = 0.06$ h were obtained for the times related to interruptions. Additionally, failure rates per zone, in failures per year, were also determined using both methods, with the corresponding values being available in Appendix C.

The six zones in which faults most contribute to the indices $ESAIFI$, $ESAIDI$, and $EENS$ are highlighted in orange in Figure 20. Additionally, the highest contributions

of faults in these zones to the indices $ESAIFI$, $ESAIDI$, and $EENS$ are shown in Figure 18. Faults in zone 4 contribute most to the indices $ESAIFI$, $ESAIDI$, and $EENS$; faults in zone 4 account for approximately 10 % of $ESAIFI$, and 12 % of $ESAIDI$ and $EENS$.

Figure 18 – Zones with the highest contribution of faults to the reliability indices obtained using the proposed method - 60-zone feeder.

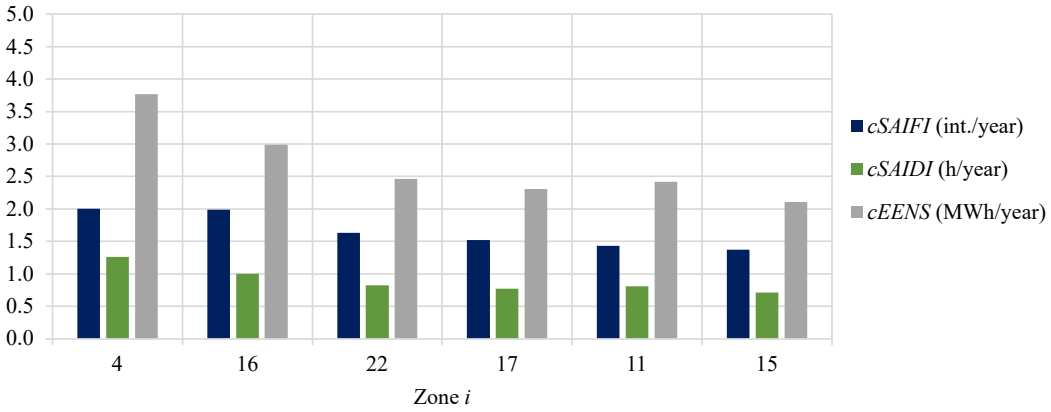

Source: ASCHIDAMINI *et al.* (2022b).

Figure 19 confirms that each method (correlated and proposed) indicates a different zone with the highest fault contribution to the indices $ESAIFI$, $ESAIDI$, and $EENS$. The correlated method estimates failure rates proportionally to the length of the zones and without considering the history of interruptions. Consequently, the zones with the highest values of fault contribution to the $ESAIFI$ correspond to the longest which, in addition, are not protected by a fuse, namely zone 4 (4.06 km), 16 (3.37 km), 17 (3.09 km), 15 (2.79 km), and 11 (2.24 km).

Figure 19 – Zones with the highest contribution of faults to the reliability indices obtained through the correlated method - 60-zone feeder.

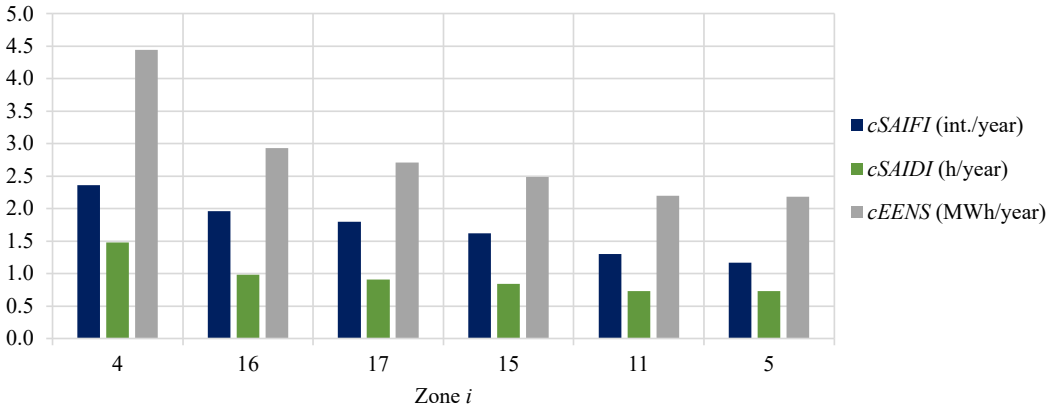

Source: ASCHIDAMINI *et al.* (2022b).

Figure 20 – Critical zones to the reliability indices for the 60-zone real primary distribution feeder.

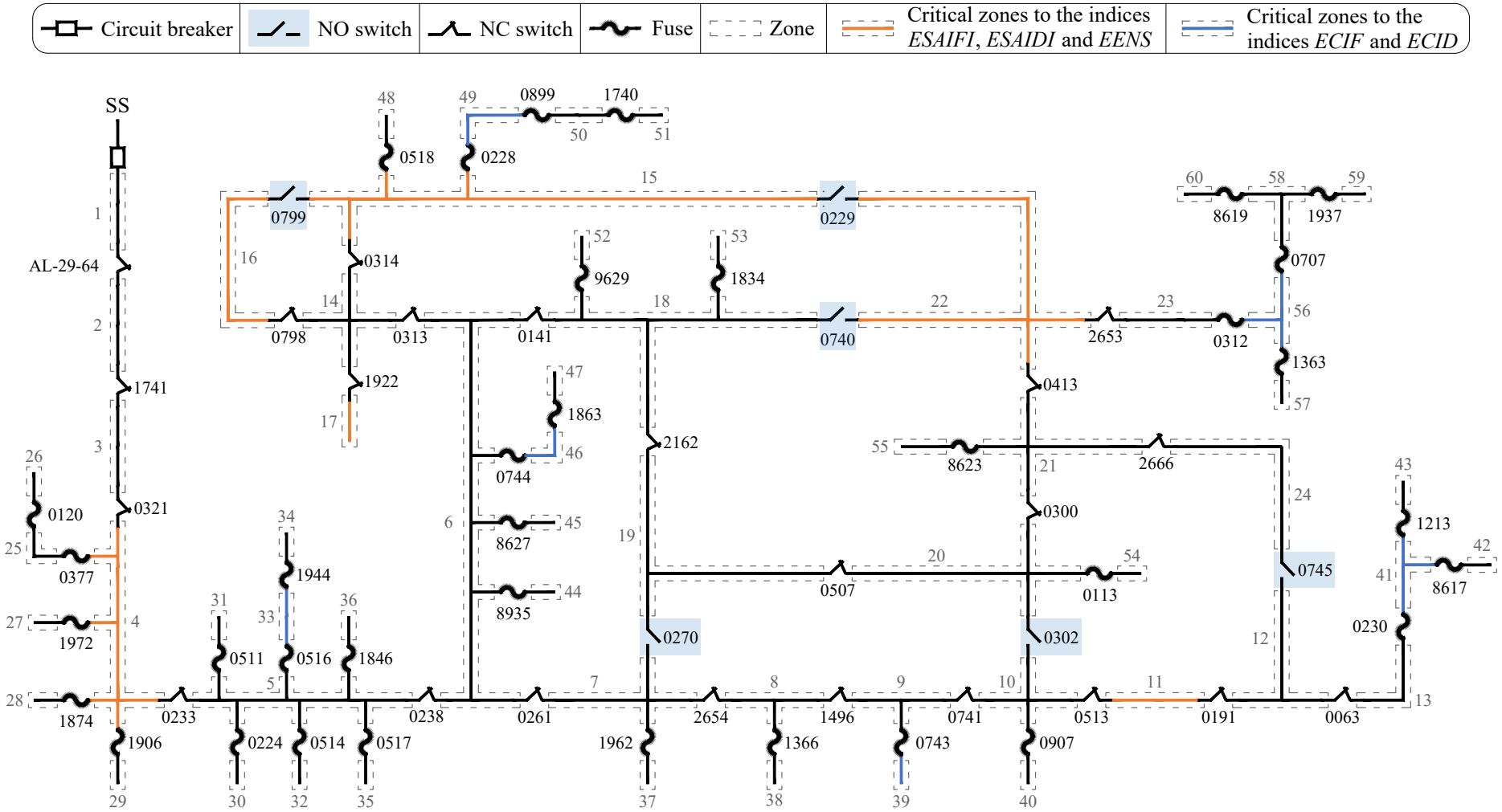

Source: ASCHIDAMINI *et al.* (2022b).

The zones with the highest expected values of indices CIF and CID estimated with the proposed method are highlighted in blue in Figure 20. The five highest expected values for the index CIF refer to zones 41, 33, 39, 56, and 46, respectively with 23.38, 22.41, 22.17, 22.10, and 21.63 interruptions/year. On the other hand, the zones with the highest expected values for the index CID are zones 41, 56, 39, 33, and 49 having, respectively, 13.12, 12.35, 12.22, 12.21, and 11.98 h/year.

The fault contribution of each zone to the indices $ESAIFI$, $ESAIDI$, and $EENS$ was obtained through the proposed algorithm. The values of these indices will be used as a basis to prioritize (i) the sectionalizing switches to be automated and (ii) the existing network zones to be replaced by conductors with lower failure rates in connection with a reconductoring plan.

5.1.2 Estimation of Reliability Considering Expansion Projects

In this section, data of the reliability estimation without expansion projects will be used to guide the i) installation of NC sectionalizing switches; ii) installation of a NO switch; iii) replacement of manual NC sectionalizing switches by remote controlled switches; and iv) replacement of bare overhead conductors by covered conductors.

5.1.2.1 Installation of NC sectionalizing switches

Initially, this study assumes that a manual type NC sectionalizing switch was installed within zone 11 of the feeder, since, among the zones with upstream NC sectionalizing switches, this zone contributes significantly to $ESAIDI$. Zone 11 of this feeder is part of the primary network and 2.24 km long, which corresponds to 4.5 % of the total length of the primary network. In addition, this zone has 654 customers and a failure rate of 1.43 failure/year.

The switch installed in zone 11, between sectionalizing switches 0513 and 0191, divides this zone into two parts, named 11a and 11b and having, respectively, 251 and 403 customers. Further, zones 11a and 11b are, respectively, 0.56 and 1.67 km long within the primary network; they exhibit failure rates of 0.36 and 1.07 failure/year, respectively. Due to the installation of the sectionalizing switch, the expected value of index CID for

zone 11a becomes 10.17 h/year, while that for zone 11b is 10.26 h/year. Thus, the expected indices CID of zones 11a and 11b are lower than the expected index CID of zone 11, whose value is 10.31 h/year.

On the other hand, the indices $ESAIDI$ and $EENS$ remained almost unchanged after the installation of the NC sectionalizing switch, as 10.86 h/year and 32.31 MWh/year were obtained, respectively, for these indices. Moreover, the frequency of interruptions is also unaffected by installation of NC sectionalizing switches. In this case, the installation of the sectionalizing switch only changed the switching conditions of customers in zones 11a and 11b, considering the occurrence of faults in these zones. Therefore, there was no impact on the restoration classification of other zones.

Adding the fault contributions of zones 11a and 11b to the $ESAIDI$ results in 0.803 h/year, a value lower than that determined for the fault contribution of zone 11 to $ESAIDI$ (0.808 h/year). Likewise, the sum of fault contributions from zones 11a and 11b to the index $EENS$ is 2.40 MWh/year and therefore lower than the contribution of zone 11 to the index $EENS$ (2.42 MWh/year).

It is noteworthy that the installation of only one sectionalizing switch did not significantly impact the reliability indices considered. However, defining the location of sectionalizing switches with priority to those zones with the highest fault contributions to the $ESAIDI$ helps in the restoration process of the zones considered more critical in terms of fault contributions to the duration of interruptions.

5.1.2.2 Installation of a NO switch

Subsequently, the installation of a NO switch with interconnection to an adjacent feeder inside zone 13 was analyzed (see Figure 17). The installation of this switch led to the indices $ESAIDI = 10.65$ h/year and $EENS = 31.69$ MWh/year, which represents a reduction of, respectively, 0.21 h/year and 0.62 MWh/year. Also note that under fault contingencies, more zones can be transferred to another feeder, thus reducing the time to restore these zones. However, the expected value of index CID for some zones may be higher, as is the case of zones (2–4), where $ECID$ increased around 0.23 h/year. This increase can be explained by the manual operation of more switches, which increases the

total time for switching and, consequently, the restoration time of these zones.

5.1.2.3 Replacement of Manual Switches by Remote Controlled Switches

To evaluate the impact on reliability coming from the replacement of manual NC sectionalizing switches by remote controlled switches, firstly, the nearest upstream sectionalizing switch inside the zone with the highest value of fault contribution to the $ESAIDI$ was replaced. The same process with the nearest sectionalizing switches upstream of the two zones with the highest contribution of faults to the $ESAIDI$ was done, and successively, with up to eight zones with the highest contribution of faults to the $ESAIDI$. The results obtained through this procedure for $ESAIDI$ and $EENS$ are shown, respectively, in Figure 21a,b, according to which $ESAIDI$ and $EENS$ decrease when the number of remote controlled switches increases. Additionally, note that without replacement of switches by remote controlled ones, these indices represent the reliability without expansion projects. It is also worth noting that the $ESAIFI$ is not affected by the installation of remote controlled switches, as the energy supply cannot be restored in a time shorter than the minimum duration of sustained interruptions. Faults on MV overhead lines need to be located before maneuvering remote controlled switches.

5.1.2.4 Replacement of Existing Bare Overhead Conductors by Covered Conductors

To assess the impact of replacement of bare overhead conductors by covered conductors on the indices $ESAIFI$, $ESAIDI$, and $EENS$, the replacement of bare conductors of zones of the network was considered. Initially, bare conductors of zone 4 were replaced, given that zone 4 has the highest contribution of faults to the $ESAIFI$. Subsequently, the conductors of up to eight zones with the highest values of fault contribution to the $ESAIFI$ were replaced by covered conductors.

Figure 22a,b, respectively, show $ESAIFI$ and $ESAIDI$ versus the number zones with bare conductors replaced by covered conductors. When no replacement of conductors occurs, no changes will take place in the network. When the replacement of bare conductors of zone 4 by covered conductors occurs, $ESAIFI = 18.66$ interruptions/year and $ESAIDI = 10.23$ h/year were obtained. Therefore, replacing the bare conductors of

Figure 21 – Impact of replacement of manual NC sectionalizing switches by remote controlled switches on reliability indices - 60-zone feeder. (**a**) $ESAIDI$. (**b**) $EENS$.

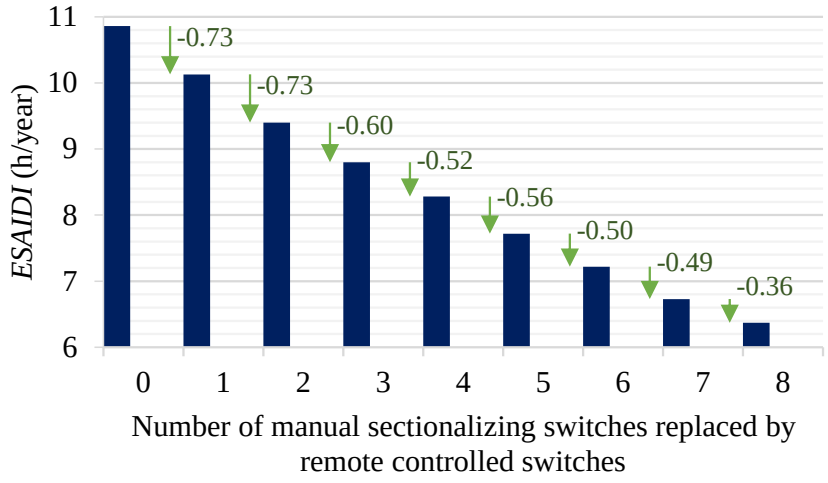

(**a**)

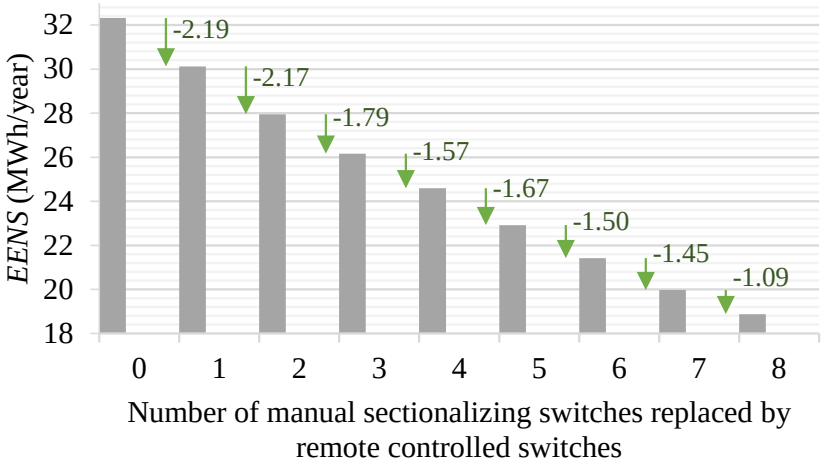

(**b**)

Source: ASCHIDAMINI *et al.* (2022b).

zone 4 by covered conductors, which corresponds to approximately 4 km and 8.14 % of the total length of the 60-zone primary distribution feeder, results in a reduction of i) 5.1 % on $ESAIFI$; and ii) 5.8 % on $ESAIDI$.

As shown in Figure 22a,b, when the bare conductors of eight zones are replaced by covered conductors, $ESAIFI = 13.53$ interruptions/year and $ESAIDI = 7.51$ h/year were obtained. Replacing the bare conductors of these eight zones by covered conductors, which corresponds to 21.5 km and 43.2 % of the 60-zone primary distribution feeder, resulted in a reduction of 31.2 % on $ESAIFI$. As a result of reduction on $ESAIFI$, the $ESAIDI$ decreased 30.9 %.

Figure 22 – Impact of replacement of bare overhead conductors by covered conductors on reliability indices - 60-zone feeder. (**a**) $ESAIFI$. (**b**) $ESAIDI$.

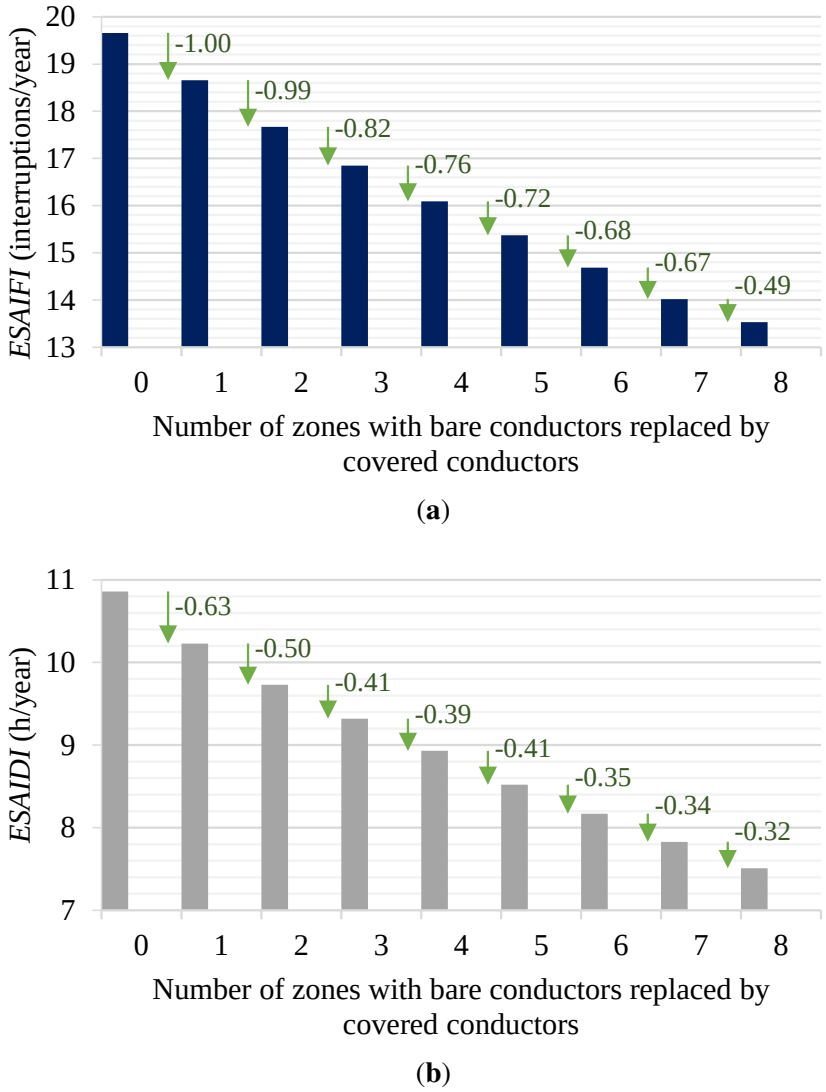

Source: ASCHIDAMINI *et al.* (2022b).

Figure 23 shows $EENS$ versus the number of zones with bare overhead conductors replaced by covered conductors. When no replacement of bare conductors is performed, there is no impact on the index $EENS$. When the bare conductors of zone 4 are replaced by covered conductors, $EENS = 30.43$ MWh/year is obtained, which represents a reduction of 1.88 MWh/year. With the replacement of bare conductors of eight zones, $EENS = 22.32$ MWh/year, therefore resulting in a reduction of 9.99 MWh/year and $30.9\,\%$ on $EENS$.

Figure 23 – Impact of replacement of bare overhead conductors by covered conductors on the index $EENS$ - 60-zone feeder.

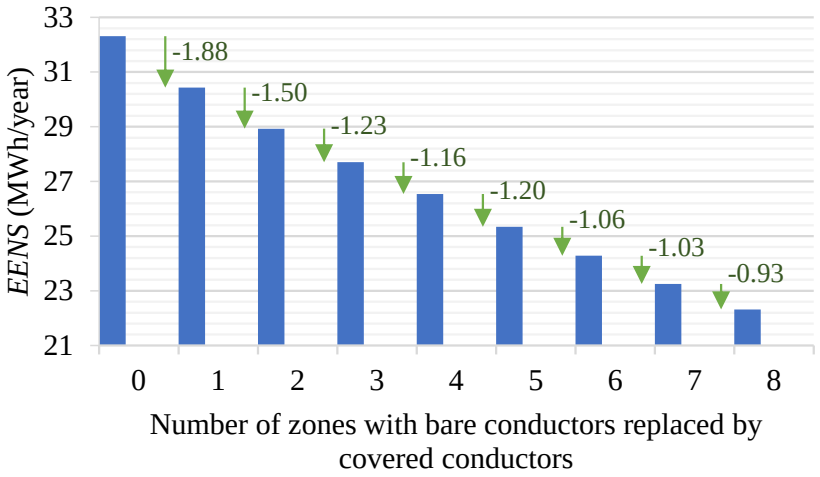

Source: Author.

The case involving replacement of bare conductors by covered conductors shows the potential of the proposed method to mitigate the frequency of interruptions, which is intimately related to the consumer satisfaction with the services provided by power distribution utilities. The results thus far discussed also highlight the importance of considering, during planning stages, changes in the network that can lead to a reduction in failure rates.

5.2 719-Zone Real Primary Distribution Network

To show the applicability of the proposed method in a large-scale primary distribution network, data from eight distribution feeders located in Southern Brazil were used. Figure 24 shows the topology of the 719-zone primary distribution network, which has eight feeders (F41 to F48). These feeders have bare overhead conductors with a total length of 506 km and operate at 13.8 kV, being supplied by the same substation. In addition, it was considered that these feeders supply $56{,}681$ customers connected at low voltage.

Figure 24 – Topology of the 719-zone real primary distribution network.

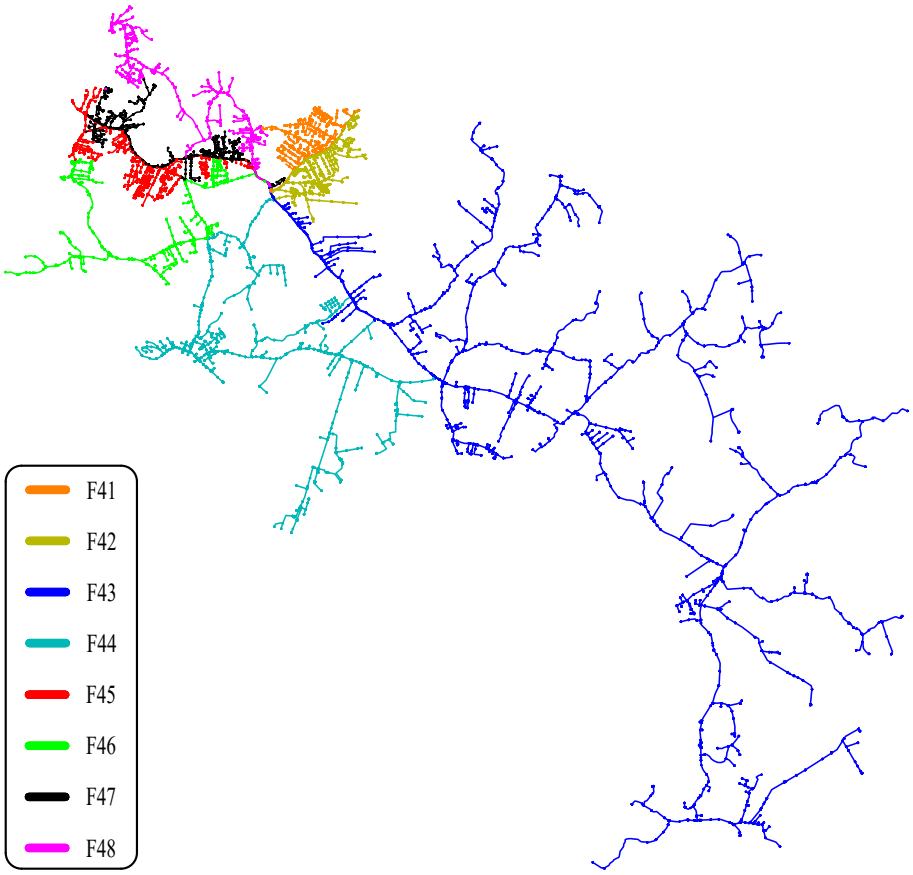

Source: Author

5.2.1 Estimation of Reliability without Expansion Projects

Initially, the data referring to the feeders of this case study were obtained from the power distribution utility to generate a database. Subsequently, based on the data of interruptions for the period of three years (2018 to 2020), the historical reliability indices of the primary distribution network were calculated, obtaining: $SAIFI_h = 9.50$ interruptions/year and $SAIDI_h = 16.53$ h/year. Likewise, ${t_R}^h = 5.92$ h and ${t_l}^h = 4.80$ h were obtained, thus leading to $p_l = 81\,\%$. In addition, the following values were assigned in the algorithm: $\Delta^s = 10^{-5}$ failure/km·year, ${t_{res}}^i = 1.7$ h, ${t_{res}}^s = 10^{-3}$ h and $p_r = 70\,\%$. The computational performance of the numerical results obtained in this section will be presented in Section 5.3.

In the estimation of reliability without expansion projects, the following reliability parameters related to time of interruptions were obtained $t_{res} = 1.95$ h, $t_l = 1.58$ h,

$t_r = 0.26$ h and $t_{sw} = 0.11$ h. The indices $ESAIFI$, $ESAIDI$ and $EENS$ resulted in 9.50 interruptions/year, 16.53 h/year and 231.90 MWh/year, respectively. It should be noted that $ESAIFI$ is approximately equal to $SAIFI_h$, as well as $ESAIDI$ is approximately equal to $SAIDI_h$, indicating that the proposed method was able to obtain the failure rates per zone and restoration times. As a further result, the $EASAI$ was calculated and resulted in $99.81\,\%$.

The ten zones with the highest values of contribution of faults to the indices $ESAIDI$, $ESAIFI$ and $EENS$, considering only zones with upstream sectionalizing switches, are shown in Table 18. The feeder of each zone is indicated, in addition to the values of l_i and ${\lambda_i}^c$. Zone 241 of feeder F43 has the highest values for these indices. It is worth noting that the network length of the zones influences the contribution of failures to the indices due to the partial consideration of failure rates per network length.

Table 18 – Ten zones with the highest values of contribution of faults in zones to the reliability indices $ESAIFI$, $ESAIDI$ and $EENS$.

Feeder	**Zone**	$\boldsymbol{cSAIFI_i}$ (int./year)	$\boldsymbol{cSAIDI_i}$ (h/year)	$\boldsymbol{cEENS_i}$ (MWh/year)	$\boldsymbol{l_i}$ (km)	${\boldsymbol{\lambda_i}}^{\boldsymbol{c}}$ (failure/year)
F43	241	0.465	0.842	11.23	8.69	3.74
F43	242	0.309	0.522	6.96	5.78	2.48
F48	56	0.213	0.388	6.33	4.30	1.85
F45	72	0.173	0.292	4.54	2.97	1.28
F46	57	0.159	0.289	3.55	2.43	1.38
F46	59	0.161	0.272	3.34	3.24	1.39
F47	59	0.112	0.204	2.84	2.37	1.02
F44	114	0.109	0.197	2.83	2.67	1.15
F45	70	0.097	0.187	2.90	1.67	0.72
F41	56	0.079	0.141	2.03	2.01	0.87

The three highest expected values for the indices CIF and CID were found in zones of the feeder F43. The highest expected values for the index CIF resulted in $ECIF_6 = 30.36$, $ECIF_{214} = 28.41$ and $ECIF_{228} = 27.16$ interruptions/year, while the highest expected values of the index CID resulted in $ECID_6 = 53.60$, $ECID_{214} = 53.03$ and $ECID_{228} = 47.73$ h/year.

The expected values of the indices CIF and CID for the zones indicated in Table 18

are shown in Table 19. Zone 114 of feeder F44 and zone 241 of feeder F43 have the highest values for these indices.

Table 19 – Expected values for the indices CIF and CID.

Feeder	**Zone**	$\boldsymbol{ECIF_j}$ (interruptions/year)	$\boldsymbol{ECID_j}$ (h/year)
F43	241	17.21	30.44
F43	242	17.21	30.12
F48	56	3.97	7.41
F45	72	7.72	13.48
F46	57	6.69	11.81
F46	59	6.69	11.81
F47	59	11.56	19.94
F44	114	19.64	33.94
F45	70	7.72	13.34
F41	56	3.33	5.94

The values of contributions of faults in zones to the indices $ESAIFI$, $ESAIDI$ and $EENS$ allow the verification of the zones in which faults most contribute to the respective reliability indices. Thus, these values can be used to guide the expansion of the primary distribution network.

5.2.2 Estimation of Reliability Considering Expansion Projects

In this section, data of the reliability estimation of the 719-zone system without expansion projects will be used to guide the i) installation of NC sectionalizing switches and ii) replacement of manual NC sectionalizing switches by remote controlled switches.

5.2.2.1 Installation of NC sectionalizing switches

This study considers that a manual type NC sectionalizing switch is installed within zone 241 of the feeder F43, as this is the zone in which faults most contribute to the $ESAIDI$ among the zones that have an upstream NC sectionalizing switch. The feeder F43 is the longest in the distribution network, with 217.1 km long in primary network, 7,054 customers, 243 protection and/or sectionalizing devices and 242 zones. Zone 241 of this feeder is part of the primary network and 8.69 km long, which corresponds to 4 % of the total length of the primary network of feeder F43. Furthermore, this zone has

319 customers and a failure rate of 3.74 failure/year.

The switch installed within zone 241 has segmented it into two zones, named 241a and 241b. These zones have, respectively, 121 and 198 customers: 4.32 and 4.37 km long primary network and a failure rate of 1.86 and 1.88 failure/year. Due to the proposed sectionalizing switch installation, the expected value of index CID from zone 241a resulted in 29.95 h/year, while the expected value of index CID from zone 241b resulted in 29.96 h/year. Thus, the indices $ECID$ of zones 241a and 241b are lower than the index $ECID$ of zone 241, whose value is 30.44 h/year.

On the other hand, the indices $ESAIDI$ and $EENS$ did not change significantly, as they resulted in 16.52 h/year and 231.33 MWh/year, respectively. The frequency of interruptions is not changed by installing NC sectionalizing switches. In this case, the installation of the sectionalizing switch only changed the switching conditions of the customers of zones 241a and 241b, considering the occurrence of failures in these zones and, therefore, there was no impact on the restoration classification of other zones.

The sum of the contributions of faults from zones 241a and 241b to the $ESAIDI$ resulted in $cSAIDI_{241ab} = 0.839$ h/year, which is therefore lower than the value found for the zone in which the switch was installed: $cSAIDI_{241} = 0.842$ h/year. Likewise, the sum of fault contributions from zones 241a and 241b to the index $EENS$ resulted in $cEENS_{241ab} = 10.66$ MWh/year, therefore being lower compared to $cEENS_{241} = 11.23$ MWh/year.

It should be noted that the installation of only one sectionalizing switch did not significantly impact the reliability indices considered. However, determining the location of installation of sectionalizing switches based on the zones with the highest values for the $cSAIDI_i$ helps in the restoration conditions of the zones that are considered more critical for fault contributions in the duration of the interruptions. Furthermore, the zones can be segmented into more parts by installing more sectionalizing switches performed by the user.

5.2.2.2 Replacement of Manual Switches by Remote Controlled Switches

Initially, the replacement of the nearest upstream manual NC sectionalizing switch to the zone with the highest value for $cSAIDI_i$ by a remote controlled switch was performed. Subsequently, the nearest upstream switches of up to ten zones with the highest values of $cSAIDI_i$ were replaced by a remote controlled switch.

Figure 25a,b shows the reduction of the indices $ESAIDI$ and $EENS$ according to the number of manual sectionalizing switches replaced by remote controlled ones. Replacing ten manual switches by remote controlled switches results in a reduction of approximately 14% in the indices $ESAIDI$ and $EENS$. Such a reduction was expected since the proposed change in network makes it possible to isolate faulty zones more quickly through remote-controlled switching. Thus, the proposed framework can be used to estimate the improvement in reliability according to the number of switches to be replaced by remote controlled ones, which is a parameter chosen by the user.

The proposed replacement of ten manual sectionalizing switches by remote controlled switches resulted in a reduction in the values of the indices $cSAIDI_i$ and $cEENS_i$ for the zones downstream of these switches, as can be observed by comparing the values presented in Table 20 and Table 18.

Table 20 – Impact of replacement of manual sectionalizing switches by remote controlled switches on the contribution of faults in zones to the indices $ESAIFI$ and $EENS$.

Feeder	**Zone**	$\boldsymbol{cSAIDI_i}$ (h/year)	$\boldsymbol{cEENS_i}$ (MWh/year)
F43	241	0.277	3.70
F43	242	0.146	1.95
F48	56	0.128	2.09
F45	72	0.082	1.28
F46	57	0.097	1.19
F46	59	0.077	0.95
F47	59	0.068	0.95
F44	114	0.065	0.93
F45	70	0.069	1.07
F41	56	0.046	0.66

The replacement of the NC sectionalizing switch nearest upstream of the zone with the

Figure 25 – Impact of replacement of manual sectionalizing switches by remote controlled switches on reliability indices. (**a**) $ESAIDI$. (**b**) $EENS$.

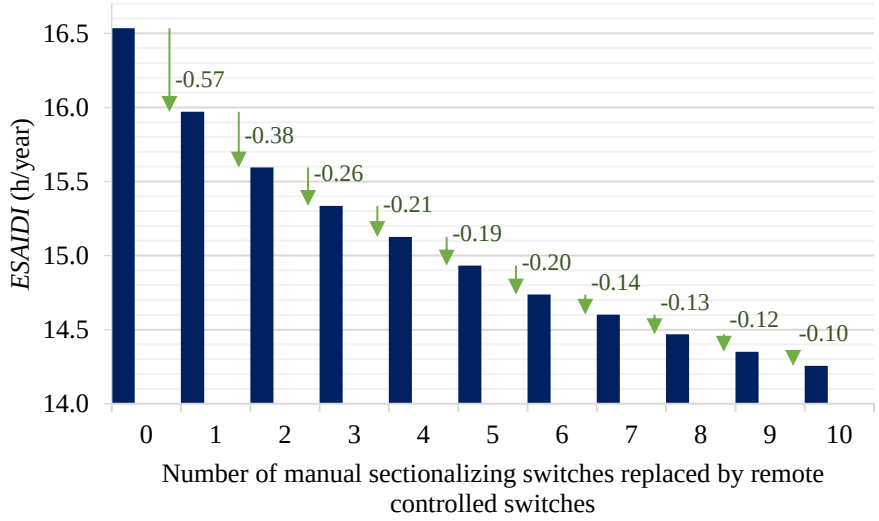

(**a**)

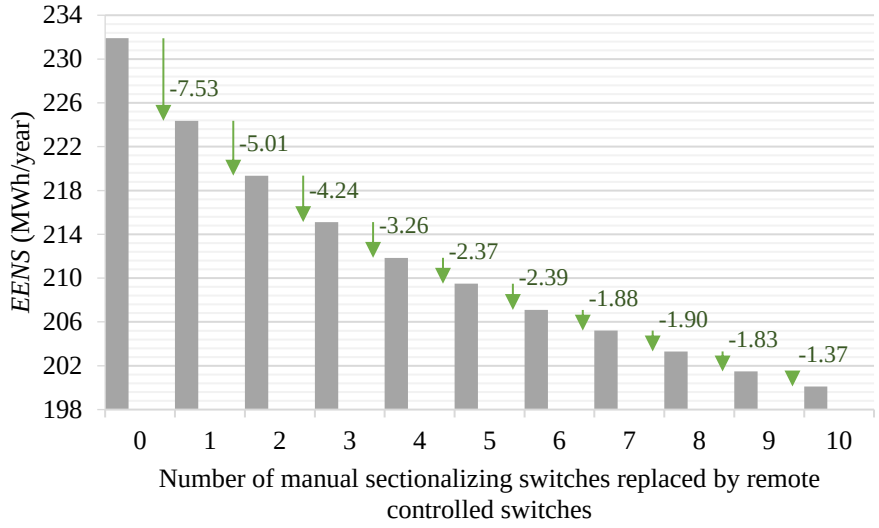

(**b**)

Source: Author.

highest value for $cSAIDI_i$ (zone 241 of feeder F43) by a remote controlled switch contributed more significantly to the reduction of $ESAIDI$ and $EENS$, because the values of $cSAIDI_{241}$ and $cEENS_{241}$ reduced 0.57 h/year and 7.53 MWh/year, respectively. On the other hand, the replacement of the NC sectionalizing switches of the zones with lower values for the $cSAIDI_i$ by remote controlled ones contributed less significantly to the reduction of the indices $ESAIDI$ and $EENS$, evidencing the advantage of considering the prioritization of expansion projects through the values of $cSAIDI_i$. Also, it is worth

noting that the contributions of faults in zones to the $ESAIFI$ were not altered by the replacement of the sectionalizing switches by remote controlled switches, as this expansion alternative does not change the failure rates of the zones.

Furthermore, due to the replacement of the ten manual sectionalizing switches upstream of the zones with the highest values for $cSAIDI_i$ by remote controlled switches, the expected value of index CID of some zones was impacted. The three highest values for the $ECID$ have been significantly reduced to $CID_6 = 46.05$, $ECID_{214} = 42.47$ and $ECID_{228} = 40.17$, all in hours per year.

Table 21 presents the results of the impact of the replacement of ten manual switches by remote controlled switches on the index $ECID$ of the zones with the highest values for $cSAIDI_i$. The expected value of index CID of the zone 56 of feeder F-48 reduced approximately 30.4 %, thus being the highest percentage reduction in this index among the zones in which the upstream sectionalizing switches were replaced by remote controlled switches.

Table 21 – Impact of replacement of manual sectionalizing switches by remote controlled switches on the expected values of index CID.

Feeder	**Zone**	$\boldsymbol{ECID_j}$ (h/year)	**Reduction on** $\boldsymbol{ECID_j}$ (%)
F43	241	22.88	24.8
F43	242	22.56	25.1
F48	56	5.16	30.4
F45	72	11.06	18.0
F46	57	8.44	28.5
F46	59	8.44	28.5
F47	59	18.71	6.2
F44	114	32.54	4.1
F45	70	10.92	18.1
F41	56	4.89	17.7

5.3 Computational Performance

In this section, tests to evaluate the computational performance of the adjustment processes of estimated reliability indices to the historical indices (Figure 12) will be presented.

To evaluate the computational performance, one hundred runs of the aforementioned processes were performed for the case studies using the real distribution networks (Section 5.1.1 and 5.2.1). In addition, the effects on reliability results and computational time coming from different values for the parameters used by the adjustment processes were evaluated. The algorithms were implemented in MatLab® (MATLAB, 2021) and executed on a computer with an Intel Core i7-10750H CPU 2.6 GHZ and 16 GB of RAM running the operating system Windows 10 and 64 bits. It is worth noting that the computational performance of execution of the proposed method can be improved by implementing the algorithm in another programming language.

5.3.1 Computational Time to Adjust the Estimated Indices to the Historical Indices for the 60-Zone Primary Distribution Feeder

In the process of adjusting the estimated reliability indices to the historical indices for the case study in the 60-zone primary distribution feeder, the following parameters were used i) $\Delta^s = 10^{-7}$ failure/km·year, ii) ${t_{res}}^i = 0.3\,\text{h}$, and iii) ${t_{res}}^s = 10^{-4}\,\text{h}$, as indicated in Section 5.1.1. The histogram of the total computational time of adjustment processes from $ESAIFI$ to $SAIFI_h$ and of adjustment from $ESAIDI$ to $SAIDI_h$, in seconds, is shown in Figure 26, where one can observe the frequency of the computational time of these processes for a total of one hundred executions.

Figure 26 – Computational time of adjusting the estimated reliability indices to historical indices for the 60-zone primary distribution feeder.

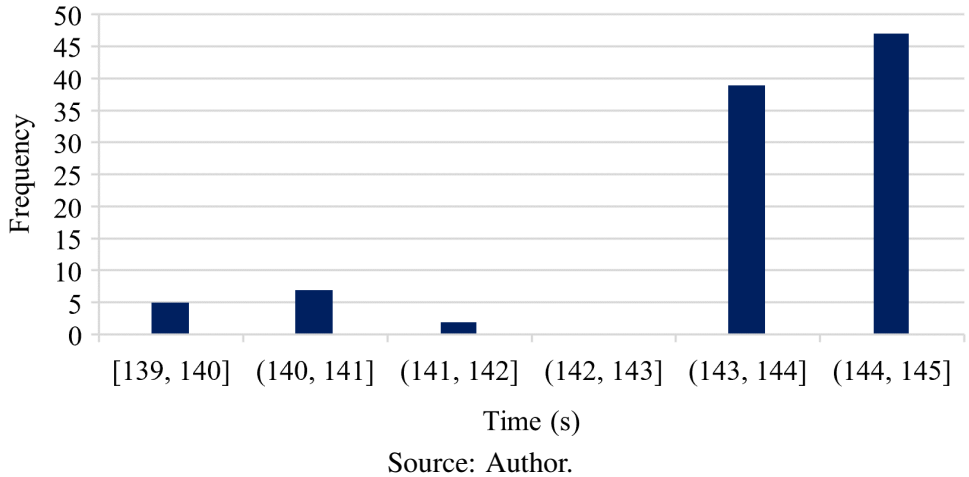

Source: Author.

The histogram of computational time observed in Figure 26 indicates that the mean is a representative value due to low dispersion. Therefore, the average computational time of the adjustment of estimated reliability indices to the historical indices of this case study, called base case, was compared with the average computational time obtained by case studies with different values for the reliability parameters used in the adjustment process.

To evaluate the average computational time of the processes of i) adjustment of $ESAIFI$ to $SAIFI_h$; ii) adjustment of $ESAIDI$ to $SAIDI_h$; and iii) the total average computational time of adjustment of both indices, different values were assigned to the parameters Δ^s (failure/km·year), ${t_{res}}^i$ (h), and ${t_{res}}^s$ (h). The results of five proposed case studies can be seen in Table 22. Among these case studies, the base case presented the highest computational time. Conversely, when the value of ${t_{res}}^s$ was raised to 10^{-3} failure/km·year, in case I, the adjustment time of $ESAIDI$ to $SAIDI_h$ was reduced to approximately $10\,\%$ of the average adjustment time of this index for the base case. This is due to the smaller number of iterations required until this process converges when using higher values of ${t_{res}}^s$.

Table 22 – Average computational time for case studies with different reliability parameters in the 60-zone primary distribution feeder.

Case	Δ^s	${t_{res}}^i$ (h)	${t_{res}}^s$ (h)	**Average Computational Time** (s)		
				$ESAIFI$ to $SAIFI_h$	$ESAIDI$ to $SAIDI_h$	Total
Base	10^{-7}	0.3	10^{-4}	85.79	57.82	143.61
I	10^{-7}	0.3	10^{-3}	83.49	5.65	88.14
II	10^{-6}	0.3	10^{-4}	8.35	56.11	64.47
III	10^{-5}	0.3	10^{-4}	0.88	55.59	56.47
IV	10^{-7}	0.6	10^{-4}	83.85	5.38	89.23
V	10^{-5}	0.6	10^{-4}	0.96	4.37	5.33

For case II (Table 22), the value of Δ^s has been raised to 10^{-6} failure/km·year, resulting in a reduction in the computational time to adjust $ESAIFI$ to $SAIFI_h$. Additionally, by increasing the value of ${t_{res}}^s$ to 10^{-5} failure/km·year, in case III, the computational time was reduced to approximately $1\,\%$ of the computational time required by adjusting $ESAIFI$ to $SAIFI_h$ in the base case.

For case IV (Table 22), the values of Δ^s and ${t_{res}}^s$ were kept equal to the values of the base case. However, the value of ${t_{res}}^i$ has been increased to 0.6 h. For this case, the average adjustment time from $ESAIFI$ to $SAIFI_h$ found was approximately equal to the time demanded by the base case (same value of Δ^s for both cases). The average adjustment time from $ESAIDI$ to $SAIDI_h$ was reduced by approximately $90\,\%$ compared to the average adjustment time of this index for the base case. This behavior in the interruption duration index was expected, due to the smaller number of iterations required to find the value of t_{res} that adjusts $ESAIDI$ to $SAIDI_h$ to a value of ${t_{res}}^i$ closest to the value of t_{res} found. Nevertheless, at the beginning of the adjustment process, the value of t_{res} is not known, and it is necessary to empirically attribute a reduced value to the parameter ${t_{res}}^i$, considering that the proposed method performs only an increase in the value of this parameter.

For case V (Table 22), the value of ${t_{res}}^i$ was assigned as 0.6 h, and the values of Δ^s and ${t_{res}}^s$ were kept equal to the values of case III. As a result, the average total time required to adjust the estimated indices to the historical reliability indices was lower than the other cases, as resulted in 5.33 s.

The reliability indices estimated by adjusting to the historical indices for each case study are presented in Table 23, where it can be noted that for the base case, the indices $ESAIFI$ and $ESAIDI$ resulted in approximately the values of $SAIFI_h$ and $SAIDI_h$, respectively. However, when the value of ${t_{res}}^s$ was increased to 10^{-3} h, in case I, the value of $ESAIDI$ obtained was different from the value of $SAIDI_h$, and the index $EENS$ found was different from the value calculated in the base case. It is important to note that the stop criterion of the analytical assessment of reliability process (illustrated by a flowchart (Figure 12)), considers the increment of ${t_{res}}^s$ in t_{res} while $ESAIDI < SAIDI_h$.

In Table 23, for case II, when the value of Δ^s is ten times greater than the value of the base case, only the value of $ESAIDI$ found was slightly different from the value of $SAIDI_h$. However, when the value of Δ^s is one hundred times greater than the value of the base case in case III, the value of $ESAIFI$ found is greater than the value of $SAIFI_h$.

Table 23 – Reliability indices estimated by adjusting to historical indices for each case in the 60-zone primary distribution feeder.

Case	$ESAIFI$ (int./year)	$ESAIDI$ (h/year)	$EENS$ (MWh/year)
Base	19.66	10.860	32.31
I	19.66	10.869	32.34
II	19.66	10.861	32.31
III	19.93	10.860	32.31
IV	19.66	10.860	32.31
V	19.93	10.860	32.31

This is because the failure rate step value in failure/km·year is too elevated to reach the accurate adjustment to the second decimal point, and because of the adjustment process runs while $ESAIFI < SAIFI_h$. For case IV, the values of indices found were equal to the values of the base case. Nonetheless, the value of ${t_{res}}^i$ is different for these cases, where the parameters Δ^s and ${t_{res}}^s$ assigned have equal values for both cases. Finally, for case V, the values of indices found were equal to the indices of case III, with approximately 10 % of the computational time required by case III.

5.3.2 Computational Time to Adjust the Estimated Indices to the Historical Indices for the 719-Zone Primary Distribution Network

The process of adjusting the estimated reliability indices to the historical indices for the case study in the 719-zone primary distribution network, developed in Section 5.2.1, will be called in this section base case. In this case study, the following parameters were used i) $\Delta^s = 10^{-5}$ failure/km·year, ii) ${t_{res}}^i = 1.7$ h, and iii) ${t_{res}}^s = 10^{-3}$ h. The computational performance evaluation for the adjustment process in this distribution network, as performed for the 60-zone primary distribution feeder, will be performed through the average computational time value for a total of one hundred executions. Three case studies were defined with reliability parameters Δ^s and ${t_{res}}^s$ different from the values used in the base case. Table 24 presents the results of computational times for each case.

As can be seen in Table 24, the total average computational time was reduced by approximately 73 % when the value of ${t_{res}}^s$ was increased by ten times, from the base case to case I. The average computational time for adjusting $ESAIFI$ to the value of

Table 24 – Reliability parameters and average computational times for case studies in the 719-zone primary distribution network.

Case	Δ^s	${t_{res}}^i$ (h)	${t_{res}}^s$ (h)	**Average Computational Time** (s)		
				$ESAIFI$ to $SAIFI_h$	$ESAIDI$ to $SAIDI_h$	Total
Base	10^{-5}	1.7	10^{-3}	50.64	285.00	335.64
I	10^{-5}	1.7	10^{-2}	56.15	33.10	89.25
II	10^{-4}	1.7	10^{-3}	7.58	131.30	138.88
III	10^{-4}	1.7	10^{-2}	7.04	14.04	21.08

$SAIFI_h$ was reduced for case II, in which $\Delta^s = 10^{-4}$ failure/km·year was adopted. For case III, 10^{-4} failure/km·year and 10^{-2} h were assigned, respectively, to Δ^s and ${t_{res}}^s$. As a consequence, 21 s was found for the total average computational time, therefore the lowest computational time required between the proposed case studies.

The reliability indices estimated by adjusting to the historical indices for each case study are presented in Table 25, where it can be observed that the increase in the value of the parameter ${t_{res}}^s$ for case I impacted in the values found for indices $ESAIDI$ and $EENS$, in a comparison with the values found for the base case.

Table 25 – Reliability indices estimated by adjusting to the historical indices for each case in the 719-zone primary distribution network.

Case	$ESAIFI$ (int./year)	$ESAIDI$ (h/year)	$EENS$ (MWh/year)
Base	9.50	16.53	231.90
I	9.50	16.56	232.25
II	10.26	16.54	232.04
III	10.26	16.60	232.94

For case II (Table 25), despite the fact that the adopted value of Δ^s had a positive impact on reducing the computational time to adjust the $ESAIFI$ to $SAIFI_h$, this case resulted in a value distant from the historical index. Finally, in case III, the reliability indices found were higher than the values of base case, however with less computational time. As a result, it is possible to verify that the adjusted values were closer to the historical values in the base case that required a greater computational effort due to the steps of failure rate and restoration time used.

6 CONCLUSION

In this thesis, a framework for inserting reliability criteria into studies of planning the expansion of primary distribution networks was introduced. Further, it was described how to determine matrices which allow estimating the most relevant reliability indices, such as ESAIFI and ESAIDI. The proposed algorithm to analytically assess reliability allows estimating reliability indices, which are adjusted to historical indices of the primary distribution network.

The potential use and advantages of the proposed framework were demonstrated through a case study using the Roy Billinton test system. To show the applicability in distribution networks with characteristics of real networks and historical data of interruptions, the framework was also demonstrated through case studies using a real primary distribution feeder and a real large-scale primary distribution network. The case studies confirmed that applying the proposed framework, significant improvements can be achieved in reliability indices. Finally, the extent of these improvements depends on the particular expansion project considered by the user.

The results presented in this thesis showed that the proposed framework can guide the location of installation of sectionalizing switches and the manual switches to be replaced by remote controlled switches, by identifying the zones in which the faults most contribute to the reliability indices. The numerical results demonstrated a positive impact on the reliability of a real feeder, which comes from the installation of a NC sectionalizing switch in the most critical zone of this feeder. Additionally, an improvement was also observed in the reliability of the real feeder as more manual sectionalizing switches are replaced

by remote controlled switches, and more bare overhead conductors of network zones are replaced by conductors with lower failure rates.

The computational performance of the adjustment processes of the estimated indices to the historical indices, was evaluated through the average computational time. Its potential for convergence with different reliability parameters and the advantages of the reliability parameters chosen for the processes (using case studies in real distribution networks) were proved.

The proposed framework can support the decision of investments in network expansion projects during planning stages. The impact on reliability coming from different expansion projects, can be measured, and compared by the user of the proposed framework, to achieve the required reliability indices imposed by regulatory agencies.

6.1 Perspectives for Future Work

Based on the results of the proposed case studies, the following extensions to the proposed framework are suggested:

- include capacity constraints to better evaluate transferable zones and model uncertainties in load and distributed energy resources;
- address other expansion projects that impact the reliability of power distribution systems, including distributed energy resources;
- the incorporation of the expansion of the network in areas without distribution network to meet new load, usually called greenfield planning (MIGUEZ *et al.*, 2002), is also an alternative for future study since the proposed framework can be adjusted to adopt different failure rates;
- the incorporation of the costs of investments in expansion projects indicated by the user of the framework is a future work since it is crucial to assess the reliability cost/worth of each alternative to expand the distribution network.

REFERENCES

ABAIDE, A. R. **Desenvolvimento de métodos e algoritmos para avaliação e otimização da confiabilidade em redes de distribuição**. 2005. PhD Thesis (in Portuguese) — Federal University of Santa Maria, Santa Maria, RS, Brazil, 2005.

ALLAN, R. *et al.* A Reliability Test System For Educational Purposes - Basic Distribution System Data and Results. **IEEE Transactions on Power Systems**, [S.l.], v. 6, n. 2, p. 813–820, 1991.

ALOTAIBI, I. *et al.* A comprehensive review of recent advances in smart grids: a sustainable future with renewable energy resources. **Energies**, [S.l.], v. 13, n. 23, 2020.

ANEEL. **Procedimentos de Distribuição de Energia Elétrica no Sistema Elétrico Nacional - PRODIST, Módulo 8**: qualidade do fornecimento de energia elétrica. 2022.

ASCHIDAMINI, G. L. *et al.* Expansion Planning of Power Distribution Systems Considering Reliability: a comprehensive review. **Energies**, [S.l.], v. 15, n. 6, 2022a.

ASCHIDAMINI, G. L. *et al.* A Framework for Reliability Assessment in Expansion Planning of Power Distribution Systems. **Energies**, [S.l.], v. 15, n. 14, 2022b.

BARAN, M.; WU, F. Network reconfiguration in distribution systems for loss reduction and load balancing. **IEEE Transactions on Power Delivery**, [S.l.], v. 4, n. 2, p. 1401–1407, 1989.

BARAN, M.; WU, F. Optimal capacitor placement on radial distribution systems. **IEEE Transactions on Power Delivery**, [S.l.], v. 4, n. 1, p. 725–734, 1989.

BILLINTON, R. A test system for teaching overall power system reliability assessment. **IEEE Transactions on Power Systems**, [S.l.], v. 11, n. 4, p. 1670 – 1676, 1996.

BILLINTON, R. **Methods to consider customer interruption costs in power system analysis**: task force 38.06.01. [S.l.]: Cigré, 2001.

BILLINTON, R.; ALLAN, R. N. **Reliability Evaluation of Engineering Systems**: concepts and techniques. 2. ed. New York: Plenum Press, 1992.

BILLINTON, R.; ALLAN, R. N. **Reliability evaluation of power systems**. 2nd. ed. [S.l.]: New York, NY, USA: Plenum Press, 1996.

BILLINTON, R.; LI, W. **Reliability Assessment of Electric Power Systems Using Monte Carlo Methods**. 1. ed. [S.l.]: Springer US, 1994.

BROWN, R. **Electric Power Distribution Reliability**. 2nd. ed. [S.l.]: Boca Raton, FL, USA: CRC Press, 2008.

CHAVES, T. *et al.* Application study in the field of solutions for the monitoring distribution transformers of the overhead power grid. **Energies**, [S.l.], v. 14, n. 19, 2021.

CHOWDHURY, A.; KOVAL, D. **Power Distribution System Reliability**: practical methods and applications. [S.l.]: Hoboken, NJ, USA: Wiley, 2009.

CONTI, S. *et al.* Reliability assessment of distribution systems considering telecontrolled switches and microgrids. **IEEE Transactions on Power Systems**, [S.l.], v. 29, n. 2, p. 598 – 607, 2014.

DAZA, E. F. B. **Utilização da metodologia AHP para alocação de equipamentos telecomandados em sistemas de distribuição para melhoria da confiabilidade.** 2010. MSc Thesis (in Portuguese) — Federal University of Santa Maria, Santa Maria, RS, Brazil, 2010.

DIAS, E. B. **Avaliação de indicadores de continuidade e seu impacto no planejamento de sistemas de distribuição.** 2002. MSc Thesis (in Portuguese) — University of São Paulo, São Paulo, SP, Brazil, 2002.

DIESTEL, R. **Graph Theory**. 5. ed. Berlin: Springer-Verlag, 2017. (Graduate Texts in Mathematics).

ESCALERA, A.; HAYES, B.; PRODANOVIć, M. A survey of reliability assessment techniques for modern distribution networks. **Renewable and Sustainable Energy Reviews**, [S.l.], v. 91, p. 344 – 357, 2018.

ESCALERA, A. *et al.* Reliability assessment of distribution networks with optimal coordination of distributed generation, energy storage and demand management. **Energies**, [S.l.], v. 12, n. 16, 2019.

ESPINO-CORTéS, F. P.; RAMíREZ-VáZQUEZ, I.; GóMEZ, P. **Electric field analysis of spacer cable systems under polluted conditions**. 2014. 231 – 234 p.

FILHO, A. C. M. **Análise de modelos de investimentos em distribuidoras de energia elétrica com foco no ativo poste.** 2014. MSc Thesis (in Portuguese) — Federal University of Pampa, Alegrete, RS, Brazil, 2014.

GEORGILAKIS, P. S.; HATZIARGYRIOU, N. D. A review of power distribution planning in the modern power systems era: models, methods and future research. **Electric Power Systems Research**, [S.l.], v. 121, p. 89 – 100, 2015.

GEORGILAKIS, P. *et al.* Optimal allocation of protection and control devices in smart distribution systems: models, methods, and future research. **IET Smart Grid**, [S.l.], v. 4, n. 4, p. 397 – 413, 2021.

GONÇALVES, R.; FRANCO, J.; RIDER, M. Short-term expansion planning of radial electrical distribution systems using mixed-integer linear programming. **IET Generation, Transmission and Distribution**, [S.l.], v. 9, n. 3, p. 256–266, 2015.

HAMIDAN, M.-A.; BOROUSAN, F. Optimal planning of distributed generation and battery energy storage systems simultaneously in distribution networks for loss reduction and reliability improvement. **Journal of Energy Storage**, [S.l.], v. 46, p. 103844, 2022.

HEIDARI, S.; FOTUHI-FIRUZABAD, M. **Reliability evaluation in power distribution system planning studies**. [S.l.]: International Conference on Probabilistic Methods Applied to Power Systems (PMAPS), Beijing, China, Oct. 16-20, 2016, 2016.

HEIDARI, S.; FOTUHI-FIRUZABAD, M.; KAZEMI, S. Power Distribution Network Expansion Planning Considering Distribution Automation. **IEEE Transactions on Power Systems**, [S.l.], v. 30, n. 3, p. 1261–1269, 2015.

IEEE. IEEE Guide for Electric Power Distribution Reliability Indices. **IEEE Std 1366-2012**, [S.l.], p. 1–43, 2012.

JOOSHAKI, M. *et al.* An Enhanced MILP Model for Multistage Reliability-Constrained Distribution Network Expansion Planning. **IEEE Transactions on Power Systems**, [S.l.], v. 37, n. 1, p. 118–131, 2022.

KERSTING, W. Radial distribution test feeders IEEE distribution planning working group report. **IEEE Transactions on Power Systems**, [S.l.], v. 6, n. 3, p. 975–985, 1991.

KüFEOğLU, S.; LEHTONEN, M. Interruption costs of service sector electricity customers, a hybrid approach. **International Journal of Electrical Power and Energy Systems**, [S.l.], v. 64, p. 588 – 595, 2015.

LI, M.-B.; SU, C.-T.; SHEN, C.-L. The impact of covered overhead conductors on distribution reliability and safety. **International Journal of Electrical Power** & **Energy Systems**, [S.l.], v. 32, n. 4, p. 281 – 289, 2010.

LI, R. *et al.* A review of optimal planning active distribution system: models, methods, and future researches. **Energies**, [S.l.], v. 10, n. 11, 2017.

LOTERO, R.; CONTRERAS, J. Distribution system planning with reliability. **IEEE Transactions on Power Delivery**, [S.l.], v. 26, n. 4, p. 2552 – 2562, 2011.

LóPEZ-PRADO, J.; VéLEZ, J.; GARCIA-LLINáS, G. Reliability evaluation in distribution networks with microgrids: review and classification of the literature. **Energies**, [S.l.], v. 13, n. 23, 2020.

MARCOS, F. *et al.* A review of power distribution test feeders in the United States and the need for synthetic representative networks. **Energies**, [S.l.], v. 10, n. 11, 2017.

MASOUM, M.; FUCHS, E. **Power Quality in Power Systems and Electrical Machines**. 2nd. ed. [S.l.]: Academic Press, 2015.

MATLAB. **(R2021a)**. Natick, MA: The MathWorks Inc., 2021.

MIGUEZ, E. *et al.* An improved branch-exchange algorithm for large-scale distribution network planning. **IEEE Transactions on Power Systems**, [S.l.], v. 17, n. 4, p. 931–936, 2002.

MIRANDA, V.; RANITO, J.; PROENA, L. Genetic algorithms in optimal multistage distribution network planning. **IEEE Transactions on Power Systems**, [S.l.], v. 9, n. 4, p. 1927–1933, 1994.

NETO, E. A. C. A. **Alocação de chaves automatizadas em redes de distribuição utilizando múltiplos critérios**. 2006. MSc Thesis (in Portuguese) — Federal University of Santa Catarina, Florianópolis, SC, Brazil, 2006.

PIHLER, J.; TIčAR, I. Design of systems of covered overhead conductors by means of electric field calculation. **IEEE Transactions on Power Delivery**, [S.l.], v. 20, n. 2 I, p. 807 – 814, 2005.

POMBO, A.; MURTA-PINA, J.; PIRES, V. A multiobjective placement of switching devices in distribution networks incorporating distributed energy resources. **Electric Power Systems Research**, [S.l.], v. 130, p. 34–45, 2016.

RESENER, M. *et al.* Optimization techniques applied to planning of electric power distribution systems: a bibliographic survey. **Energy Systems**, [S.l.], v. 9, n. 3, p. 473 – 509, 2018.

RODIGHERI, A. **Simulação da confiabilidade de redes primárias de distribuição considerando faltas temporárias, equipamentos religadores, e manobras de**

restauração. 2013. MSc Thesis (in Portuguese) — Federal University of Santa Catarina, Florianópolis, SC, Brazil, 2013.

SOUSA, R. S. **Alocação estocasticamente robusta de chaves automáticas em rede de distribuição de energia elétrica.** 2018. MSc Thesis (in Portuguese) — Federal University of Santa Maria, Santa Maria, RS, Brazil, 2018.

SPERANDIO, M. **Planejamento da automação de sistemas de manobra em redes de distribuição**. 2008. PhD Thesis (in Portuguese) — Federal University of Santa Catarina, Florianópolis, SC, Brazil, 2008.

TABARES, A. *et al.* An Enhanced Algebraic Approach for the Analytical Reliability Assessment of Distribution Systems. **IEEE Transactions on Power Systems**, [S.l.], v. 34, n. 4, p. 2870–2879, 2019.

TABARES, A. *et al.* Multistage reliability-based expansion planning of ac distribution networks using a mixed-integer linear programming model. **International Journal of Electrical Power** & **Energy Systems**, [S.l.], v. 138, p. 107916, 2022.

VIEIRA POMBO, A.; MURTA-PINA, J.; FERNãO PIRES, V. Multiobjective formulation of the integration of storage systems within distribution networks for improving reliability. **Electric Power Systems Research**, [S.l.], v. 148, p. 87–96, 2017.

WACKER, G.; BILLINTON, R. Customer Cost of Electric Service Interruptions. **Proceedings of the IEEE**, [S.l.], v. 77, n. 6, p. 919–930, 1989.

WANG, C. *et al.* Fault incidence matrix based reliability evaluation method for complex distribution system. **IEEE Transactions on Power Systems**, [S.l.], v. 33, n. 6, p. 6736–6745, 2018.

WILLIS, H. **Power Distribution Planning Reference Book**. 2nd. ed. [S.l.]: New York, NY, USA: Marcel Dekker, 2004.

XIE, K.; ZHOU, J.; BILLINTON, R. Fast algorithm for the reliability evaluation of

large-scale electrical distribution networks using the section technique. **IET Generation, Transmission and Distribution**, [S.l.], v. 2, n. 5, p. 701 – 707, 2008.

ZHANG, T. *et al.* Optimal Design of the Sectional Switch and Tie Line for the Distribution Network Based on the Fault Incidence Matrix. **IEEE Transactions on Power Systems**, [S.l.], v. 34, n. 6, p. 4869 – 4879, 2019.

ZHANG, T. *et al.* Analytical Calculation Method of Reliability Sensitivity Indexes for Distribution Systems Based on Fault Incidence Matrix. **Journal of Modern Power Systems and Clean Energy**, [S.l.], v. 8, n. 2, p. 325–333, 2020.

ZIDAN, A. *et al.* Fault Detection, Isolation, and Service Restoration in Distribution Systems: state-of-the-art and future trends. **IEEE Transactions on Smart Grid**, [S.l.], v. 8, n. 5, p. 2170 – 2185, 2017.

APPENDIX A

NUMERICAL RESULTS OF ANALYTICAL ASSESSMENT OF RELIABILITY FOR THE 3-ZONE EXAMPLE FEEDER

In this appendix, numerical results of the analytical assessment of reliability for the 3-zone example feeder (Figure 11) will be presented using constant values for reliability parameters. In this example, the following reliability parameters were chosen: $\lambda_1 = \lambda_2 = \lambda_3 = 5$ failures/year, $l_1 = l_2 = l_3 = 1$ km, $N_1 = N_2 = N_3 = 4$ customers, $TC = 12$ customers, and $C_1 = C_2 = C_3 = 8$ MWh/year. Additionally, constant values were also assigned for the parameters related to time of interruptions $t_l = 1$ h, $t_c = 0.25$ h, and $t_r = 0.5$ h.

The matrix IQM resulted in:

$$IQM = \begin{array}{c} \begin{matrix} 1 & 2 & 3 \end{matrix} \\ \begin{bmatrix} 5 & 5 & 5 \\ 5 & 5 & 5 \\ 5 & 5 & 5 \end{bmatrix} \end{array} \begin{matrix} 1 \\ 2 \\ 3 \end{matrix} \tag{A.1}$$

From the matrix IQM, the expected index CIF of zones were obtained, resulting in: $ECIF_1 = ECIF_2 = ECIF_3 = 15$ interruptions/year.

The matrix CWIQM was obtained using the matrix IQM, resulting in:

$$CWIQM = \begin{array}{c} \begin{matrix} 1 & 2 & 3 \end{matrix} \\ \begin{bmatrix} 20 & 20 & 20 \\ 20 & 20 & 20 \\ 20 & 20 & 20 \end{bmatrix} \end{array} \begin{matrix} 1 \\ 2 \\ 3 \end{matrix} \tag{A.2}$$

From the matrix CWIQM, the value of $ESAIFI$ was obtained, which resulted in 15 interruptions/year. The values of fault contribution in zones to the $ESAIFI$ were also obtained through the matrix CWIQM, and resulted in $cSAIFI_1 = cSAIFI_2 = cSAIFI_3 = 5$ interruptions/year.

The matrix IDM was assembled using the matrix IQM, and resulted in:

$$IDM = \begin{matrix} \\ 1 \\ 2 \\ 3 \end{matrix} \begin{matrix} \begin{matrix} 1 & 2 & 3 \end{matrix} \\ \begin{bmatrix} 8.75 & 6.25 & 6.25 \\ 7.50 & 10.00 & 7.50 \\ 6.25 & 6.25 & 8.75 \end{bmatrix} \end{matrix} \tag{A.3}$$

From the matrix IDM, the expected index CID of zones were obtained, which resulted in: $ECID_1 = ECID_2 = ECID_3 = 22.5$ h/year.

Subsequently, the matrix CWIDM was generated using the matrix IDM, and resulted in:

$$CWIDM = \begin{matrix} \\ 1 \\ 2 \\ 3 \end{matrix} \begin{matrix} \begin{matrix} 1 & 2 & 3 \end{matrix} \\ \begin{bmatrix} 35 & 25 & 25 \\ 30 & 40 & 30 \\ 25 & 25 & 35 \end{bmatrix} \end{matrix} \tag{A.4}$$

From the matrix CWIDM, the $ESAIDI$ was obtained, resulting in 22.5 h/year. The values of fault contribution in zones to the $ESAIDI$ were also obtained through the matrix CWIDM, and resulted in $cSAIDI_1 = 7.08$ h/year, $cSAIDI_2 = 8.33$ h/year, and $cSAIDI_3 = 7.08$ h/year.

The matrix CWIM resulted in:

$$CWIM = \begin{matrix} \\ 1 \\ 2 \\ 3 \end{matrix} \begin{matrix} \begin{matrix} 1 & 2 & 3 \end{matrix} \\ \begin{bmatrix} 70 & 50 & 50 \\ 60 & 80 & 60 \\ 50 & 50 & 70 \end{bmatrix} \end{matrix} \tag{A.5}$$

From the matrix CWIM, the index $EENS$ was obtained, and resulted in 61.65 kWh/year. The contribution of faults in zones to the index $EENS$ were obtained through the matrix CWIM, and resulted in $cEENS_1 = 19.41$ kWh/year, $cEENS_2 = 22.83$ kWh/year, and $cEENS_3 = 19.41$ kWh/year.

Finally, Table 11 shows all the reliability indices obtained for the 3-zone example

feeder.

Table A.1 – Reliability indices obtained for the 3-zone example feeder.

Index	**Value** (int./year)	**Index**	**Value** (h/year)	**Index**	**Value** (kWh/year)
$ESAIFI$	15	$ESAIDI$	22.5	$EENS$	61.65
$cSAIFI_1$	5	$cSAIDI_1$	7.08	$cEENS_1$	19.41
$cSAIFI_2$	5	$cSAIDI_2$	8.33	$cEENS_2$	22.83
$cSAIFI_3$	5	$cSAIDI_3$	7.08	$cEENS_3$	19.41
$ECIF_1$	15	$ECID_1$	22.5	–	–
$ECIF_2$	15	$ECID_2$	22.5	–	–
$ECIF_3$	15	$ECID_3$	22.5	–	–

APPENDIX B

ADDITIONAL DATA – CASE STUDY USING THE DISTRIBUTION NETWORK AT BUS 5 OF THE RBTS

In this appendix, data concerning parameters of the distribution network at bus 5 of the RBTS, used in the case study presented in Section 4.1, are made available. Data in this appendix are excerpted, modified, and reproduced with permission, from the following paper that I co-authored:

- **Aschidamini, G.L.**; da Cruz, G.A.; Resener, M.; Leborgne, R.C.; Pereira, L.A. A Framework for Reliability Assessment in Expansion Planning of Power Distribution Systems. Energies 2022, 15. doi:10.3390/en15145073.

Data of this appendix have been adapted from the above paper to fit the scope and formatting of the thesis.

Table B.1 shows the length per zone of the distribution network, in km. This parameter was calculated based on the lengths of each feeder section in (BILLINTON, 1996). Zone 1 of feeder F1 and zone 4 of feeder F4 have 2.10 km of primary distribution network length, thus being the longer zones of this distribution network.

Table B.1 – Length per zone of the distribution network at bus 5 of the RBTS.

	Zone	**1**	**2**	**3**	**4**	**5**
Length (km)	F1	2.10	1.95	1.80	1.60	–
	F2	1.15	1.15	1.45	1.15	1.95
	F3	1.60	1.65	1.45	1.95	–
	F4	1.95	1.95	1.15	2.10	–

The number of customers connected in each zone of the distribution network is shown in Table B.2. This parameter was calculated based on the data of number of customers connected at each load-point in (BILLINTON, 1996). Zone 4 of feeder F4 has 435 customers, therefore being the zone with most customers in this network.

Table B.2 – Customers per zone of the distribution network at bus 5 of the RBTS.

	Zone	**1**	**2**	**3**	**4**	**5**
Customers	F1	420	241	241	15	–
	F2	1	195	195	195	196
	F3	15	241	1	16	–
	F4	420	16	15	435	–

The average load level per zone of the distribution network, in MW, is shown in Table B.3. This parameter was calculated based on the data of average load level per load-point in (BILLINTON, 1996). Zone 2 and zone 3 of feeder F1 present the highest values for the average load level among the zones of this distribution network.

Table B.3 – Average load level per zone of the distribution network at bus 5 of the RBTS.

	Zone	**1**	**2**	**3**	**4**	**5**
Average load level (MW)	F1	0.8538	1.0418	1.0418	0.4089	–
	F2	0.6247	0.3213	0.3213	0.3213	0.6999
	F3	0.4089	0.7957	0.6247	0.7875	–
	F4	0.8538	1.0336	0.4089	0.7384	–

The matrices of the analytical assessment of reliability for feeders F1, F3 and F4, which have 4 zones, are shown in (B.1), (B.2), (B.3), (B.4), and (B.5).

$$IQM = \begin{array}{c} \begin{matrix} 1 & 2 & 3 & 4 \end{matrix} \\ \begin{bmatrix} \lambda_1 & \lambda_1 & \lambda_1 & \lambda_1 \\ \lambda_2 & \lambda_2 & \lambda_2 & \lambda_2 \\ \lambda_3 & \lambda_3 & \lambda_3 & \lambda_3 \\ \lambda_4 & \lambda_4 & \lambda_4 & \lambda_4 \end{bmatrix} \end{array} \begin{matrix} 1 \\ 2 \\ 3 \\ 4 \end{matrix} \tag{B.1}$$

$$CWIQM = \begin{array}{c} \begin{matrix} 1 & 2 & 3 & 4 \end{matrix} \\ \begin{bmatrix} \lambda_1 N_1 & \lambda_1 N_2 & \lambda_1 N_3 & \lambda_1 N_4 \\ \lambda_2 N_1 & \lambda_2 N_2 & \lambda_2 N_3 & \lambda_2 N_4 \\ \lambda_3 N_1 & \lambda_3 N_2 & \lambda_3 N_3 & \lambda_3 N_4 \\ \lambda_4 N_1 & \lambda_4 N_2 & \lambda_4 N_3 & \lambda_4 N_4 \end{bmatrix} \begin{matrix} 1 \\ 2 \\ 3 \\ 4 \end{matrix} \end{array} \tag{B.2}$$

$$IDM = \begin{bmatrix} \lambda_1(t_l + t_{sw} + t_r) & \lambda_1(t_l + t_{sw}) & \dots \\ \lambda_2(t_l + t_{sw} + t_{sw}) & \lambda_2(t_l + t_{sw} + t_{sw} + t_r) & \dots \\ \lambda_3(t_l + t_{sw} + t_{sw}) & \lambda_3(t_l + t_{sw} + t_{sw}) & \dots \\ \lambda_4(t_l + t_{sw}) & \lambda_4(t_l + t_{sw}) & \dots \end{bmatrix} \begin{bmatrix} \lambda_1(t_l + t_{sw}) & \lambda_1(t_l + t_{sw}) \\ \lambda_2(t_l + t_{sw} + t_{sw}) & \lambda_2(t_l + t_{sw} + t_{sw}) \\ \lambda_3(t_l + t_{sw} + t_{sw} + t_r) & \lambda_3(t_l + t_{sw} + t_{sw}) \\ \lambda_4(t_l + t_{sw}) & \lambda_4(t_l + t_{sw} + t_r) \end{bmatrix} \tag{B.3}$$

$$CWIDM = \begin{bmatrix} \lambda_1(t_l + t_{sw} + t_r)N_1 & \lambda_1(t_l + t_{sw})N_2 & \dots \\ \lambda_2(t_l + t_{sw} + t_{sw})N_1 & \lambda_2(t_l + t_{sw} + t_{sw} + t_r)N_2 & \dots \\ \lambda_3(t_l + t_{sw} + t_{sw})N_1 & \lambda_3(t_l + t_{sw} + t_{sw})N_2 & \dots \\ \lambda_4(t_l + t_{sw})N_1 & \lambda_4(t_l + t_{sw})N_2 & \dots \end{bmatrix} \begin{bmatrix} \lambda_1(t_l + t_{sw})N_3 & \lambda_1(t_l + t_{sw})N_4 \\ \lambda_2(t_l + t_{sw} + t_{sw})N_3 & \lambda_2(t_l + t_{sw} + t_{sw})N_4 \\ \lambda_3(t_l + t_{sw} + t_{sw} + t_r)N_3 & \lambda_3(t_l + t_{sw} + t_{sw})N_4 \\ \lambda_4(t_l + t_{sw})N_3 & \lambda_4(t_l + t_{sw} + t_r)N_4 \end{bmatrix} \tag{B.4}$$

$$CWIM = \begin{bmatrix} \lambda_1(t_l + t_{sw} + t_r)C_1 & \lambda_1(t_l + t_{sw})C_2 & \dots \\ \lambda_2(t_l + t_{sw} + t_{sw})C_1 & \lambda_2(t_l + t_{sw} + t_{sw} + t_r)C_2 & \dots \\ \lambda_3(t_l + t_{sw} + t_{sw})C_1 & \lambda_3(t_l + t_{sw} + t_{sw})C_2 & \dots \\ \lambda_4(t_l + t_{sw})C_1 & \lambda_4(t_l + t_{sw})C_2 & \dots \end{bmatrix} \begin{bmatrix} \lambda_1(t_l + t_{sw})C_3 & \lambda_1(t_l + t_{sw})C_4 \\ \lambda_2(t_l + t_{sw} + t_{sw})C_3 & \lambda_2(t_l + t_{sw} + t_{sw})C_4 \\ \lambda_3(t_l + t_{sw} + t_{sw} + t_r)C_3 & \lambda_3(t_l + t_{sw} + t_{sw})C_4 \\ \lambda_4(t_l + t_{sw})C_3 & \lambda_4(t_l + t_{sw} + t_r)C_4 \end{bmatrix} \tag{B.5}$$

The matrices of the analytical assessment of reliability for feeder F2 are shown in (B.6), (B.7), (B.8), (B.9), and (B.10).

$$IQM = \begin{array}{c} \begin{matrix} 1 & 2 & 3 & 4 & 5 \end{matrix} \\ \begin{bmatrix} \lambda_1 & \lambda_1 & \lambda_1 & \lambda_1 & \lambda_1 \\ \lambda_2 & \lambda_2 & \lambda_2 & \lambda_2 & \lambda_2 \\ \lambda_3 & \lambda_3 & \lambda_3 & \lambda_3 & \lambda_3 \\ \lambda_4 & \lambda_4 & \lambda_4 & \lambda_4 & \lambda_4 \\ \lambda_5 & \lambda_5 & \lambda_5 & \lambda_5 & \lambda_5 \end{bmatrix} \end{array} \begin{matrix} 1 \\ 2 \\ 3 \\ 4 \\ 5 \end{matrix} \tag{B.6}$$

$$CWIQM = \begin{array}{c} \begin{matrix} 1 & 2 & 3 & 4 & 5 \end{matrix} \\ \begin{bmatrix} \lambda_1 N_1 & \lambda_1 N_2 & \lambda_1 N_3 & \lambda_1 N_4 & \lambda_1 N_5 \\ \lambda_2 N_1 & \lambda_2 N_2 & \lambda_2 N_3 & \lambda_2 N_4 & \lambda_2 N_5 \\ \lambda_3 N_1 & \lambda_3 N_2 & \lambda_3 N_3 & \lambda_3 N_4 & \lambda_3 N_5 \\ \lambda_4 N_1 & \lambda_4 N_2 & \lambda_4 N_3 & \lambda_4 N_4 & \lambda_4 N_5 \\ \lambda_5 N_1 & \lambda_5 N_2 & \lambda_5 N_3 & \lambda_5 N_4 & \lambda_5 N_5 \end{bmatrix} \end{array} \begin{matrix} 1 \\ 2 \\ 3 \\ 4 \\ 5 \end{matrix} \tag{B.7}$$

$$IDM = \begin{bmatrix} \lambda_1(t_l + t_{sw} + t_r) & \lambda_1(t_l + t_{sw}) & \lambda_1(t_l + t_{sw}) & \dots \\ \lambda_2(t_l + t_{sw} + t_{sw}) & \lambda_2(t_l + t_{sw} + t_{sw} + t_r) & \lambda_2(t_l + t_{sw} + t_{sw}) & \dots \\ \lambda_3(t_l + t_{sw} + t_{sw}) & \lambda_3(t_l + t_{sw} + t_{sw}) & \lambda_3(t_l + t_{sw} + t_{sw} + t_r) & \dots \\ \lambda_4(t_l + t_{sw} + t_{sw}) & \lambda_4(t_l + t_{sw} + t_{sw}) & \lambda_4(t_l + t_{sw} + t_{sw}) & \dots \\ \lambda_5(t_l + t_{sw}) & \lambda_5(t_l + t_{sw}) & \lambda_5(t_l + t_{sw}) & \dots \end{bmatrix}$$

$$\begin{bmatrix} \lambda_1(t_l + t_{sw}) & \lambda_1(t_l + t_{sw}) \\ \lambda_2(t_l + t_{sw} + t_{sw}) & \lambda_2(t_l + t_{sw} + t_{sw}) \\ \lambda_3(t_l + t_{sw} + t_{sw}) & \lambda_3(t_l + t_{sw} + t_{sw}) \\ \lambda_4(t_l + t_{sw} + t_{sw} + t_r) & \lambda_4(t_l + t_{sw} + t_{sw}) \\ \lambda_5(t_l + t_{sw}) & \lambda_5(t_l + t_{sw} + t_r) \end{bmatrix} \tag{B.8}$$

$$CWIDM = \begin{bmatrix} \lambda_1(t_l + t_{sw} + t_r)N_1 & \lambda_1(t_l + t_{sw})N_2 & ... \\ \lambda_2(t_l + t_{sw} + t_{sw})N_1 & \lambda_2(t_l + t_{sw} + t_{sw} + t_r)N_2 & ... \\ \lambda_3(t_l + t_{sw} + t_{sw})N_1 & \lambda_3(t_l + t_{sw} + t_{sw})N_2 & ... \\ \lambda_4(t_l + t_{sw} + t_{sw})N_1 & \lambda_4(t_l + t_{sw} + t_{sw})N_2 & ... \\ \lambda_5(t_l + t_{sw})N_1 & \lambda_5(t_l + t_{sw})N_2 & ... \end{bmatrix}$$

$$\begin{bmatrix} \lambda_1(t_l + t_{sw})N_3 & \lambda_1(t_l + t_{sw})N_4 & ... \\ \lambda_2(t_l + t_{sw} + t_{sw})N_3 & \lambda_2(t_l + t_{sw} + t_{sw})N_4 & ... \\ \lambda_3(t_l + t_{sw} + t_{sw} + t_r)N_3 & \lambda_3(t_l + t_{sw} + t_{sw})N_4 & ... \\ \lambda_4(t_l + t_{sw} + t_{sw})N_3 & \lambda_4(t_l + t_{sw} + t_{sw} + t_r)N_4 & ... \\ \lambda_5(t_l + t_{sw})N_3 & \lambda_5(t_l + t_{sw})N_4 & ... \end{bmatrix}$$

$$\begin{bmatrix} \lambda_1(t_l + t_{sw})N_5 \\ \lambda_2(t_l + t_{sw} + t_{sw})N_5 \\ \lambda_3(t_l + t_{sw} + t_{sw})N_5 \\ \lambda_4(t_l + t_{sw} + t_{sw})N_5 \\ \lambda_5(t_l + t_{sw} + t_r)N_5 \end{bmatrix} \tag{B.9}$$

$$CWIM = \begin{bmatrix} \lambda_1(t_l + t_{sw} + t_r)C_1 & \lambda_1(t_l + t_{sw})C_2 & ... \\ \lambda_2(t_l + t_{sw} + t_{sw})C_1 & \lambda_2(t_l + t_{sw} + t_{sw} + t_r)C_2 & ... \\ \lambda_3(t_l + t_{sw} + t_{sw})C_1 & \lambda_3(t_l + t_{sw} + t_{sw})C_2 & ... \\ \lambda_4(t_l + t_{sw} + t_{sw})C_1 & \lambda_4(t_l + t_{sw} + t_{sw})C_2 & ... \\ \lambda_5(t_l + t_{sw})C_1 & \lambda_5(t_l + t_{sw})C_2 & ... \end{bmatrix}$$

$$\begin{bmatrix} \lambda_1(t_l + t_{sw})C_3 & \lambda_1(t_l + t_{sw})C_4 & ... \\ \lambda_2(t_l + t_{sw} + t_{sw})C_3 & \lambda_2(t_l + t_{sw} + t_{sw})C_4 & ... \\ \lambda_3(t_l + t_{sw} + t_{sw} + t_r)C_3 & \lambda_3(t_l + t_{sw} + t_{sw})C_4 & ... \\ \lambda_4(t_l + t_{sw} + t_{sw})C_3 & \lambda_4(t_l + t_{sw} + t_{sw} + t_r)C_4 & ... \\ \lambda_5(t_l + t_{sw})C_3 & \lambda_5(t_l + t_{sw})C_4 & ... \end{bmatrix}$$

$$\begin{bmatrix} \lambda_1(t_l + t_{sw})C_5 \\ \lambda_2(t_l + t_{sw} + t_{sw})C_5 \\ \lambda_3(t_l + t_{sw} + t_{sw})C_5 \\ \lambda_4(t_l + t_{sw} + t_{sw})C_5 \\ \lambda_5(t_l + t_{sw} + t_r)C_5 \end{bmatrix} \tag{B.10}$$

APPENDIX C
ADDITIONAL DATA AND RESULTS – CASE STUDY USING THE 60-ZONE REAL PRIMARY DISTRIBUTION FEEDER

In this appendix, additional data and results of the 60-zone real primary distribution feeder used in the case study presented in Section 5.1 are made available. Data in this appendix are excerpted, modified, and reproduced with permission, from the following paper that I co-authored:

- **Aschidamini, G.L.**; da Cruz, G.A.; Resener, M.; Leborgne, R.C.; Pereira, L.A. A Framework for Reliability Assessment in Expansion Planning of Power Distribution Systems. Energies 2022, 15. doi:10.3390/en15145073.

Data of this appendix have been adapted from the above paper to fit the scope and formatting of the thesis.

Table C.1 shows the parameters per zone of the 60-zone real primary distribution feeder. For each zone, the id of the switch upstream of the zone and the type of switch (CB, NC switch or fuse) are shown. Additionally, the values of the following parameters are presented for each zone: i) length, ii) number of customers, iii) average load level, and iv) initial failure rate.

Table C.1 – Data per zone of the 60-zone real primary distribution feeder.

Zone number	**Switch**		**Length** (km)	**Customers**	**Average load level** (MW)	**Initial failure rate** (failure/year)
	id	**type**				
1	-	CB	-	-	-	-
2	AL-29-64	NC	0.0517	0	0	0
3	1741	NC	0.1182	0	0	0
4	0321	NC	4.0608	100	0.03658	0
5	0233	NC	2.0175	231	0.08960	0
6	0238	NC	1.3854	232	0.09489	0
7	0261	NC	0.5976	144	0.05359	0.3333
8	2654	NC	0.1904	28	0.00691	0
9	1496	NC	1.0407	289	0.10930	0
10	0741	NC	1.3178	572	0.13756	0.3333
11	0513	NC	2.2380	654	0.18362	0.3333
12	0191	NC	1.4691	340	0.11496	0
13	0063	NC	2.0144	1,000	0.24581	0.3333
14	0313	NC	0.7927	158	0.05075	0
15	0314	NC	2.7929	624	0.15951	0
16	0798	NC	3.3673	498	0.10170	0.3333
17	1922	NC	3.0902	827	0.19273	0
18	0141	NC	1.6114	327	0.12997	0
19	2162	NC	0.6507	324	0.12392	0
20	0507	NC	0.7877	93	0.03123	0
21	0300	NC	0.6270	155	0.04392	0
22	0413	NC	1.9635	430	0.09779	0.6667
23	2653	NC	0.2103	23	0.00706	0
24	2666	NC	0.7128	157	0.04267	0
25	0377	FUS	0.8224	135	0.02565	0.6667
26	0120	FUS	0.0249	1	0.00234	0
27	1972	FUS	0.6592	1	0.00140	1.3333
28	1874	FUS	0.1089	1	0.00014	0
29	1906	FUS	0.0269	1	0.00014	0
30	0224	FUS	0.4970	74	0.01294	1.0000
31	0511	FUS	0.4414	115	0.02811	1.3333
32	0514	FUS	0.2150	35	0.00952	0.6667
33	0516	FUS	0.2582	16	0.00287	3.6667
34	1944	FUS	0.0155	0	0	0
35	0517	FUS	0.1378	60	0.01596	0
36	1846	FUS	0.1089	0	0	0
37	1962	FUS	0.0081	0	0	0
38	1366	FUS	0.0131	0	0	0
39	0743	FUS	3.1459	1,230	0.28809	2.0000
40	0907	FUS	1.3134	357	0.08588	1.0000

Continued on next page

Table C.1 – Data per zone of the 60-zone real primary distribution feeder (Continued).

Zone number	**Switch**		**Length** (km)	**Customers**	**Average load level** (MW)	**Initial failure rate** (failure/year)
	id	**type**				
41	0230	FUS	2.8964	701	0.21472	3.3333
42	8617	FUS	0.0190	1	0.00995	0
43	1213	FUS	0.0720	0	0	0
44	8935	FUS	0.0177	1	0.00018	0
45	8627	FUS	0.0176	0	0	0
46	0744	FUS	0.7057	100	0.02660	2.6667
47	1863	FUS	0.0177	0	0	0
48	0518	FUS	0.3478	245	0.05513	1.3333
49	0228	FUS	1.8779	656	0.14025	2.0000
50	0899	FUS	1.2165	2	0.00014	0.3333
51	1740	FUS	0.0307	0	0	0
52	9629	FUS	0.0127	0	0	0
53	1834	FUS	0.0160	0	0	0
54	0113	FUS	0.0125	0	0	0
55	8623	FUS	0.0124	0	0	0
56	0312	FUS	0.9842	4	0.00391	3.0000
57	1363	FUS	0.0391	1	0.00715	0
58	0707	FUS	0.5942	3	0.00093	0
59	1937	FUS	0.0358	1	0.00374	0
60	8619	FUS	0.0320	0	0	0

Table C.2 shows additional results for the case study of reliability without expansion projects of the 60-zone real primary distribution feeder presented in Section 5.1.1. For each zone, the following results are presented i) failure rate; ii) contribution of faults in zones to the indices $ESAIFI$, $ESAIDI$ and $EENS$; and iii) indices $ECIF_j$ and $ECID_j$.

Table C.2 – Reliability without expansion projects of the 60-zone real primary distribution feeder.

Zone number	**Calculated failure rate** (failure/year)	$\boldsymbol{cSAIFI_i}$ (int./year)	$\boldsymbol{cSAIDI_i}$ (h/year)	$\boldsymbol{cEENS_i}$ (MWh/year)	$\boldsymbol{ECIF_j}$ (int./year)	$\boldsymbol{ECID_j}$ (h/year)
1	-	-	-	-	-	-
2	0.0254	0.0254	0.0146	0.0437	18.6192	9.6231
3	0.0581	0.0581	0.0367	0.1098	18.6192	9.6308
4	1.9975	1.9975	1.2614	3.7714	18.6192	9.8957
5	0.9924	0.9924	0.6238	1.8650	18.6192	10.0273
6	0.6815	0.6815	0.4240	1.2663	18.6192	10.1177

Continued on next page

Table C.2 – Reliability without expansion projects of the 60-zone real primary distribution feeder (Continued).

Zone number	**Calculated failure rate** (failure/year)	$cSAIFI_i$ (int./year)	$cSAIDI_i$ (h/year)	$cEENS_i$ (MWh/year)	$ECIF_j$ (int./year)	$ECID_j$ (h/year)
7	0.6273	0.6273	0.3497	1.0467	18.6192	10.2009
8	0.0937	0.0937	0.0521	0.1557	18.6192	10.1301
9	0.5119	0.5119	0.2939	0.8776	18.6192	10.1856
10	0.9816	0.9816	0.5565	1.6600	18.6192	10.2479
11	1.4342	1.4342	0.8084	2.4178	18.6192	10.3079
12	0.7227	0.7227	0.3784	1.134	18.6192	10.2135
13	1.3242	1.3242	0.6879	2.0578	18.6192	10.3891
14	0.3899	0.3899	0.2237	0.6657	18.6192	10.1694
15	1.3738	1.3738	0.7108	2.1138	18.6192	10.2999
16	1.9897	1.9897	1.0046	2.9946	18.6192	10.4333
17	1.5201	1.5201	0.7736	2.3062	18.6192	10.3710
18	0.7926	0.7929	0.4436	1.3306	18.6192	10.2228
19	0.3201	0.3201	0.1791	0.5371	18.6192	10.1601
20	0.3875	0.3875	0.2158	0.6454	18.6192	10.1691
21	0.3084	0.3084	0.1726	0.516	18.6192	10.1586
22	1.6325	1.6325	0.8236	2.4611	18.6192	10.3342
23	0.1034	0.1034	0.0516	0.1546	18.6192	10.3479
24	0.3506	0.3506	0.1756	0.525	18.6192	10.2051
25	1.0712	0.0132	0.0076	0.0158	19.6904	10.5113
26	0.0122	0	0	0	18.6314	9.9027
27	1.6576	0.0002	0.0001	0.0013	20.2768	10.8483
28	0.0536	0	0	0	18.6728	9.9265
29	0.0132	0	0	0	18.6324	9.9033
30	1.2445	0.0084	0.0048	0.0093	19.8637	10.7425
31	1.5505	0.0163	0.0094	0.0025	20.1697	10.9183
32	0.7724	0.0025	0.0014	0.0042	19.3916	10.4712
33	3.7937	0.0055	0.0032	0.0063	22.4129	12.2074
34	0.0076	0	0	0	18.6268	10.0317
35	0.0678	0.0004	0.0002	0.0006	18.6870	10.0663
36	0.0535	0	0	0	18.6728	10.0581
37	0.0040	0	0	0	18.6232	10.2032
38	0.0064	0	0	0	18.6257	10.1338
39	3.5475	0.3986	0.2291	0.5873	22.1667	12.2242
40	1.6461	0.0537	0.0308	0.0812	20.2653	11.1938
41	4.7581	0.3047	0.1751	0.5871	23.3773	13.1234
42	0.0093	0	0	0.0001	18.6286	10.3945
43	0.0354	0	0	0	18.6546	10.4095
44	0.0087	0	0	0	18.6279	10.1227
45	0.0086	0	0	0	18.6279	10.1227
46	3.0138	0.0275	0.0158	0.0461	21.6330	11.8496

Continued on next page

Table C.2 – Reliability without expansion projects of the 60-zone real primary distribution feeder (Continued).

Zone number	**Calculated failure rate** (failure/year)	$cSAIFI_i$ (int./year)	$cSAIDI_i$ (h/year)	$cEENS_i$ (MWh/year)	$ECIF_j$ (int./year)	$ECID_j$ (h/year)
47	0.0087	0	0	0	18.6279	10.1227
48	1.5044	0.0337	0.0193	0.0477	20.1236	11.1644
49	2.9237	0.1752	0.1007	0.2356	21.5429	11.9800
50	0.9317	0.0002	0.0001	0.0001	19.5509	10.8353
51	0.0151	0	0	0	18.6343	10.3086
52	0.0063	0	0	0	18.6255	10.2264
53	0.0079	0	0	0	18.6271	10.2273
54	0.0062	0	0	0	18.6254	10.1726
55	0.0061	0	0	0	18.6253	10.1621
56	3.4841	0.0013	0.0007	0.0078	22.1033	12.3501
57	0.0192	0	0	0.0001	18.6384	10.3589
58	0.2923	0.0001	0	0.0002	18.9115	10.5159
59	0.0176	0	0	0	18.6368	10.3580
60	0.0157	0	0	0	18.6350	10.3570